AD-A054 438 ARMY MILITARY PERSONNEL CENTER ALEXANDRIA VA F/G 20/11
DEVELOPMENT OF AN EMPIRICAL RELATIONSHIP FOR THE PREDICTION OF --ETC(U)
MAY 78 T J RUSNAK

UNCLASSIFIED NL

1 OF 3
ADA
054438

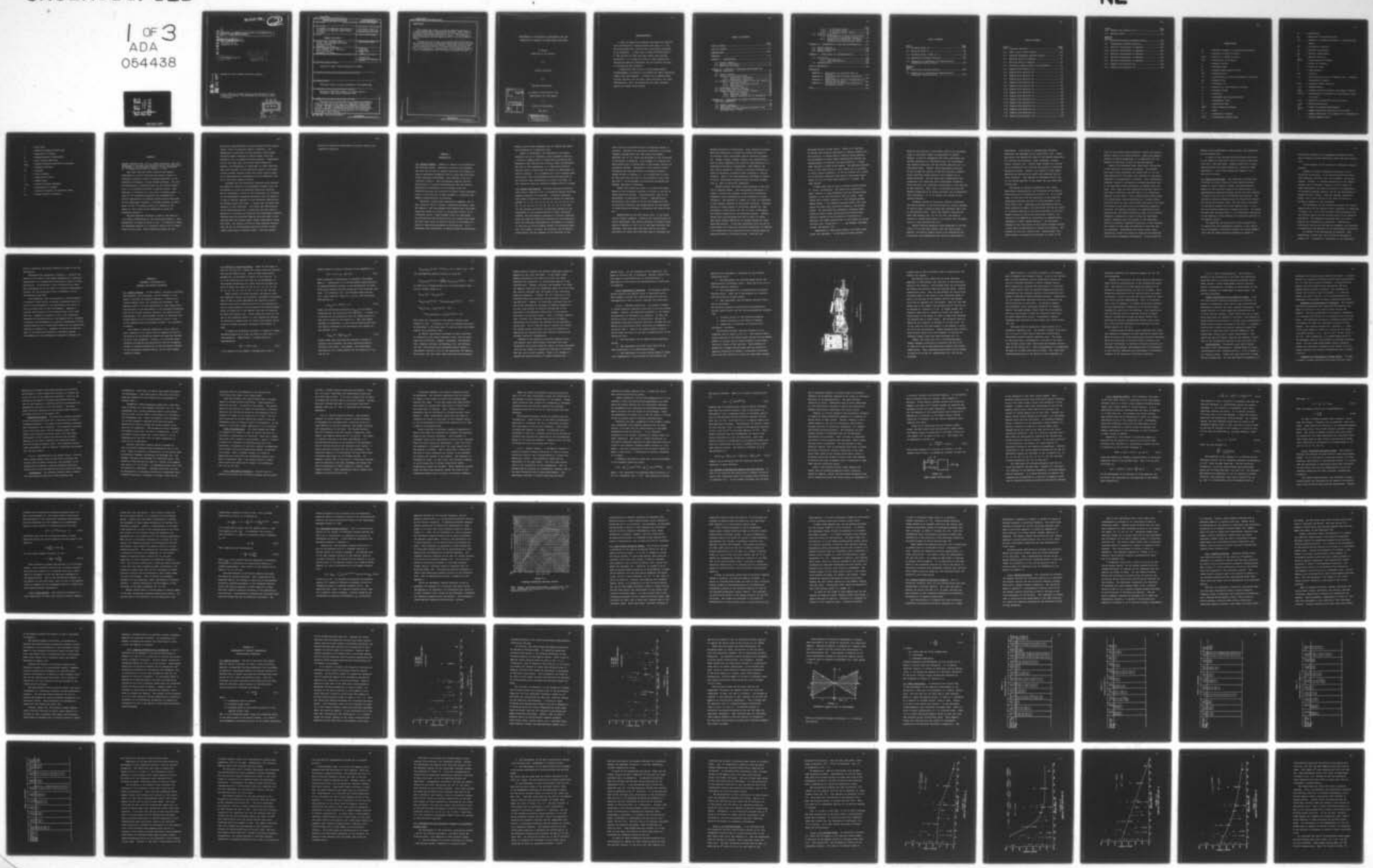

FOR FURTHER TRAN

AD A054438

DEVELOPMENT OF AN EMPIRICAL RELATIONSHIP FOR THE PREDICTION OF DAMPING IN STEEL-FRAMED BUILDINGS.

TERRANCE JOHN RUSNAK, MAJOR
HQDA, MILPERCEN (DAPC-OPP-E)
200 Stovall Street
Alexandria, VA 22332

3 May 78

Final Report, 3 May 1978

219p.

Approved for public release; distribution unlimited

A thesis submitted to Purdue University, West Lafayette, IN 47907 in partial fulfillment of the requirements for the degree of Doctor of Philosophy.

391 191

UNCLASSIFIED
SECURITY CLASSIFICATION OF THIS PAGE (When Data Entered)

REPORT DOCUMENTATION PAGE		READ INSTRUCTIONS BEFORE COMPLETING FORM
1. REPORT NUMBER	2. GOVT ACCESSION NO.	3. RECIPIENT'S CATALOG NUMBER
4. TITLE (and Subtitle) Development of an Empirical Relationship for the Prediction of Damping in Steel-Framed Buildings		5. TYPE OF REPORT & PERIOD COVERED Final Report, 3 May 1978
		6. PERFORMING ORG. REPORT NUMBER
7. AUTHOR(s) TERRANCE JOHN RUSNAK		8. CONTRACT OR GRANT NUMBER(s)
9. PERFORMING ORGANIZATION NAME AND ADDRESS Student, HQDA, MILPERCEN (DAPC-OPP-E) 200 Stovall Street Alexandria, VA 22332		10. PROGRAM ELEMENT, PROJECT, TASK AREA & WORK UNIT NUMBERS
11. CONTROLLING OFFICE NAME AND ADDRESS HQDA, MILPERCEN, ATTN: DAPC-OPP-E 200 Stovall Street Alexandria, VA 22332		12. REPORT DATE 3 May 1978
		13. NUMBER OF PAGES 203
14. MONITORING AGENCY NAME & ADDRESS (if different from Controlling Office)		15. SECURITY CLASS. (of this report) Unclassified
		15a. DECLASSIFICATION/DOWNGRADING SCHEDULE

16. DISTRIBUTION STATEMENT (of this Report)

Approved for public release; distribution unlimited

17. DISTRIBUTION STATEMENT (of the abstract entered in Block 20, if different from Report)

18. SUPPLEMENTARY NOTES

PhD Thesis; Purdue University; Department of Civil Engineering

19. KEY WORDS (Continue on reverse side if necessary and identify by block number)

Earthquakes; Vibrations; Dynamics; Structural Analysis; Structural Design; Damping; Buildings; Steel

20. ABSTRACT (Continue on reverse side if necessary and identify by block number)

Test data from the forced vibration and ambient experiments on actual structures are used as input to a regression analysis routine to develop equations for the prediction of damping in steel-framed buildings. The data is categorized by building height and building width (the dimension in the direction parallel to the applied forces). The best resulting equation is used as the basis for a new design methodology to predict damping.

DD FORM 1 JAN 73 1473 EDITION OF 1 NOV 65 IS OBSOLETE

UNCLASSIFIED
SECURITY CLASSIFICATION OF THIS PAGE (When Data Entered)

Item 20 cont.

This methodology consists of using the prediction equation in a situation where a set of conditions are satisfied. These conditions pertain to the particular characteristics of the structure and the approximate level of excitation which is expected. It is anticipated that this methodology will be especially useful in the early stages of design.

Included also are two types of sensitivity analysis which indicate the amount of variation in displacement response that can be expected by using the developed prediction equation. The results of both of these analyses indicate that the use of the developed equations results in good, usable predictions of damping values. Both the English and Metric systems of measurement are used to develop the regression equations.

DEVELOPMENT OF AN EMPIRICAL RELATIONSHIP FOR THE PREDICTION OF DAMPING IN STEEL-FRAMED BUILDINGS

A Thesis

Submitted to the Faculty

of

Purdue University

by

Terrance John Rusnak

In Partial Fulfillment of the

Requirements for the Degree

of

Doctor of Philosophy

May 1978

ACKNOWLEDGMENTS

I wish to express my sincerest gratitude and appreciation to Professors C. Douglas Sutton and James T. P. Yao who have guided this work and have contributed profoundly to my education. I would like to thank Professors Robert H. Lee and Dale W. Thoe for their advice and interest, and Doctor W. E. Fisher from the U.S. Army Construction Engineering Research Laboratory for his interest and help in originating this research.

I would also like to give a long overdue public acknowledgement of thanks to my parents for their continuing support and encouragement. I would like to deeply thank my wife, Marlene, and two sons, Terry and Scott, for their understanding, love, and especially for their patience during the course of my studies.

TABLE OF CONTENTS

LIST OF TABLES

LIST OF FIGURES

NOMENCLATURE

A_i	= solution statement in decision-tree format
a	= quantity in Taylor's series
B,B( )	= function in Taylor's series
COV	= coefficient of variation
c	= damping constant
D	= building width
$\underline{D}$	= dynamic magnification factor
E[]	= expected value
F( )	= distribution (or joint distribution) function
F_d	= damping force
f	= frequency, Hz
f( )	= density (or joint density) function
H	= building height
k	= stiffness
L	= earthquake participation factor
ℓ	= consequence (loss)
M*	= generalized mass
MDOF	= multi-degree-of-freedom
m	= mass
P ( )	= probability function
p(t)	= harmonically varying load

p	=	probability
p_o	=	amplitude of excitation force
Q_i	=	question, or problem statement, in decision-tree format
R^2	=	correlation statistic
S_a	=	spectral acceleration
S_d	=	spectral displacement
S_v	=	spectral velocity
SDOF	=	single-degree-of-freedom
T	=	period of vibration
$\underline{T}$	=	index set (time)
t	=	time parameter
Var	=	variance
w_D	=	total area per cycle (in damping force - harmonic displacement diagram)
$X(f)$	=	frequency domain function
$X(t)$	=	random process
$\underline{X(t)}$	=	response function denoting the Duhamel integral
$X(z,t)$	=	displacement of structure at each spanwise point z at time t
$x(t)$	=	generally the position vector of mass m
$\ddot{x}_g(t)$	=	ground acceleration
$\vec{x}_{max}$	=	vector of maximum displacements
$\cap$	=	symbol indicating intersection of two sets
ε	=	symbol indicating "is a subset of" or "belongs to"
ζ	=	viscous damping ratio

μ = mean value

ξ = hysteretic damping coefficient

ρ = amplitude of response

$\underline{\rho}$ = maximum harmonic displacement

ρ_p = peak response amplitude

ρ_{max} = maximum response amplitude at resonance

σ = standard deviation

σ^2 = variance

τ = time parameter

$\vec{\Phi}$ = shape factor vector

Ω = sample space

ω, ω_n = natural circular frequency

$\underline{\omega}$ = observation or outcome

$\bar{\omega}$ = circular frequency of excitation force

ω_D = damped vibration frequency

ABSTRACT

Rusnak, Terrance John. Ph.D., Purdue University, May 1978. Development of an Empirical Relationship for the Prediction of Damping in Steel-Framed Buildings. Major Professors: Dr. C. Douglas Sutton and Dr. James T. P. Yao.

Test data from the forced vibration and ambient experiments on actual structures are used as input to a regression analysis routine to develop equations for the prediction of damping in steel-framed buildings. The data are categorized by building height and the building dimension in the direction parallel to applied forces. This dimension is referred to in the text as building width. A total of 267 regression equations are attempted with various combinations of building height and building width as the independent variables. The best equation is determined by the R^2 statistic which is a measure of the amount of error which can be explained by using the regression equation.

The best equation resulting is used as the basis of a new design methodology for the prediction equation. This methodology is simple and easy to use. It consists of using the developed equation in a situation where a set of conditions are satisfied. These conditions pertain to the

particular characteristics of the structure and the approximated level of excitation which is expected. The methodology is pertinent to free standing, steel moment-resisting frame buildings of regular shape, which are founded on soil of adequate bearing capacity. Characteristics of the input data set dictate these conditions. Further, the methodology is applicable to those locations where the intensity of the excitation force is low enough to keep induced stresses within the linear elastic range. It is anticipated this methodology will be especially useful in the early stages of design.

Included also are sensitivity analyses which indicate the amount of variation in displacement response that can be expected by using the developed prediction equation. This is expressed in terms of the coefficients of variation of the displacement responses determined when the equation is used to predict damping for nine different combinations of building height and width. A second type of sensitivity analysis is also performed. This shows the effectiveness of the developed equation in predicting the mean value of damping in a structure by comparing the displacement response obtained when the predicted damping value was used to that obtained when the highest and/or lowest experimental values were used. The results of both of these analyses indicate that the use of the developed equations results in good, usable predictions of damping values. Both the English

and Metric systems of measurement are used to develop the regression equations.

CHAPTER I

INTRODUCTION

<u>1.1 General Remarks</u>. Damping is similar to the weather in the following sense. Everyone is aware of its existence but very few are able to predict accurately its essence in term of measurable parameters even by using detailed analytical techniques and methods. This analogy is not all-inclusive, however. While weathermen study the patterns and histories of certain meteorological data and develop predictions (estimations) of the weather which are reasonably accurate and relatively reliable, design engineers enjoy no such facility in their attempts at estimating the damping characteristics of buildings.

Engineers, relying upon engineering judgement, are in many instances able to assume a reasonable and useful value for damping. But this assumed value depends upon individual experience which, by virtue of its personal nature, is an intangible entity. These assumed values are determined from estimations and decisions which are subjectively-based and thus their worth is directly related to the extent and amount of experience possessed by the predictor. It is preferable that estimations of damping values be objectively

based so that biased judgements can be reduced and experience relegated to a supporting role.

Herein is developed a new methodology that design engineers can use to determine, with reasonable facility, a value for damping which is determined from certain key parameters that describe the structure under consideration. The crux of this methodology is an empirically-derived equation which is based upon the results of experiments in actual buildings. It is presented as a tool of design that uses certain real and measurable quantities pertinent to the building under consideration as input, and thus, is that objective means for predicting damping which is sought.

1.2 General Philosophies. Recently developed analytical tools play an important role in estimating damping and other dynamic properties of structures. Structural engineers rely almost exclusively on analytical models and numerical methods [1, 2, 11, 12, 13, 14, 21, 25, 27, 28, 29, 31, 32, 34, 36, 41, 42, 50, 51, 53, 65, 68, 73, 75, 77, 80, 82] for the analysis and design of structures because of the advancement in the state-of-the-art of these analytical methods, and the expanding technology of digital computers which has made the analytical approach more cost-effective. With the continuing development of refinements in elements to use with the Finite Element Concept in structural analysis, for example, virtually any structure can be modeled analytically, and the response of the structure to any

given load can be predicted with an acceptable degree of accuracy. Estimation of structural properties is included. Computer programs exist for both static and dynamic analyses; SAP IV [1], which was developed at the University of California at Berkeley, is an example of a general purpose program that is widely used in the dynamic analysis of structural systems. Discussions in more specific detail concerning the state-of-the-art in estimating damping values follows in Chapter II. It is sufficient to state at this point that the bulk of the research in this area has been in the development of analytical procedures and methods, and their refinements.

Foutch [25] points out there is at least one consequence of the structural engineer's reliance on and use of these analytical methods. Experimentation, that is the performance of experiments, suffers. Experimentation, particularly that needed to verify the assumptions made in analytical modeling, has lagged behind the application of these analytical methods in advancing the state-of-the-art.

Experimentation has been taking place in the broad area of dynamic response. Recently the characteristics of actual earthquakes like the San Fernando, California earthquake of February 9, 1971 [3, 47] have been monitored and recorded; these data have then been used as the input excitation for tests that have been made to determine the

dynamic properties of structures. Also, extensive programs have been undertaken to assess and analyze the behavior of virtually every conceivable type of structural component. Beams, columns, frames, panels, even connections as well as other components are suited to experimentation in a laboratory environment; consequently, these members are continually exposed to a variety of testing procedures in order to determine information about response to various loadings. Most of the experimentation performed in search of new or confirming information about structural properties is done on structural components.

Another popular and widely used technique is the testing of physical models. This experimental technique, of course, involves the assembly of small-scale structural components into configurations which represent an actual structure. The response of a model to a test is correlated to the response expected in the actual structure. Recently, testing of planar models of structural systems has been performed on shake tables [66, 86] in order to determine the dynamic properties of the prototype systems. Shaking tables have been developed and used in order to obtain data about dynamic properties of systems exposed to large amplitude motions. It has been determined that the use of other means of testing, like vibration generators, is limited to low amplitude force application which usually keeps the material tested in its elastic range. This will be

discussed shortly in more detail. While it is feasible to develop more powerful generators to vibrate systems into the inelastic, or elasto-plastic ranges to study behavior, the development of shake tables theoretically enables the accomplishment of basically the same objective. A shake table operates on small-scale models. The permanent deformation, or even destruction of these models due to yielding or other inelastic behavior, is not as critical as it would be if vibration generators were used on full-scale structures (or even on larger-scale models) to produce the same results.

A shake table can be used to simulate ground motions of actual earthquakes. The tables are classified as small, medium, or large depending upon the maximum weight capacity of the test structures they can shake. Small tables have a weight capacity of a few thousand pounds; medium tables - a few hundred thousand pounds; and large tables can shake test structures weighing a few million pounds. For more detailed information regarding shake tables and their usage, particularly the medium-scale facility located at the University of California at Berkeley, the reader should refer to the reports by Clough and Tang [19], Clough and Li [17], and Stephen, Bouwkamp, Clough, and Penzien [72].

Experiments on small-scale models, like shake table tests, are important. In the areas of post-yielding

behavior and failures of structures, much of our knowledge today is the direct result of experiments on models. However, it must be remembered that these experiments are usually conducted in a laboratory where the environment, the loading conditions, and the testing apparatus are in a controlled state. Further, these experiments generally do not include the testing of the non-structural elements which contribute significantly to the response of an actual structure. Nor are they able to demonstrate the interaction of a structure with a deformable foundation, which certainly can contribute significantly to the behavior of the structure. What, then, is the means by which the dynamic properties of an actual structure can be determined with confidence? It is, of course, the testing of the actual structure.

Vibration testing of full-scale (actual) structures has been performed in the United States for several decades. In earlier years, vibration tests were dependent upon wind or microseismic waves. While this ambient technique has been used recently [22, 78, 83, 85, 88], the scope of testing is limited since there is no control over the application of the exciting force [25].

Forced vibration generators were developed in the mid-1930's [7] to give this control over the input forces. However, the earlier models proved to be ineffective and unreliable, and consequently they were not used widely in

experiments. A new system of synchronized vibration generators was developed in the early 1960's [38]. These generators have enabled the study of the dynamic properties of a variety of structures: dams, buildings, bridges, towers, reactors, etc. Usually these studies are carried out in conjunction with and with the purpose of verifying analytical studies. However, the results of such experimentation are particularly useful when examined from another viewpoint. This approach is developed herein, and it will become apparent to the reader the role these test results play.

The nature of vibration generators, their usage, associated instrumentation, and discussion of the obtainable output will be presented in Chapter II. It is sufficient to note here that the generators in use today are essentially improved versions of those developed in the early 1960's [39]. Refinements and improvements such as those reported by Hudson [39] and Foutch [25] may be viewed as a natural outgrowth of evolving technology in the area. Dynamic testing of full-scale structures, however, will continue to be hampered by limitations in implementation, regardless of these "modernizations." One limitation inherent in the very nature of full-scale structure testing is that tests to destruction are simply not feasible. The reasons for this are obvious [39]. Nevertheless, full-scale testing is necessarily conducted, at least at the

level of the current state-of-the-art, within the linearly elastic range of the tested material. While this hampers studies of certain properties, it is sufficient for the purpose of this work, as will be outlined shortly.

Schiff [69] discusses other, more subtle limitations in the testing of full-scale structures. He contends that since large structures are unique, and it is a one-time operation for the owner, the incentive to test after completion of construction is lacking. Once a building is occupied, testing is disruptive to normal operations even if low amplitude forced excitations or ambient tests are used. Thus, there are few incentives to perform tests on full-scale structures, and this adds to the limitations inherent in such tests. Also, testing during construction of a building has similar difficulties. Strictly from a practical point of view, Schiff notes that even if the owner is willing to have tests run on his partially completed structure, the general contractor is responsible during construction, and unless provision is made in the contract documents, permission to test is often not obtainable. Further, depending upon the purpose of the experiment, testing of partially completed structures is done randomly, and results of such tests are peculiar to the time they are performed. Experimental data which result, then, necessarily reflect the status of construction completion which could be misleading information. In the search for

damping values undertaken in this project, this phenomenon was encountered [65].

In spite of the difficulties/limitations which exist in the conduct of full-scale structure testing, many such tests have been performed. Dynamic properties of prototype structures have been obtained as a result of these experiments. One of these properties, damping, is of particular interest.

1.3 Objective and Scope. Data have been collected from full-scale structure testing of steel moment-resistant frames of various heights, widths, and configurations. Damping is the principal property of concern herein, so experimentally-determined damping values have been compiled in tabular form for ease of reference and usability. The regression analysis technique from the Statistical Program for the Social Sciences (SPSS) [58] was used to establish a correlation between the viscous damping ratio, ζ, and the two building dimensions of height and width. (It should be noted that building width, D, is consistently used herein as the dimension of the building in a direction parallel to the applied forces.)

To summarize, the objectives of this research are: to compile data and subsequently tabulate it into useful form; to develop a correlation between the viscous damping ratio and the chosen building parameters by means of

statistical analyses of the assembled experimental data; and to develop a design methodology based upon this correlation.

A brief summary of the contents of subsequent chapters follows:

Chapter II contains information pertinent to the collection of the data. It has descriptions of the vibration generators and their use, and of ambient testing procedures. Further, it includes discussions on the various methods used to determine damping from the results of these experiments; and sections devoted to an explanation of Earthquake Response Spectra, and the use and purpose of moment-resistant frames. Numerical methods, analytical models, and a brief outline of the state-of-the-art in estimating damping is also discussed.

The development of the correlation between the viscous damping ratio and the chosen building parameters is presented in Chapter III. As it will be shown, these parameters are the building height and the building width in the direction considered. The regression technique which was used to develop this correlation is explained. Additionally, sensitivity testing and reliability assessment are presented to demonstrate the usability of the established correlations.

In Chapter IV the methodology is presented. This methodology is based upon the correlation developed in Chapter III. Included is a discussion of the information

which is needed by the design engineer in order to use the methodology.

Conclusions are presented in Chapter V. Sections are devoted to the value of the design methodology in practical applications, its limitations and potential areas of future application. A discussion is also included giving views and recommendations on the nature of reporting experimental results, and the directions future refinements of this methodology should take.

Four appendices also are presented to further develop or present in more detail incidental information which is used in the development of the methodology, but which is not an integral part of this development. Appendix A contains descriptions of the buildings used in the input data set. Appendix B contains a list of the regression equations for the predictions of the damping ratio. Appendix C contains the development of a spectral displacement versus viscous damping ratio relationship needed for the sensitivity analysis in Chapter III. Appendix D contains the development of the prediction equation in the Metric system corresponding to the development contained in Chapter III.

CHAPTER II

EQUIPMENT, PROCEDURES AND METHODS FOR DAMPING ESTIMATION

2.1 General Remarks. In this chapter, the means (including the equipment, the procedures, and the methods) in use today to estimate the damping parameter ζ (taken as the viscous damping ratio) are reviewed and discussed. The emphasis herein is on the explanation of those means which are pertinent to the development of the proposed methodology, such as the forced vibration generator, and ambient tests. Consequently, only those methods utilized to determine this viscous damping ratio from experimental results - such as the bandwidth and log decrement methods - are discussed in detail.

As a means of eventual comparison, and in order to give coverage to the entire field of damping estimation, an overview of the analytical models and numerical methods in use is also presented. Finally, it is believed these detailed discussions and descriptions would be incomplete without a thorough presentation of the principles inherent in the earthquake response spectra, and in steel moment-resisting frames.

<u>2.2 Testing of Actual Buildings</u>. There are two types of tests of concern here, namely the forced vibration generator test and the ambient test. Both of these experimental methods will be discussed in detail in this section. It is to be noted that all data used in the development of the proposed methodology are taken from the available results of these two types of test [9, 10, 11, 12, 25, 30, 43, 44, 45, 55, 59, 60, 62, 65, 73, 83, 84, 85, 86, 88].

These results of forced vibration and ambient tests are compatible because the equipment, procedures and methods used in each of these experiments are basically similar. Results from forced vibration tests will be compatible to and in close agreement with the results from ambient experiments if conditions in the ambient tests are as reported by Ward and Crawford [88]. These conditions relate to the use of the bandwidth method, or other appropriate methods of calculating damping when the wind or microtremor excitations are random and nearly stationary with respect to time.

A random (or stochastic) process is a family of random variables, indexed by an index set which in this case is a time parameter. Symbolically, a random process is represented by:

$$X(t) \equiv \{X(t);\ t\varepsilon \underline{T}\} \tag{2-1}$$

It is implied in this symbolic representation that a

random process is really a function of two arguments, or:

$$X(t) \equiv \{X(t, \underline{\omega});\ t\varepsilon\underline{T},\ \underline{\omega}\varepsilon\Omega\} \tag{2-2}$$

where $\underline{\omega}$ denotes an observation or outcome in the sample space Ω. "Stationary" is a term describing characteristics of random processes relating to the satisfaction of conditions which indicate certain properties to be invariant with time. To illustrate, for a real-valued random process, $X(t)$, with a specific value of t, say t_1, the first-order distribution is:

$$F_{X(t_1)}(x) \equiv P(X(t_1) \leq x) \tag{2-3}$$

where this distribution function, $F_{X(t_1)}(x)$ is finite, *nondecreasing, and continuous* from the right. In words, it is defined as the probability that the random process is less than or equal to the value of x. When the random variable is continuous, it has an associated density function which is defined as its derivative with respect to the variable x; or:

$$f_{X(t_1)}(x) = \frac{\partial}{\partial x} F_{X(t_1)}(x) \tag{2-4}$$

Higher order joint distribution functions relating to multiple time instances, and their associated density functions also exist. For example, the second-order distribution of a random process for two values of t—t_1 and t_2—is:

$$F_{X(t_1)X(t_2)}(x_1,x_2) \equiv P(X(t_1) \leq x_1 \cap X(t_2) \leq x_2) \quad (2\text{-}5)$$

Its corresponding density function is given by:

$$f_{X(t_1)X(t_2)}(x_1,x_2) = \frac{\partial^2}{\partial x_1 \partial x_2} F_{X(t_1)X(t_2)}(x_1,x_2) \quad (2\text{-}6)$$

In order for a random process X(t) to be stationary, then, for all integer values of n:

$$f_{X(t_1)}(x_1) = f_{X(t_1+a)}(x_1)$$

$$f_{X(t_1)X(t_2)}(x_1,x_2) = f_{X(t_1+a)X(t_2+a)}(x_1,x_2) \quad (2\text{-}7)$$

$$\vdots$$

$$f_{X(t_1)X(t_2)\ldots X(t_n)}(x_1,x_2,\ldots x_n) =$$

$$= f_{X(t_1+a)X(t_2+a)\ldots X(t_n+a)}(x_1,x_2,\ldots x_n)$$

This shows the invariance of the density function with respect to time. A process is said to be weakly stationary, or stationary in the wide sense if just the first two orders display this invariance [89].

In ambient experiments performed on steel structures in conjunction with forced vibration tests, such as those reported by Petrovski, Stephen, Gartenbaum, and Bouwkamp [62], Stephen, Hollings, and Bouwkamp [73], and Trifunac [84, 85], difficulties were encountered which tended to invalidate a portion or all of the estimations for damping. The authors [62] felt their study satisfied the stationary

random process criterion and obtained comparable values of damping for the first two modes. In the higher modes, damping estimations were found to be very low, which indicated the possibility of insufficient density of the recorded data. Stephen, Hollings, and Bouwkamp [73] found the damping values for the fundamental mode to be very large. The authors concluded that the length of the time-series used was inadequate. Trifunac [84, 85] found only a few instances where the stationary random process criterion was satisfied. However, he found that even when this criterion was satisfied his estimates of damping appeared to be very large because of spectral overlap due to the proximity of corresponding frequencies in North-South, East-West, and torsional modes. Later, in another ambient test, Trifunac [83] obtained good results of damping estimations by rectifying the problems he had previously encountered. He not only was able to satisfy the stationary random process criterion, but also was effective in separating the translational and torsional vibrations by optimum location of seismometers.

Because of the success in obtaining damping values from ambient tests which compare favorably with those estimations from forced vibration tests, all data considered valid by the respective authors are included in the basic data set used in this research. There is no attempt to expound the relative merits of forced vibration and

ambient tests. For the purposes of this comparison, the paper by Trifunac [84] is suggested. Because results from both types of experimentation are included herein, a description of the nature and characteristics of each test is presented.

2.2.1 Experimental Apparatus. The equipment used in forced vibration and ambient tests is described herein. This hardware includes the vibration generators and the instrumentation used to monitor response and record data.

2.2.1.1 Vibration Generators. As stated in Chapter I, forced vibration generators have been in use for several decades. However, the generation equipment in its present configuration was developed only recently. In 1958, the California State Division of Architecture, through the Earthquake Engineering Research Institute, arranged for its design and construction which eventually was completed in the early 1960's. Some of the general design criteria which became the basis of the major characteristics of the system are [38]:

1. The requirement for an inertia force generation system.

2. The requirement for small units which can be used individually or in sychronized groups.

3. The requirement to excite various modes of vibration independently; thus the need for distributing the

applied force throughout a structure by using several sychronized units.

4. The requirement for accurate speed control and sychronization of multiple units. (This led to the use of rotating eccentric weights.)

5. The requirement for a unidirectional horizontal exciting force. (This led to the adoption of a counter-rotating eccentric weight system.)

6. The requirement that extraneous vertical forces not be introduced.

The vibration generator system which was developed to satisfy these criteria has the following essential features [38]:

1. Accurate control of the exciting frequency

2. Stable operation at low levels of damping

3. Capability to distribute an exciting force throughout a structure.

The eccentric-weight vibration generator in its completed form is shown in Fig. 2.1. This machine essentially consists of an electric motor driving two pie-shaped baskets or rotors, each of which produces a centrifugal force as a result of the rotation. These baskets are mounted on a common vertical shaft and are rotated in opposite directions to produce a sinusoidal rectilinear force from the resultant of their two centrifugal forces.

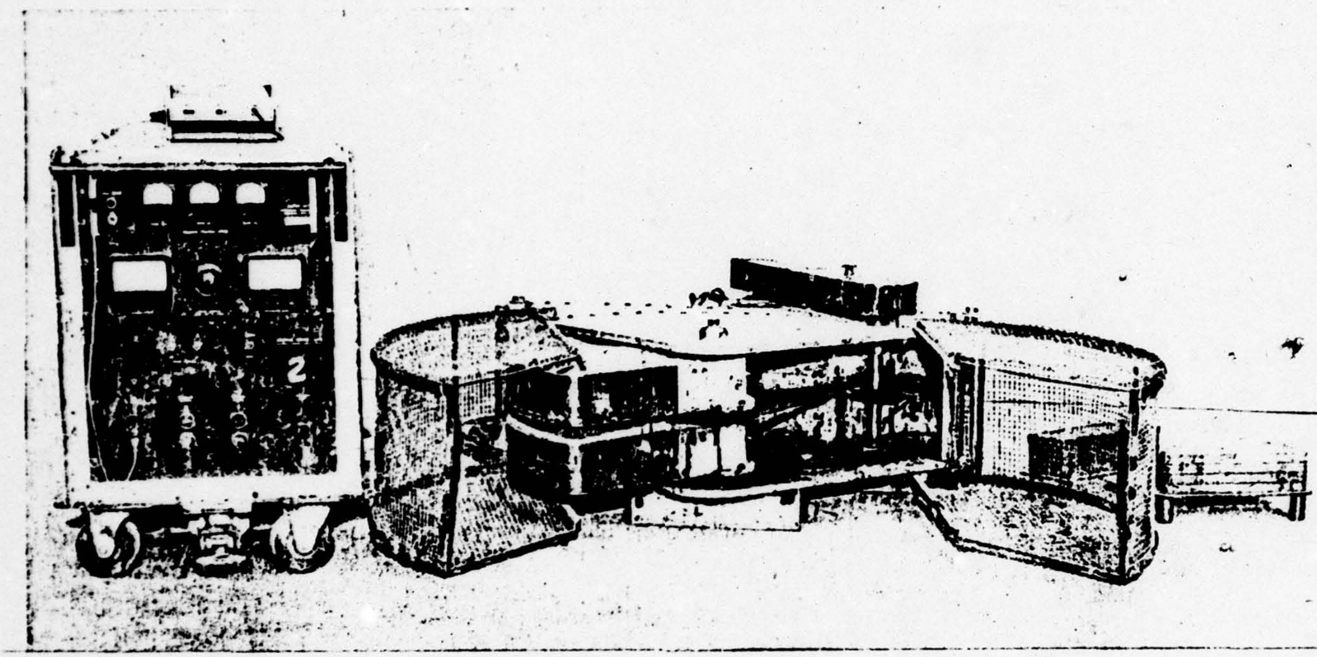

FIGURE 2.1

VIBRATION GENERATOR

A peak value of this sinusoidal force is exerted when the baskets are aligned.

The maximum force output for one such vibration generator is 5000 pounds, the limit due to the structural design of the machine. This maximum force can be attained by varying the eccentric mass and rotating speed. Several combinations exist. This is true because the output force is proportional to the square of the rotational speed as well as to the mass of the baskets and the lead weights which can be inserted into the baskets. When all the lead plates are in the basket, the maximum force of 5000 lb can be exerted at a speed of 2.5 Hz. At higher speeds, the eccentric mass must be reduced by varying the number of lead weights in the basket in order to keep from exceeding the maximum 5000 lb force output. The practical range of operation for a machine is between 0.5 Hz and 10 Hz. At 0.5 Hz, with all the lead weights in the baskets, a force of 200 lb can be generated. Graphs displaying the relationship between output force and frequency of rotation for different basket loads have been developed [62, 73].

Hudson [38] notes that with a noncounterbalanced basket assembly eccentricity variations from 455 in-lb to 7888 in-lb can be developed using standard lead weight combinations. Thus, approximate horizontal inertia forces of from 50 lb to 800 lb, respectively, at 1 Hz, can be produced.

Speed control is a critical variable in the measurement of damping from resonant curves. Prior to the development of these machines, earlier techniques involved the use of a run-down procedure to obtain resonant curves. This, essentially, requires the excitation of a structure at a speed greater than the maximum frequency desired and disconnecting the vibrating apparatus thus permitting the system to decelerate slowly through resonance. Theoretically, the steady-state resonance curve can be derived from the deceleration vs time curve. In practice, however, this procedure led to inaccurate estimates of damping because the speed changes, which could not be controlled, were not slow enough to allow the structural amplitudes to reach steady-state values. Consequently, damping estimates thus obtained are much higher than actual values [38, 59].

The speed control adapted for these machines is an Electronic Amplidyne unit. The eccentric weight drive motor is a 1.5 hp D.C. motor driven from this electronically controlled rotating magnetic amplifier unit. The speed of the drive motor corresponds to a setting of the reference voltage control that constitutes the frequency adjustment on the control unit. This correspondence is accomplished by means of a closed loop control system. For a much more thorough description of the details of the components of

vibration generators the reports by Hudson [37, 38, 40] are recommended.

Another characteristic of these vibration generators which should be mentioned here is the synchronized operation. The control unit allows multiple machines to be operated in synchronization, or 180° out of phase. This allows the distribution of the exciting force throughout a structure in such a way that the various modes of vibration can be excited independently. Also, in structures with a line of symmetry, it enables either pure torsional or pure translational vibrations to be excited without changing the position of the machines. This synchronization of multiple units is obtained by means of speed control, accomplished through the master control unit, and position control, accomplished through selsyn units. For a more detailed description and discussion see the Hudson reports [37, 38, 40].

A recent state-of-the-art paper concerned with vibration generating equipment has been authored by Hudson [39]. While he states that these synchronized vibration generators which were developed in the early 1960's continue to be the main "workhorses" in testing full-scale structures, he introduces new systems, and suggests that the development of the vibration generator was instrumental in developing interest in the testing of full-scale structures.

2.2.1.2 Other Instrumentation. This section is devoted to the description of the other instrumentation which was used on the forced vibration generator tests. These include a linear displacement control vibration system, accelerometers, equipment for measurement of frequency, equipment for measurement of phase angles, and recording equipment.

Linear Displacement Control Vibration System. Since the rotating mass vibration generators are difficult to operate at frequencies lower than 0.5 Hz, this system was developed to determine the lower resonant frequencies. The system consists of a mass supporting platform with low friction rollers attached. These rollers are set on round steel bars which are affixed to the floor. The platform is moved horizontally by means of a closed loop servocontrolled double-acting actuator connected to the floor. A standard servo-control console and function generator supply the input to a 5 gpm servo-valve with the feedback in the displacement coming from a linear potentiometer. This system was used by Stephen, Hollings and Bouwkamp in their test of the Transamerica Building in San Francisco [73].

Accelerometers. Transducers were used to detect horizontal floor accelerations. Statham Model A4 linear accelerometers with a maximum rating of ± 0.25 g seemed to be a popular choice. Foutch [25] used these with a Brush carrier preamplifier. He also used Ranger seismometers to

determine the relative motion between two points. Nielsen's system [60] consisted of Statham strain gage accelerometers of ± 2 g and 100 Hz natural frequency. He amplified the signals with both Brush carrier amplifiers, and dual channel Sanborn carrier recorders. Rea, Bouwkamp and Clough [65] initially used the Statham ± 1 g accelerometers, but had to use the ± 0.25 g accelerometers for subsequent tests because of smaller vibration amplitudes.

Equipment for Measurement of Frequency. The vibration excitation frequencies were determined by measuring the speed of rotation of the electric motor driving the baskets. This was accomplished by attaching a tachometer to a rotating shaft driven by a transmission belt from the motor. The tachometer generated a sinusoidal signal with a frequency 300 times the frequency of rotation of the baskets. The maximum accuracy was, therefore, ± 1 count in the total number of counts in a period of one second (the gating period), i.e., $\pm \frac{1}{3}$ of 1% at 1 Hz and $\pm \frac{1}{9}$ of 1% at 3 Hz. This information is a standard description of the equipment used for this purpose in vibrating generator tests. For the linear displacement control vibration system, the excitation frequencies were preset on a frequency generator and could be incrementally set to within 0.001 Hz.

Equipment for Measurement of Phase Angles. In order to obtain a signal indicating the basket position, which

determined the phase relationship between the excitation and response, a small magnet was attached to a basket and a coil of wire to the supporting structure. The coil was affixed so the magnet's circular path passed close by, thus at each passing an electrical pulse was generated and subsequently recorded on the oscillograph. The pulse signal could be generated for any desired basket location by proper position of the magnet [65].

Recording Equipment. The electrical signals generated by the instrumentation were fed to amplifiers and then to recording equipment. Two types of oscillographic recorders were discussed in the literature - the Honeywell Visicorder with 6 inch wide chart, and the Honeywell Model 1858 Graphic Data Acquisition System with 8 inch wide chart. The digital counter reading was observed and recorded manually on the chart alongside the associated traces for the frequency-response tests. The equipment used by other researchers, such as Jennings, Matthiesen and Hoerner [43, 44] was similar.

2.2.1.3 Instrumentation for Ambient Tests. Since by their nature ambient tests of multistory buildings use natural wind to induce vibrations, the equipment is not exceptionally elaborate, although sensitive measuring devices have to be used because the input forces are small.

Seismometers. The measuring devices used to record the wind-induced vibrations of the buildings were

seismometers. There are, of course, many makes and models of seismometers. Only those used in the tests from which data was compiled for this project will be discussed in further detail.

Kinemetrics Range Seismometers, Model SS-1, have been used to measure the wind-induced vibrations [62, 73]. This seismometer has a strong permanent magnet as the seismic inertial mass, moving within a stationary coil attached to the seismometer case. Small rod magnets at the periphery of the coil produce a reversed field which provides a destabilizing force to extend the natural period of the mass and its suspension. The seismometer natural frequency and damping ratio were 1 Hz and 0.7 respectively. It has a constant voltage output for a given velocity at all frequencies greater than 1 Hz; at lower frequencies it falls off at 12 dB/octave.

Trifunac used Earth Sciences Ranger Seismometers [83] and similar Teledyne Ranger Seismometers [83] in his work. These are similar in construction to the devices used by Petrovski, Stephen, Gartenbaum, and Bouwkamp [62], and Stephen, Hollings, and Bouwkamp [73] described above. The period for these devices is close to 1 second, with damping also set at 0.7 of critical. At frequencies lower than 1 Hz, the falloff is 6 dB/octave. Trifunac notes that this may be advantageous in recording vibrations of structures with a fundamental period of 2 seconds, or longer, since the low

frequency modes do not dominate in the records thus facilitating the study of the higher modes.

Ward and Crawford [88] used Willmove Mark II Seismometers to record building vibrations. These operate on basically the same principle as the others. The seismometer can be oriented in either the horizontal or vertical direction and the natural period of the suspension can be adjusted to values in the range 0.6 to 5.0 sec. For the tests reported the natural period was chosen so that the fundamental mode of vibration would not predominate at the expense of the higher modes; damping was 0.65 of critical.

Other instrumentation. Two other categorized items of equipment are needed in order to convert the data to a form which is appropriate for analysis. These are a signal conditioner and a magnetic tape recorder. Again, a variety of models are available and depending upon one's own prejudices, allegiances or even more tangible circumstances like economic status and testing environment, a selection can be made. What is needed, though, is a means of amplifying and controlling the seismometer signals and a means of recording them. The relative merits of those used on pertinent tests can be found in the references [62, 73, 83, 85, 88].

2.2.2 Experimental Procedure. One will note in reading this section the differences between the two types

of tests - forced vibration generator and ambient. There are, of course, advantages and disadvantages associated with each type of test. It is not a purpose here to state or analyze the relative merits of the two methods. Because data was collected and used in this project from both methods, each type of test is described and discussed separately.

2.2.2.1 Forced Vibration Testing. The procedure inherent in forced vibration testing includes placement of equipment and instrumentation, precision control of these devices at and near resonance, and proper recording and interpretation of the data. The forced-vibration test will normally yield the resonant frequencies, mode shapes, and damping capacities of a structure. The number of vibration exciters to be used individually or in synchronization depends on the purpose of the experiment and the characteristics of the structure to be tested. A single generator suffices for low rise buildings. Two generators appear to be satisfactory for most multi-story structures above about ten to fifteen stories. For example, Nielsen [60] in his test of a nine-story building used one generator, while Rea, Bouwkamp, and Clough [65] used two generators in their study of a 15-story steel framed structure. Other experiments tend to support this somewhat arbitrary dividing line.

To estimate damping, the resonant frequencies must be determined. The vibration generators must be located to create a force output to excite the building modes required for study. It has been found that these generators cannot be located near nodal points of those modes for which data is required. Also, location of the generators must be considered in eliminating modal interference. Modal interference occurs when two modes of vibration are close to each other in the frequency domain. It can be eliminated by locating the generators at or near a node of the unwanted mode.

Once a location is selected, resonant frequencies of each of the modes are determined by sweeping the frequency range of the vibration generator. This frequency is increased slowly until acceleration traces on the recording chart are large enough for measurement. Above this level the frequency is increased until the upper speed limit of the machine is reached. Care is exercised to insure that the 5000 lb force limitation per machine is not exceeded by altering the weights in the baskets. The frequency is increased in steps. At each value, the vibration response is given enough time to become steady-state before acceleration traces are recorded. These frequency-interval steps are small near resonance (where the slope of the frequency-response curve is great), and larger elsewhere.

Where the linear displacement vibration system was used [73] the input displacement signal was maintained at the maximum allowable displacement of the system. Steady-state vibrations were induced for incrementally increased frequencies and the building response was recorded. Frequency-intervals of as low as 0.001 Hz were used near resonance.

The frequency-response curves are plotted from the recorded data. These curves, in the form of acceleration amplitude vs. frequency, are for a force which increases with the square of the exciting frequency. Since linear stiffness and damping is assumed, a normalized curve equivalent to that for a constant force can be obtained by dividing each acceleration amplitude by the corresponding square of its exciting frequency. Damping ratios can then be determined from these normalized curves.

2.2.2.2 Ambient Testing. An assumption inherent in measuring ambient building vibrations is that the actual structural behavior can be approximated by a linear one-dimensional system. This assumption simplified the measurement of the mode shapes. The first step usually taken is the calibration of the seismometers. This is accomplished by locating all seismometers together, and in the same orientation while taking measurements. This measurement provides a relative amplitude and phase

calibration between channels which includes the entire data collection/recording system.

After calibration, and for each subsequent run (a run consists of the time during which measurements are taken while the sensing devices are in a particular location), the seismometers are relocated for simultaneous measurements of motion over the height of the building. Since the frequencies of concern are in the low range, a low-pass filter is usually used to eliminate unwanted noise.

Recalling the basic assumption in the analysis regarding a reasonably flat frequency spectrum for the input forces, it follows that the identification of the modal frequencies would be difficult. It is, therefore, convenient to use Fourier transforms to analyze these low level vibrations. The result of these calculations is the Fourier amplitude spectrum (or power spectrum) which is a plot of the standard frequency domain function vs. frequency. The model frequencies of the structure appear as peaks in these plots. A discussion of Fourier transforms is in order.

A measured time-series signal X(t) can be transformed to the frequency domain by using:

$$X(f) = \frac{1}{2\pi} \int_{-\infty}^{\infty} x(t)e^{-i\omega t}dt = \frac{1}{2\pi} \int_{-\infty}^{\infty} x(t)e^{-i2\pi ft}dt \qquad (2\text{-}8)$$

where: X(f) represents the frequency domain function, $\omega = 2\pi f$ ($f \equiv$ frequency) and $i = \sqrt{-1}$. This equation is called

the direct transform. There is an inverse transform which is:

$$x(t) = \int_{0}^{\infty} X(f)e^{i2\pi ft}df \qquad (2\text{-}9)$$

Together the two equations are called a Fourier Transform Pair since the direct transform maps a time-series (or time domain) into a frequency-series (or frequency domain), and its corresponding inverse transform reverses the process [62, 73, 89]. Note that X(f) is a complex number with both amplitude and phase. The magnitude (or absolute value) of this variable, $|X(f)|$ is known as the amplitude spectrum of x(t), and $|X(f)|^2$ is the power spectrum of f(t). Thus, these recordings from the seismometers are input to the Fourier transform as a set of time-series. Each time-series function is transformed to the frequency domain and after all calculations are made, a standard Fourier amplitude spectrum results. The output is smoothed by $\frac{1}{4}$, $\frac{1}{2}$ and $\frac{1}{4}$ weights as:

$$|X_i(f)|_{sm} = \frac{1}{4}|X_{i-1}(f)| + \frac{1}{2}|X_i(f)| + \frac{1}{4}|X_{i+1}(f)| \qquad (2\text{-}10)$$

Damping can be estimated from the resulting amplitude spectrum, or power spectrum.

<u>2.3 Methods of Determining Damping from Test Results.</u> In 1967 it was reported that definitions of damping varied so widely that conclusions about this property were difficult to correlate [61]. It was further concluded that the best

way to determine damping of various types of structural elements and assemblages composed of all types of structural materials is by experimentation. The same thinking continues to exist. Researchers such as those referenced in this dissertation continue to ponder the questions of damping definitions, mechanisms, and actual values.

Damping, as is most generally and universally accepted, is simply an energy dissipation property of a material or system which is under stress. However, damping is not a simple property, and thus its estimation, particularly through numerical or analytical techniques, is a complex and thought-provoking process. The estimation of this complex property is dependent upon the circumstances surrounding its existence. Thus, in order to understand the nature of this property being measured, these circumstances must be stipulated. For the purposes of this research, damping will be determined from tests of actual structures excited by vibration generators or the wind. Since these tests do not produce forces which excite a structure beyond the linearly elastic range, the problem of defining the type of damping which is measured in these tests becomes relatively easier.

Even in the linearly elastic range, damping can result from the energy dissipation within a material (material damping), and/or from the energy dissipation due to the interaction among the various parts or components of

a structure (system or structural damping). In the measurement of damping from test results, total damping is obtained. Total damping includes material and structural damping, and there is no further attempt to subdivide the estimated values into these components. This is acceptable for the purposes of this study because the estimation of damping for a structure is of primary concern without regard for a breakdown into the various components which comprise this value.

Since we are concerned with the linearly elastic range, the most widely used and practically useful model for damping forces on structures is the ideal linear viscous damper [35] as shown in Fig. 2.2. This damper can be expressed as follows [6]:

$$F_d = c\frac{\partial X(z,t)}{\partial t} = c\dot{X}(z,t) \qquad (2\text{-}11)$$

which shows damping as a function of velocity. In the methods which follow, an assumption inherent in their use

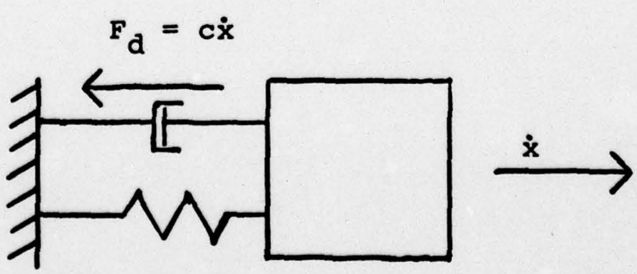

FIGURE 2.2

IDEAL LINEAR VISCOUS DAMPER

is the existence of the ideal viscous damper. When measuring damping values from tests which produce responses only in the linear elastic range, this assumption is well founded. Further, others have stated that so long as the damping remains small (less than 10% of critical) the concept of viscous damping can be used [60]. Outside this range, either another method must be used, or an equivalent damping factor must be calculated. An equivalent damping factor, referred to as the equivalent viscous damping of a system is defined in terms of a viscous damper which expends energy per cycle at the same rate as the actual dissipation mechanism. This is a practical approach and in most cases the approximation simplifies the analysis and yields relatively accurate results. In the cases pertinent to this research, the concept of viscous damping is applicable because of the underlying assumptions. Detailed discussions of the various types of damping and the use of equivalent damping are available in the literature [31, 32, 34, 35, 36, 48, 49, 50, 54, 63, 64, 67, 80, 82] and thus, further elaboration will not be made here.

All techniques for estimating damping from test results are based on the same idea. Reponse of a structure is a function of its physical properties, including damping, and of excitation. If a known excitation is applied, the response can be predicted as a function of damping, which can be inferred by matching predicted and measured response.

2.3.1 Bandwidth Method. This technique, also known as the half-power method, is applicable to the displacement resonant curve of a linear, single degree-of-freedom system (SDOF) with a small amount of viscous damping. It is a particularly effective technique when the value of damping, ζ, is less than 10%. At extremely low values, however, some difficulties may be encountered if there is a problem identifying points on the resonance curve. Furthermore, since this technique relies upon the measurement of the frequency difference at points around the resonant frequency, measurement of this difference is often difficult at small values of damping.

Essentially, this method of calculating damping is derived from the equation of motion for an elastic SDOF structure that responds to a harmonically varying load p(t) of amplitude p_o and circular frequency $\bar{\omega}$:

$$m\ddot{x}(t) + c\dot{x}(t) + kx(t) = p_o \sin \bar{\omega}t \qquad (2\text{-}12)$$

where the symbols are standard representations of structural properties found in any dynamics text. Eqn. 2-12 can also be written as:

$$\ddot{x}(t) + 2\zeta\omega\dot{x}(t) + \omega^2 x(t) = \frac{p_o}{m} \sin \bar{\omega}t \qquad (2\text{-}13)$$

In the development of the solution of this equation, one can derive the expression for the amplitude of the steady-state response as:

$$\rho = \frac{P_o}{k} \{[1 - (\frac{\bar{\omega}}{\omega})^2]^2 + 4\zeta^2 (\frac{\bar{\omega}}{\omega})^2\}^{-1/2} \qquad (2\text{-}14)$$

The response is thus a function of frequency, and when the exciting frequency, $\bar{\omega}$, approximately equals the natural frequency, ω, the system is in resonance, and a large amplitude response can result. It is obvious from Eqn. 2-14 that only a value for damping, ζ, keeps the resonant amplitude from approaching infinite bounds. For a damped system, the peak response occurs when the slope of the frequency-response curve is zero, and thus it can be found by setting the derivative with respect to $\bar{\omega}$ equal to zero. It will then be found that ρ_p, the peak response, occurs at:

$$\bar{\omega}/\omega_n = (1 - 2\zeta^2)^{1/2} \qquad (2\text{-}15)$$

Thus, the peak response is:

$$\frac{\rho_p k}{P_o} = \frac{1}{2\zeta(1-\zeta^2)^{1/2}} \qquad (2\text{-}16)$$

The bandwidth of the response, $\Delta\omega$, is defined as the difference between the two frequency responses corresponding to $1/\sqrt{2}$ times the peak amplitude. The two excitation frequencies, $\bar{\omega}_1$ and $\bar{\omega}_2$, which produce these half-power points can be found from Eqns. 2-14 and 2-16. For detailed development the references [6, 18, 63] should be studied. Utilizing these equations, which are in terms of $\bar{\omega}_1$, $\bar{\omega}_2$, ω_n, and ζ, a relationship giving the bandwidth can be

obtained, i.e.:

$$\Delta\omega = \bar{\omega}_2 - \bar{\omega}_1 = 2\zeta\omega_n \tag{2-17}$$

Thus, the damping factor can be approximated as:

$$\zeta = \frac{1}{2} \frac{\Delta\omega}{\omega_n} \tag{2-18}$$

In order to measure damping from a resonant curve, only the resonant frequency and the bandwidth need to be known. These factors are inherent in the frequency-response plots which result from forced vibration generator experiments. The values of damping obtained using this method in conjunction with these experiments are considered valid even though there is some variance from the basic assumptions underlying its development and disadvantages in its use [6, 12, 18, 65, 69, 73].

2.3.2 Logarithmic Decrement Method. This might be possibly the simplest and most frequently used experimental method. As its alternative titles may indicate, the Free-Vibration Decay Method or Time-Response Method, it is based upon the measurement of amplitudes during free vibrations. In such tests, this can be accomplished by turning the vibration generators off after reaching a steady-state situation.

For lightly damped systems, this technique is appropriate because the vibrations do not damp out too quickly once a free vibration state has been established. Greater

accuracy can be obtained by measuring response peaks on a plot of displacement vs. time graph several cycles apart. The development of the logarithmic decrement method begins with the expression for the response of an underdamped system in free vibration in rotating-vector form [18]:

$$x(t) = \rho e^{-\zeta\omega t}(\cos \omega_D t - \theta) \qquad (2\text{-}19)$$

Considering the ratio of two positive peaks, m cycles apart and taking the natural logarithm of both sides of the equation:

$$\ln\left(\frac{x_n}{x_{n+m}}\right) = 2\underline{m}\pi\zeta \frac{\omega}{\omega_D} \qquad (2\text{-}20)$$

or, for lightly damped structures [6, 18]:

$$\zeta = \frac{1}{2\pi\underline{m}} \ln\left(\frac{x_n}{x_{n+\underline{m}}}\right) \qquad (2\text{-}21)$$

This technique is widely used because it is relatively simple. Once a structure has been set in motion, and the exciting force removed, it is possible with only a small amount of equipment to show the amplitude dependence of the damping factor. Some of the difficulties inherent in the method, on the other hand, limit its use to the determination of damping for the fundamental mode in a system with well separated natural frequencies.

2.3.3 Other Methods. This section is devoted to a brief description of other means used to calculate damping

values which are used herein. One of these, termed the 90° out-of-phase method, is a variation of the bandwidth method. Essentially, when modal interference is present the bandwidth or other common methods are not suitable for calculating damping. However, a modification to the bandwidth method can be used if the recorded phase of the force with respect to the response allows the response to be separated into its in-phase and 90° out-of-phase components. When the 90° out-of-phase acceleration is plotted vs. frequency, the frequency-response curve becomes more defined and sharper, thus allowing the damping values to be more readily determined. The procedure for calculating damping is basically the same as the bandwidth (or half power) method as described above, except that 1/2 the peak amplitude is used to determine the bandwidth instead of $1/\sqrt{2}$. The rationale behind such a technique takes advantage of the fact that when considering modal interference, the response of modes lower than the one considered is almost entirely in-phase with the excitation, while higher modes are 180° out-of-phase. Thus if the 90° out-of-phase component can be determined, modal interference is greatly reduced. A thorough description and development of this technique is available elsewhere [25, 43, 44].

Another method used is a multi-degree-of-freedom (MDOF) to the SDOF system-based dynamics magnification factor. Referring back to the expression for the amplitude of the

steady-state response as given in Eqn. 2-14, a dynamic magnification factor, $\underline{D}$, is defined as:

$$\underline{D} \equiv \frac{\rho}{p_o/k} = \{[1 - (\frac{\bar{\omega}}{\omega_n})^2]^2 + 4\zeta^2(\frac{\bar{\omega}}{\omega_n})^2\}^{-1/2} \quad (2\text{-}22)$$

It is noted that $\underline{D}$ varies with the damping ratio, ζ, and the frequency ratio, $\frac{\bar{\omega}}{\omega_n}$. At resonance, the exciting force frequency, $\bar{\omega}$, equals the response natural frequency, ω_n, or:

$$\underline{D} = \frac{1}{2\zeta} \quad (2\text{-}23)$$

Thus, damping can be determined by:

$$\zeta = \frac{1}{2\underline{D}} = \frac{1}{2}\frac{p_o}{k\rho_{max}} \quad (2\text{-}24)$$

where ρ_{max} is the maximum response amplitude at resonance. This method is appropriate for determining damping of closely spaced modes. More details on this method can be found in [6, 18, 60, 63].

Two other methods of calculating damping were used, and should be briefly explained. One is essentially the bandwidth method, but instead of using one of the measured structural response parameters in the frequency-response curve, the Fourier spectrum, or power spectrum is used. The other method is based on the decay of the autocorrelation function. Autocorrelation diagrams are calculated from raw data through the use of electronic digitizers. The

effective damping of the structure can be estimated by measuring peaks of successive cycles of the autocorrelation function and using calculations similar to the logarithmic decrement method [77, 88].

2.4 Earthquake Response Spectra. This is a brief introduction to the concept of earthquake response spectra and their use in determining the response of structures to earthquake excitations. A more detailed explanation and discussion appears in Appendix C.

Essentially, the earthquake response spectrum is a plot of the maximum value of a response function vs. natural period (or natural frequency). The maximum value of one type response function is the spectral velocity (or more accurately, the pseudo-velocity because it is not exactly equal to the maximum velocity for a damped system) denoted, S_v, and is calculated from the Duhamel integral [16]:

$$S_v = X_{max} \equiv \left[\int_0^t \ddot{x}_g(\tau) e^{-\zeta\omega(t-\tau)} \sin\omega(t-\tau) d\tau\right]_{max} \quad (2\text{-}25)$$

A plot of S_v vs. T is obtained by averaging the response spectra of a number of different earthquake records and normalizing them to a standard intensity level. The resulting plot, then, is a series of smooth curves, each for a specific value of damping. Similar graphs can be constructed for spectral displacement, S_d, by dividing

spectral velocity by the circular frequency, and for spectral acceleration, S_a, by multiplying spectral velocity by the circular frequency. A combined earthquake response spectra diagram can be obtained by presenting all three graphs on a single plot using tripartite paper as shown in Figure 2.3. Thus, for an earthquake of a given intensity, the associated combined spectra can be used to determine the spectral displacement, velocity, and acceleration for a given structure, if its natural period and damping are known. This technique is applicable to SDOF systems and to those MDOF systems which can be approximated by a SDOF system using the generalized coordinate approach. The response spectrum technique can be used for elastic systems [16] as well as inelastic systems [57]. It is also the method of calculating response in the modal analysis method, where a vibration system is separated into its principal modes [74]. The spectrum analysis technique is used in the sensitivity analysis portion of this dissertation. This is described more fully in Chapter III and Appendix C.

While the earthquake response spectrum is used to determine the response of a structure with known period and damping to an earthquake (or earthquake-like) force of a given intensity level, Blume [8] has developed a procedure for estimating damping using the spectra. This procedure, called Spectral Response Reconciliation, involves

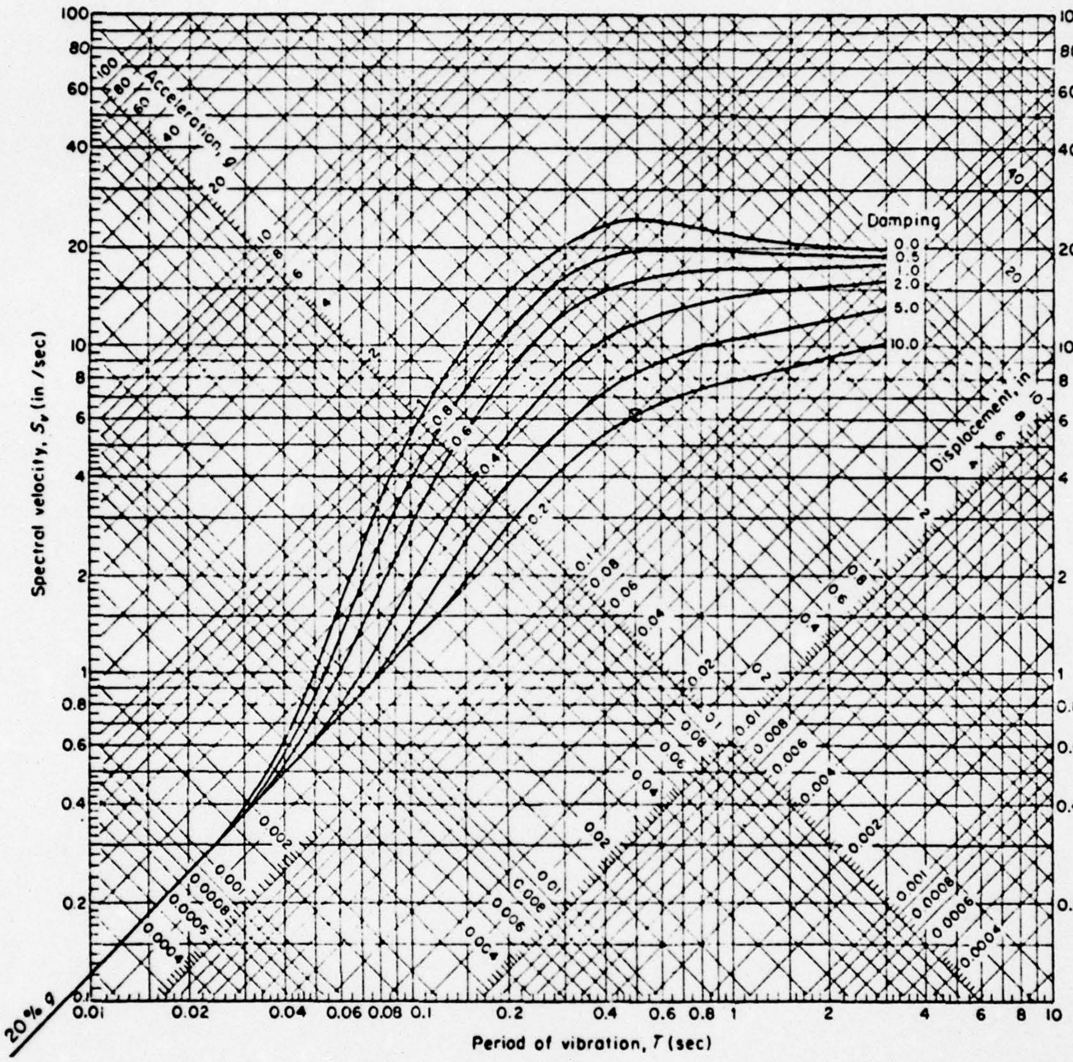

FIGURE 2.3

COMBINED EARTHQUAKE RESPONSE SPECTRA

From: Wiegel, Earthquake Engineering, Prentice-Hall, Inc., 1970. Reproduced by permission of Prentice-Hall, Inc., Englewood Cliffs, N.J.

reconciliation of spectral response with measured real building motion to obtain damping under actual response to ground motion of any intensity. The procedure, as developed and described in detail in the reference [8], basically relates building response displacement to mass, modal deformation, frequency, damping, and free field motion. By measuring/recording all variables except damping from tests or computations, this variable can thus be estimated.

2.5 Steel Moment-Resisting Frames. This section includes a discussion of the general philosophy behind the use of moment-resisting frames. It is not an attempt to review the entire concept of rigid frame design; many texts are available which treat this subject in detail, complete with examples, such as those by McGuire [52], and by Tall, Beedle and Galambos [76]. Moreover, no attempt will be made to present design procedures or philosophies, as those can be obtained from the many design pamphlets and guidelines, such as in the references [24, 70, 79, 90], most of which are explicit, thorough, and complete with examples. Rather, herein is a presentation of the rationale behind the use of steel moment-resistant frames in seismic design, and how they fulfill the requirements of the seismic provisions of building codes. It will be noted that in the foregoing discussion of steel moment-resisting frames, some rationale for their use is based upon response when in the inelastic range. While non-linear, inelastic response is

beyond the scope of this dissertation, the principles and concepts of moment-resisting frames are also applicable when response is in the linearly elastic range.

A tall building designed to resist earthquakes usually uses a moment-resisting frame as the main lateral load-carrying structural system. By using contemporary building codes as the basis for design of these buildings, the engineer can provide an economical structure with adequate rigidity and toughness. The seismic provisions of these codes allow for the use of reduced values for design coefficients [23, 87] when (a) a moment resisting frame is a part of the structural system, and (b) it is capable of independently resisting a portion of (at least 25%) or the entire lateral force. Only that a moment-resisting frame exists as an integral part of a structural system is relevant herein, not its lateral load-carrying capacity.

A frame is basically constructed of horizontal members (beams or girders), and vertical members (columns). A series of interconnected frames are used to form a building. Usually frames are designed/analyzed as two-dimensional frameworks oriented in the direction parallel to that of the expected predominant lateral loading. This approach is particularly useful in the design of short, or low-rise buildings. The frames are connected in the direction perpendicular to them by shear walls or some other form of

rigid bracing. In taller structures, frames are constructed in both principal directions forming a space frame.

A space frame depends upon its own bending stiffness for the lateral stability of the structure. It resists the earthquake forces through the bending of its columns and beams (girders). In a major earthquake large deformations will occur in the structure. The space frame will be effective if it can deform inelastically without losing its lateral resistance or vertical load carrying capacity. Contemporary design philosophy requires the inclusion of a moment-resisting frame as a necessary safety precaution to prevent total collapse of a tall building during a major earthquake [23, 70]. Supplemental elements, like concrete shear walls, which are usually included to add rigidity to withstand low amplitude earthquakes and wind forces, will possibily fail during a high intensity earthquake. The largest moments in the frame usually occur in the connections between the beams (or girders) and columns. These connections should be designed as rigid joints which develop the full plastic capacity of the members framing into the joint. Connections, then, should be designed so that first failure occurs in a member [5].

In order for the frame to truly depend upon its own bending stiffness to insure adequate lateral resistance, a space frame must be ductile. Ductility is a property of concern in the inelastic range. A ductile structure

is able to dissipate energy while it is yielding, without fracturing [5, 70]. Ductile moment-resisting frames should be an integral portion of the lateral load resisting structural system in structures exceeding 160-feet in height, or about 13 stories [23, 70]. Note that contemporary west coast design philosophy includes some flexibility in the selection of the structural system for buildings between 10 and 20 stories high [23].

Space frames with adequate ductility can be constructed in either steel or reinforced concrete. Proponents of each - usually the respective material manufacturers, or trade associations - are ready to offer the advantages of one over the other. No attempt is made herein to explore or present these arguments. It is sufficient to note that steel is one acceptable material for use in the design of multistory buildings with earthquake loadings [90], and that steel moment-resisting frames are the structures which are studied in this dissertation.

2.6 Present Methods of Estimating Damping. From an analytical viewpoint there are many methods which have been established to estimate damping. This topic has been a popular one during the past 15 to 20 years, and much has been reported in the literature regarding the theoretical determination of damping coefficients.

The identification of damping and other structural parameters from measured structural responses to a known

disturbance, regardless of method, is termed an inverse or indirect approach in structural dynamics. The other broad category of methods for solving structural dynamics problems is the direct approach, in which the response of a given structure to a known dynamic loading condition is computed. The overall concept which deals with the inverse approach is system identification [15, 33, 53, 81], which has been investigated intensively by many researchers in recent years.

Building system identification includes the analytical models and numerical methods which are briefly described in the following. Only a representative portion of the system identification field is presented herein to give the reader an introduction to the inverse approach, and to provide a basis for comparison with the methodology to be present in Chapter IV.

<u>2.6.1 Analytical Models</u>. This technique for determining damping requires the analytical modeling of a structure and usually involves the use of digital computer programs which have a dynamic analysis capability. The analytical model is exposed to a representative forcing function and the dynamic analysis algorithm is used to estimate structural parameters of the building. This technique is usually used in conjunction with experiments on the same structure as a means for comparing experimental and analytical values of each parameter.

Most of the experiments used in this report were complemented by analyses of the structures by means of analytical models. Damping values obtained from the tests were compared with those estimated by means of the analytical models [12, 25, 62, 65, 73]. Analytical models have come into common use in recent years due to the development and refinements of the finite element concept of structural analysis [36]. The finite element method uses a substitute structure which is composed of a number of separate finite elements. The finite-element structure is built by assembling the component elements in a member so as to maintain the structural behavior characteristics which are to be modeled [20].

A researcher usually has a choice in the use of the finite element method. He can choose elements which are already developed, or develop his own, depending upon the behavior he wishes to model. For the Parsons building, Foutch [25] developed an element which was based on the structural design calculations and structural drawings for the building. Few additional assumptions were necessary. He developed the finite element model using a modified version of SAP IV [1], a general purpose program developed at the University of California at Berkeley. SAP was used by Stephen, Hollings and Bouwkamp [73] to model the Transamerica Building. A quarter of the building was modeled for analysis so as to keep the computer requirements

to a minimum. Briefly, other computer programs used to determine damping in reported tests are: MACTUB, which was developed for the analysis of multistory tube structures consisting of an assembly of plane frames [62]; FRMDYN, which was used to compute the translational vibration mode shapes, natural frequencies, steady state and linear responses; DINFRA, which was used to determined torsional mode shapes and corresponding natural frequencies; and NONLIN, which was used to compute nonlinear translational response after yielding [65].

2.6.2 Numerical Methods. Numerical methods differ from analytical models in that some form of numerical procedure is formulated to derive from the basic equations of motion the required structural parameters mathematically. What follows is a brief description of some of the methods which have appeared in the literature recently. The reader should recognize some of the qualities inherent in the following methods and how these methods differ from using analytical models and the methodology to be described shortly.

Beliveau [2] formulated a method for identifying damping from modal information within a general Bayesian framework based on eigenvalue and eigenvector pertubations, and a modified Newton-Raphson scheme. This is used to modify parameter estimates when natural frequencies, associated damping constants, mode shapes and phase angles

are known. He uses actual data from a 9-story steel structure to illustrate the method. Hart and Collins [31] propose a method which also develops damping matrices from modal test data, as does Hasselman [34].

Tanaka, Yoshizawa, Osawa, and Morishita [77] present the numerical method analog to the modified logarithmic decrement method for determining damping using the power spectrum presented earlier. It is based on the development of the autocorrelation function of an output to a stationary random input. Corotis and Vanmarcke [21] develop a procedure to estimate the equivalent viscous damping of oscillatory systems using stationary random processes in terms of spectral parameters, and nonstationary random processes in terms of time-dependent parameters. The shape factor function is determined from an analysis of the segmented time history of an earthquake input, and the damping value estimated from a shape factor-damping relationship. Hart and Vasudevan's [32] theory of the linear system transfer function is also based on the Fourier spectrum.

Both the reports by Gersch, Nielsen, and Akaike [29] and by Sweet, Schiff, and Kelley [75] outline a maximum likelihood computational procedure for determining the damping. These procedures, independently arrived at, rely upon the development of the logarithm of the likelihood function. Partial derivatives are then taken with respect

to the damping variable and equated to zero to determine the damping.

The expected damping coefficient is determined by equating the expected energy dissipation caused by inelastic behavior to the dissipation of the equivalent viscous damper in the procedure outlined by Torres and Mote [82]. Also, the damping ratio is determined from a relationship among total energy ratio, potential energy and damping developed by Raggett [64].

Caravani and Thomson [14] determine damping from frequency response as an optimization problem. Response data are sequentially processed by an algorithm which refines the estimation of damping at each frequency point. This is the Identification Algorithm, and it should be carried out over the frequency interval centered at the lowest natural frequency.

The autoregressive-moving average (AR-MA) time series corresponds to a stationary randomly excited differential equation. The obtained AR-MA parameters are used to express the damping and natural frequency parameters of a structural system. These procedures are presented by Gersch [27] and Gersch and Foutch [28].

Finally, Ibanez [41, 42] develops a modal damping matrix from the equations of motion, where damping is a function of mass, frequency, mode shape, and stiffness. Using Taylor's expansion and a criterion function, Ibanez

develops a variable which is a function of mass, frequency, damping, and structure stiffness. By integrating with respect to damping and setting the result equal to zero, a value for damping is obtained.

2.6.3 Damping Determination by Assumption. Prior to beginning the development of the design methodology of Chapters III and IV, it is pertinent to discuss the current status of damping estimation. As noted above, methods for estimating damping do exist in various forms. Experimental, analytical and numerical methods are all appropriate and acceptable procedures for determining this parameter, but, in practically all cases these methods are used for the analysis of existing structures. At the present there is apparently no adequate method available for objectively estimating the value of damping coefficients for structures during the early stages of design. Instead, there is a reliance on experience and engineering judgement, and a value is assumed for damping. The purpose of this research is to fill this apparent void by establishing an objective procedure for the estimation (prediction) of damping coefficients for use in the design of steel moment-resisting frame buildings.

CHAPTER III

DEVELOPMENT OF DAMPING CORRELATIONS WITH BUILDING PARAMETERS

3.1 General Remarks. The use of test data from experiments on actual structures to relate a basic structural property to measurable building parameters has a precedent. An empirical relationship between the natural period of a building and its height and width was developed many years ago by the U.S. Coast and Geodetic Survey. Over 500 buildings and other structures were tested and from these data the following simple formula for estimating the natural period of a building was derived:

$$T = .05 \frac{H}{\sqrt{D}} \qquad (3\text{-}1)$$

where:

T = fundamental period, seconds

H = building height, feet

D = building width in the direction parallel to the applied forces, feet.

Eqn. 3-1 has become the primary means for estimating period in the early stages of the design process. It is one of the recommended relationships given in the seismic provisions

of the Uniform Building Code [87]. Because the values obtained from this empirical relation may differ significantly from the actual values in individual buildings, the Uniform Building Code provides for alternatives to this formula for certain types of structures. However, this formula continues to be widely used in structural design; and its obvious practical value certainly demonstrates the potential worth of empirically-derived relationships for the design of structures.

It is logical to suggest that empirical relations for estimating other building properties would be equally valuable. In the 1930's, Blume [7] foresaw the possibilities of estimating damping from information obtained by observing the vibrations of actual buildings. Damping appears to have some of the same basic relationships to measurable building parameters as natural period. An analysis of the data collected for the purpose of this study indicates a definite trend exists when damping is plotted versus building height as shown in Fig. 3.1. This plot shows that damping decreases with increasing building height. This decreasing trend is to be expected for damping in the linearly elastic range from available knowledge about the nature of damping. If two structures are of the same type, configuration and construction, i.e., similar except for height, damping in the taller structure would generally be less than that in the shorter, more rigid

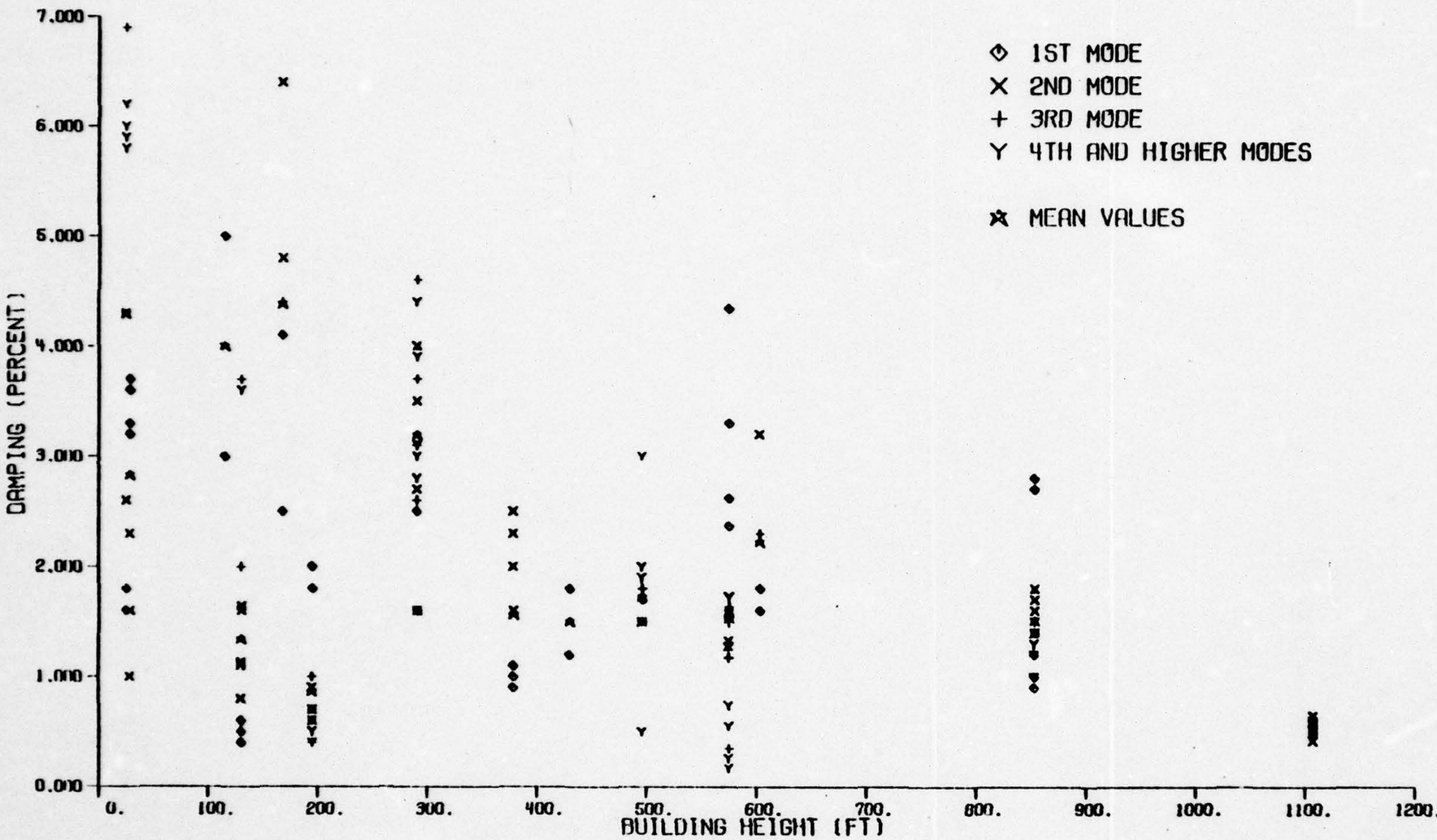

FIGURE 3.1

BUILDING HEIGHT VS DAMPING

structure because of the inter-relationships among damping, flexibility and mass.

Intuitively, one would expect that damping might also be related to building width. It should be noted that building width refers to the building dimensions in the direction parallel to the applied forces. While a plot of damping versus building width as shown in Fig. 3.2 is inconclusive, with no apparent tend existing, it is logical to presume that because of these same characteristics of damping, building width should be considered in developing an empirical relationship. This presumption was found to be valid in this study; the best correlations were obtained for relationships which included both building height and width.

For the sake of simplicity, it was decided to consider only building height and building width in the derivations. These were the only measurable parameters common to all buildings that constituted the data base used for developing the empirical relationships. A listing of these buildings with descriptions thereof is given in Appendix A. It should be noted that while differences do exist among these buildings, they are all basically steel-framed and moment-resisting structures. Further, they all have a moderate amount of non-structural internal elements (partitions, doors, curtain walls, etc.), necessary structural elements (floors, elevator/stairwell shafts, etc.),

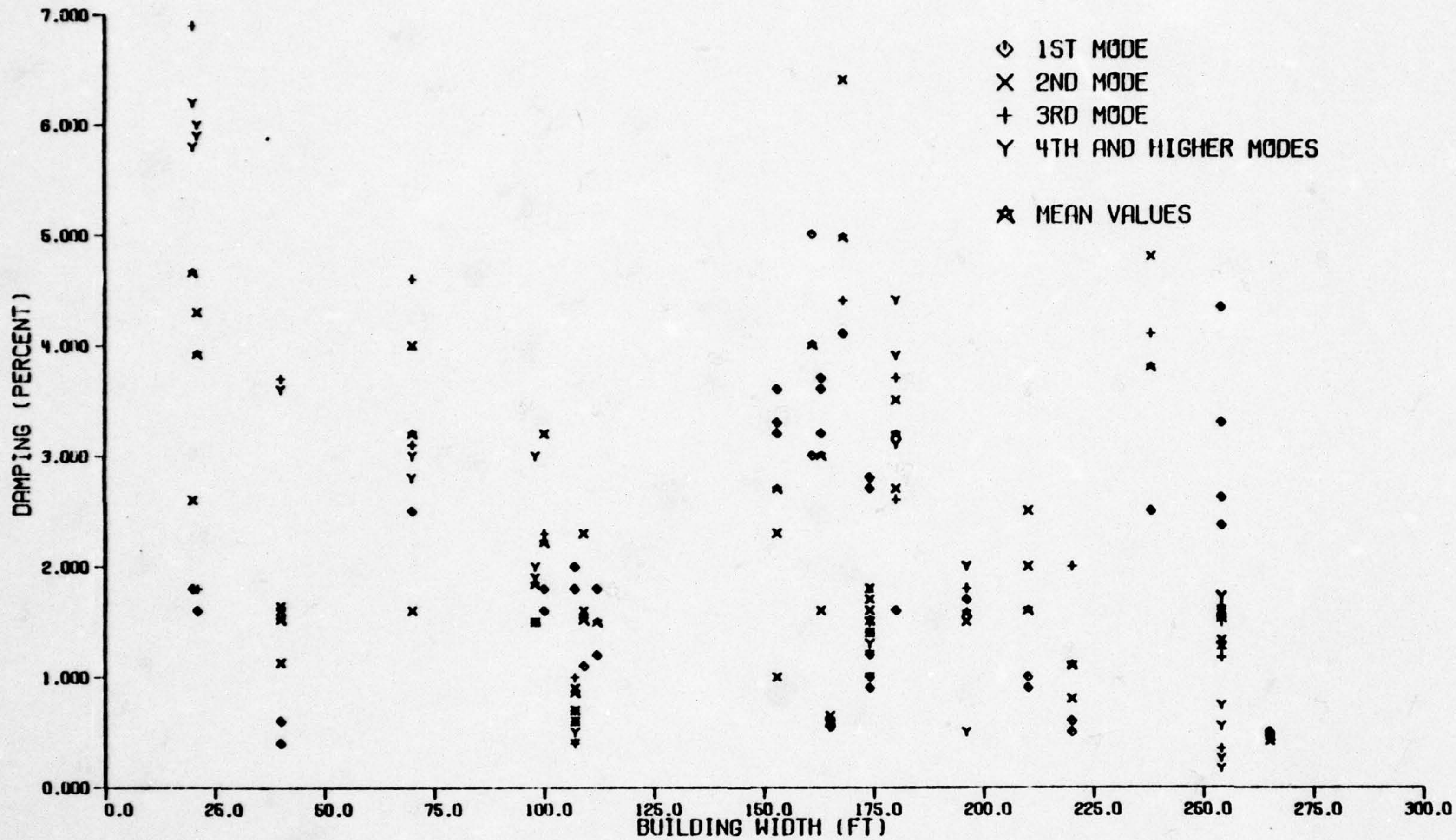

FIGURE 3.2

BUILDING WIDTH VS DAMPING

and all are founded on soil of sufficient bearing capacity to support the design loads so that piling is not needed.

Aside from the height and width differences, the buildings differ in shape, in material of the non-structural and supporting elements, and in underground building extensions. (No reentrant corner buildings, with accompanying high stress concentrations, are included.) Because these differences are imprecisely defined in a quantitative sense and to an extent unmeasurable, it was assumed that their inclusion would constitute unwarranted refinements of the basic damping vs. height, width relationships. Consequently, the development of factors to represent these more subtle differences among buildings is not included in this study.

With building height and building width as the independent variables, the damping values are collected independent of mode, and thus of frequency. The assumption inherent in this decision is that frequency (or period) and damping are statistically independent. This is based upon the apparent lack of a frequency-damping relationship - refer to Figs. 3.1 and 3.2. In separate studies of reinforced concrete buildings, Gallo and Ang [26] made the same basic assumption. They concluded that for individual tests damping seemed to vary with period (or frequency), but when data from different sources were collected together this effect vanished.

This property of frequency independence is perhaps best described by the concept of hysteretic (or structural) damping. Hysteretic damping is produced by a damping force which is in phase with the velocity but proportional to the displacements [18]. This concept is depicted by the force-displacement diagram for hysteretic damping during a typical cycle of harmonic displacement for a SDOF system in Fig. 3.3:

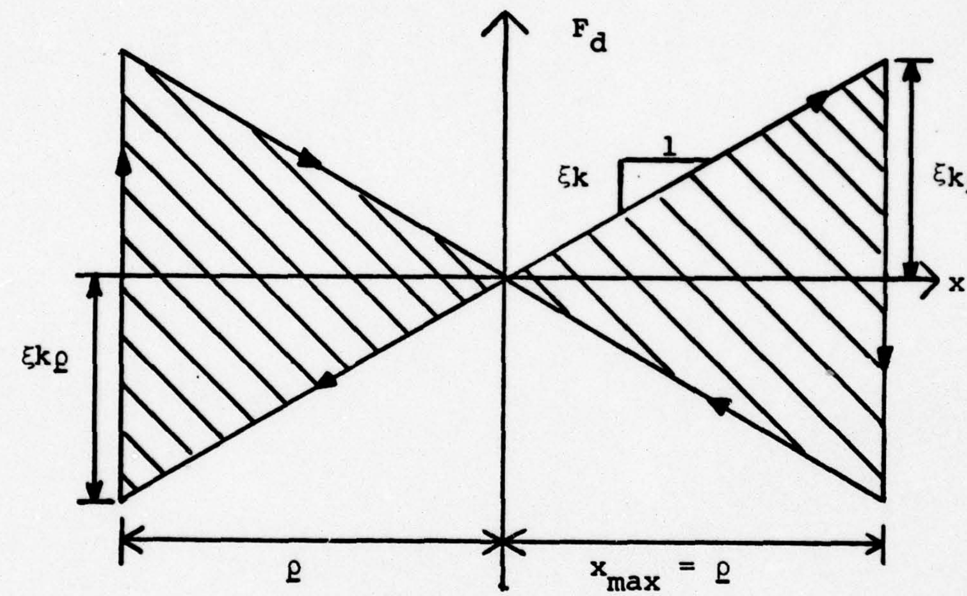

FIGURE 3.3

HYSTERETIC DAMPING FORCE VS DISPLACEMENT

where the hysteretic-damping coefficient, ξ, is given by the equation,

$$\xi = \frac{w_D}{2k\underline{\rho}^2} \qquad (3\text{-}2)$$

in which:

w_D = total area per cycle (shaded area)

k = stiffness

$\underline{\rho}$ = maximum displacement

Further discussion and development of this concept can be found in various texts and references. It is general practice, however, to utilize an equivalent viscous damping ratio, ζ, to express the damping of a structure regardless of the actual internal energy dissipation mechanism as was indicated in Chapter II (section 2.3).

3.2 Table Development. An essential and critical step in the development of the empirical relationship is the collection of data and its arrangement in a useful, tabular form. This was done for the data used in this research. Table 3.1 shows the damping values, in terms of ζ, presented as a function of building height, given in feet. Herein, as in all of the tables and figures, ζ is the equivalent viscous-damping ratio expressed in percent form. Table 3.2 gives a similar presentation of ζ vs. building width. Table 3.3 is a chart showing the damping values as they vary with both building height and building width. These damping values were obtained from the results of experiments conducted on the buildings described in Appendix A. The

TABLE 3.1

BUILDING HEIGHT VS ζ

Reference	86	12	55	55,60	25	65	43,85	10	88	83	62	88	73	22,78
Height (ft)	25	28.5	115	130	168	195	291	379	430	496	575	603	853	1107
Stories (#)	2	2	7	9	12	15	22	27	34	39	44	44	60	100
Mean	4.29	2.83	4.0	1.34	4.38	0.86	3.19	1.56	1.5	1.72	1.53	2.22	1.51	.54
ζ (%)	1.6	3.2	3.0	0.4	4.1	2.0	2.5	1.0	1.2	1.5	2.37	1.8	1.4	0.5
	1.8	3.3	5.0	0.6	2.5	1.8	1.6	1.1	1.8	1.7	2.62	1.6	0.9	0.6
	2.6	3.6		0.5	6.4	0.9	1.6	0.9		1.5	3.30	3.2	1.2	0.46
	4.3	3.2		0.6	4.8	0.7	2.7	1.1		1.5	4.34	2.3	1.0	0.55
	6.9	3.7		0.4	4.4	0.7	4.0	2.5		1.5	1.57		2.8	0.42
	1.8	3.6		0.6	4.1	0.6	3.5	1.6		1.8	1.6		2.7	0.6
	5.8	1.0		0.8		0.6	3.1	2.0		1.5	1.22		1.6	0.65
	6.0	2.3		1.1		0.4	3.7	2.3		2.0	1.28		1.4	
	6.2	1.6		1.33		1.0	4.6			3.0	1.18		1.8	
	5.9			1.64		0.7	2.6			2.0	1.64		1.7	
				0.8		0.5	2.8			2.0	0.35		1.2	
				1.6		0.4	3.9			0.5	1.17		1.2	
				2.0		0.9	3.0			1.9	0.74		1.5	
				3.7			3.1				1.72		1.5	
				2.0			4.0				1.72		1.3	
				3.6			4.4				0.26		1.0	
											1.73		1.8	
											1.49		1.2	
											0.17			
											0.55			

TABLE 3.2

BUILDING WIDTH VS ζ

References	86	86	55,60	43,85	83	88	65	10	88	12	55
Width (ft)	20	21	40	70	98	100	107	109	112	153	161
Mean	4.66	3.92	1.52	3.2	1.84	2.22	0.86	1.52	1.5	2.7	4.0
ζ (%)	1.8	1.6	0.4	2.5	1.5	1.8	2.0	1.1	1.2	3.3	3.0
	2.6	4.3	0.4	1.6	1.5	1.6	1.8	1.1	1.8	3.2	5.0
	6.9	1.8	0.6	4.0	1.5	3.2	0.9	2.3		3.6	
	5.8	6.0	0.6	3.1	1.5	2.3	0.7	1.6		1.0	
	6.2	5.9	1.6	4.6	3.0		0.7			2.3	
			1.13	2.8	2.0		0.6				
			1.64	3.0	1.9		0.6				
			3.7	4.0			0.4				
			3.6				1.0				
							0.7				
							0.5				
							0.4				
							0.9				

TABLE 3.2 CONTINUED

References	12	22,78	25	73	43,85	83	10	55,60	25	62	22,78
Width (ft)	163	165	168	174	180	196	210	220	238	254	265
Mean	3.0	0.6	4.97	1.51	3.19	1.58	1.6	1.11	3.8	1.53	.46
ζ (%)	3.2	0.55	4.1	1.4	1.6	1.7	0.9	0.5	2.5	4.34	0.5
	3.7	0.6	6.4	0.9	2.7	1.5	1.0	0.6	4.8	2.62	0.46
	3.6	0.6	4.4	1.2	3.5	1.8	2.5	0.8	4.1	2.37	0.42
	1.6	0.65		1.0	3.7	2.0	2.0	0.8		3.3	
				2.8	2.6	2.0		1.1		1.57	
				2.7	3.9	0.5		2.0		1.6	
				1.6	3.1			2.0		1.33	
				1.4	4.4					1.28	
				1.8						1.18	
				1.7						1.64	
				1.2						0.35	
				1.2						1.17	
				1.5						1.27	
				1.5						1.72	
				1.3						0.26	
				1.0						0.74	
				1.8						1.73	
				1.2						1.49	
										0.17	
										0.55	

TABLE 3.3

BUILDING HEIGHT, WDITH VS ζ

References	86	86	12	12	55	55,60	55,60	25	25	65	43,85
Height (ft)	25	25	28.5	28.5	115	130	130	168	168	195	291
Width (ft)	20	21	153	163	161	40	220	168	238	107	70
Mean	4.66	3.92	2.7	3.0	4.0	1.52	1.11	4.97	3.8	0.86	3.2
ζ (%)	1.8	1.6	3.3	3.2	3.0	0.4	0.5	4.1	2.5	2.0	2.5
	2.6	4.3	3.2	3.7	5.0	0.4	0.6	6.4	4.8	1.8	1.6
	6.9	1.8	3.6	3.6		0.6	0.8	4.4	4.1	0.9	4.0
	5.8	6.0	1.0	1.6		0.6	0.8			0.7	3.1
	6.2	5.9	2.3			1.6	1.1			0.7	4.6
						1.13	2.0			0.6	2.8
						1.64	2.0			0.6	3.0
						3.7				0.4	4.0
						3.6				1.0	
										0.7	
										0.5	
										0.4	
										0.9	

TABLE 3.3 CONTINUED

References	43,85	10	10	88	83	83	62	88	73	22,78	22,78
Height (ft)	291	379	379	430	496	496	575	603	853	1107	1107
Width (ft)	180	109	210	112	98	196	254	100	174	165	265
Mean	3.19	1.52	1.6	1.5	1.84	1.58	1.53	2.22	1.51	0.6	0.46
ζ (%)	1.6	1.1	0.9	1.2	1.5	1.7	4.34	1.8	1.4	0.55	0.5
	2.7	1.1	1.0	1.8	1.5	1.5	2.62	1.6	0.9	0.6	0.46
	3.5	2.3	2.5		1.5	1.8	2.37	3.2	1.2	0.6	0.42
	3.7	1.6	2.0		1.5	2.0	3.3	2.3	1.0	0.65	
	2.6				3.0	2.0	1.57		2.8		
	3.9				2.0	0.5	1.6		2.7		
	3.1				1.9		1.33		1.6		
	4.4						1.28		1.4		
							1.18		1.8		
							1.64		1.7		
							0.35		1.2		
							1.17		1.2		
							1.27		1.5		
							1.72		1.5		
							0.26		1.3		
							0.74		1.0		
							1.73		1.8		
							1.49		1.2		
							0.17				
							0.55				

mean values for each set of data are also given.

Tabulation of the data into this form facilitated the development of the correlation between ζ and the building parameters. The tables were also used to develop the graphs of Fig.'s 3.1 and 3.2. The horizontal line(s) appearing in the columns of the tables separate the data by modes, with the fundamental mode presented first, followed by higher, succeeding modes in numerical order.

The variation in the amount of data available and collected in this research is also easily seen by the tabular presentations. While only the fundamental modal damping values were obtained and reported in some experiments, the data contain experimental results which report damping values from as many as seven modes. Data were collected and used from the translational modes only, although torsional modes were excited and similar modal data reported. It was felt that the use of the torsional modal data in the development of the correlations undertaken herein involved resolutions to achieve compatibility with translational modal data which could not be justified. These resolutions included the determination of the composition of the torsional modal damping value and how it relates to the concept of planar equivalent viscous-damping. Conceivably the torsional modes might include internal damping mechanisms which are not presented in pure translational modes. Further, it was felt a redistribution of the

torsional damping values into representative translational components could not be made. Consequently, the torsional damping values were excluded from this study.

As previously noted, the data used herein were collected from experiments which were conducted on actual buildings. For the most part these buildings were either in the final stages of construction or completed when the experiments took place. Consequently, the damping values obtained are representative of a free-standing structure, complete with its full complement of non-structural elements, and thus are excellent input for this study.

One notable exception is the East Building of the University of California at San Francisco which was tested by Rea, Bouwkamp and Clough [65]. The total experiment was actually a series of tests conducted from the summer of 1964 through the fall of 1965. One of the most striking features of the experiment was that the damping values obtained from the tests conducted during the summer of 1964 were significantly less than those obtained from tests conducted during the summer of 1965. The authors concluded that this increase was attributable to the interaction between the East Building and its service tower, and thus the damping values were for a system of connected buildings. Consequently, the values obtained in 1965 were directly applicable to building systems with this type of construction

only and were not representative values for an isolated building.

It was decided, then, to use only the damping values obtained from the 1964 tests in this research. While far from being a complete building, the structure did have its major structural elements erected, and some of the non-structural elements emplaced as well. Windows, doors, some internal partitions, and the mechanical ductwork, however, were still lacking. Since these items contribute to damping, the values obtained from these tests are relatively low. Nevertheless, it is believed that these disparities do not invalidate the use of these damping values in this research. It is felt that the construction of the building had progressed to the extent that the damping values obtained from the summer of 1964 tests could be considered equivalent to those exhibited by a lightly damped structure of similar configuration. In other words, a steel moment-resisting framed building with a large number of open bays and light exterior and interior wall construction would have somewhat lower values of damping than a similarly structured building with a large number of non-structural elements. Since both types of buildings are to be represented by the correlation developed in this research, the damping values obtained from the summer 1964 tests are included herein.

The data in the tables also include damping values obtained from different, yet compatible methods. Methods for determining the damping ratio from test results, like the bandwidth method and the logarithmic decrement method, are presented in Chapter II. Given the circumstances of testing and the associated assumptions inherently reflected in these test data, all of the described methods are applicable. Consequently, included in the data are damping values for particular structures [10, 65, 73, 88] which were obtained by two different methods. Since these methods are based upon different test procedures and involve the use of different test results, they are considered independent and are treated as separate observations in the data even though the same researcher(s) performed the two tests. Also included in the data are results from different tests of the same building performed by different researchers at different times [22, 43, 44, 55, 60, 78, 85]. These data, too, are included as independent damping values for purposes of the statistical analyses.

3.3 Development of the Correlation Between ζ and Building Height, Width

The development of the functional relationship between ζ and the two building parameters - building height and building width - was completed in three distinct steps:

1. The development of the best correlation(s) between ζ and building height, independent of building width.

2. The development of the best correlation(s) between ζ and building width, independent of building height.

3. The development of the best correlation(s) between ζ and various combinations of building height and building width.

The third step was based upon the results obtained in the first two steps, and thus necessarily followed sequentially.

In the development of each relationship, both the raw data and the mean values of the data were used as input to the REGRESSION subroutine of the Statistical Program for the Social Sciences (SPSS) as given by Nie, Brent and Hull [58]. (The mean value used was the mean of the damping values found for each building height (or width) used. Means are given in Tables 3.1-3.3.) The basic concept of this Program and its pertinence to this dissertation research is discussed in Appendix C. Generally, the use of the regression analysis program requires a trial and error procedure whereby the basic form of the expression relating the dependent variable and the independent variable(s) is developed externally and the entered as a potential regression equation. The program carries out the calculations required to determine the coefficient(s) in the regression equation which produce the best fit to the input data. An indication of best fit is the R^2 statistic which is a measure of the amount of error which can be explained by using the regression equation. The R^2

statistic was used as the primary indicator of correlation between the dependent variables, ζ, and the independent variable combinations tried.

A total of 267 regressions were tried. These are all listed, along with their respective R^2 statistic and other pertinent data, in Appendix B. It should be noted that both the raw data and the mean values were used in the regression trials. It was discovered while running the equations that the raw data generally yielded poor correlations as measured by the R^2 statistic. It is believed the main reason for these poor correlations is the possibility that not all of the phenomena producing the damping of a structure are well correlated or even tied to building height, or building width, or a *combination*. Further, wide variations in the reported damping values could be attributed to differences in experimental technique among researchers, differences in equipment and instrumentation usage, differences in measurement and calculation tolerances, and the like. With the lack of an apparent consistent testing and reporting procedure, these differences are bound to exist. They become much more evident in a study such as this where the results of these experiments are collected for subsequent analysis and use.

In spite of these differences and the possibility of contributions to damping by other lesser-related (or even non-related) factors, it was still felt that damping of a

structure was related to building height and/or to building width. Fig. 3.1 showed that a definite trend did exist between damping and building height which supported the contention. To determine this correlation, then, the mean values of the damping ratios for each given building height (and width) were used. The use of these mean values as the input data had two advantages: (1) the elimination of the observed variations in the raw data set due to the inconsistent testing and reporting procedures, and (2) the realization of high correlation values.

The determination of what qualified as a "high correlation" was necessarily subjective in nature. While it is intuitively obvious that the closer the R^2 statistic was to 100 percent then the better the regression equation, practical limits had to be imposed to keep the relationship simple. Accordingly, it was arbitrarily decided that an R^2 value of 80 percent or higher would be considered a high correlation, and the corresponding equation, therefore, would be considered an acceptable relationship.

3.3.1 ζ vs. Building Height. It is concluded from the regression analyses using building height as the sole independent variable that an inverse relationship is the best among those tried (see Appendix B). This was determined from the results of analyses which used mean values for input data. The best correlation obtained was for Eqn. 23 which had an R^2 value of 79.5%, or very close to the

selected 80% criterion. When all data were used, a much lower correlation (R^2 = .12113) was obtained. Eqn. 23 is presented in Fig. 3.4.

An exponential type of relationship also yielded high correlation values. Subsequently, it will be shown that when both building height and width were used as the independent variables, the best correlation was obtained with a combination of inverse and exponential terms.

The relationship yielding the best correlation (R^2 = .45252) for the complete data set was an equation including inverse terms (Eq. 29). This equation is presented in Fig. 3.5. Note that this relationship is satisfactory only when the building height is greater than 250 feet. Thus, its value as an independent equation for predicting damping is limited.

Fig.'s 3.6 and 3.7 show Eqns. 11 and 12 which represent the best correlations of the other types of relationships which were attempted. It should be noted from comparing these two figures that the exponential relationship (Fig. 3.7) is better. Also, mean values were used to develop these two relationships.

3.3.2 ζ vs. Building Width. As indicated in section 3.1, there did not appear to be a definite trend evident in the plot of the damping values vs. building width (Fig. 3.2). This observation was confirmed by results of the regression analyses. For each of the several types of

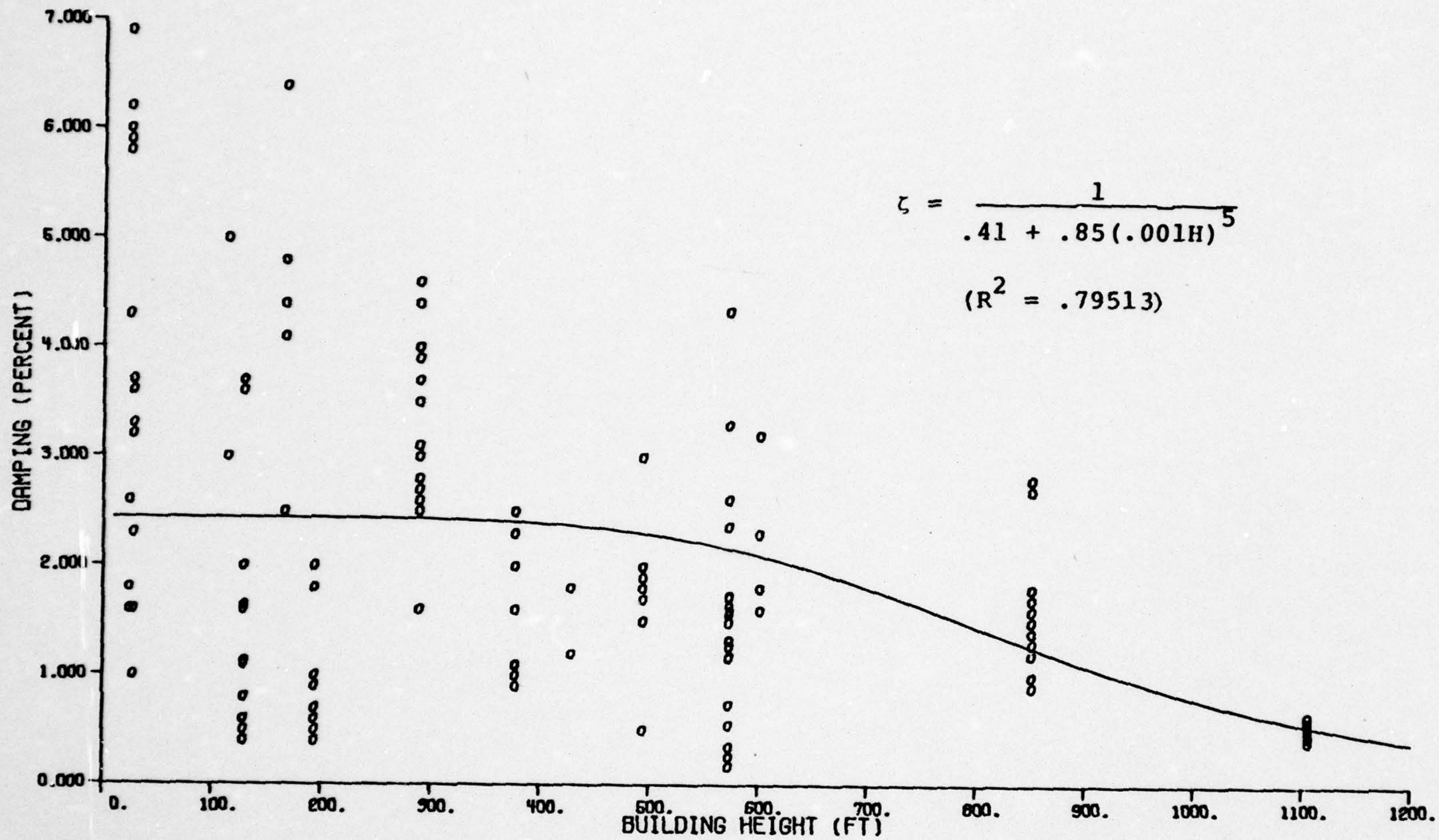

FIGURE 3.4
DAMPING FROM EQUATION 23

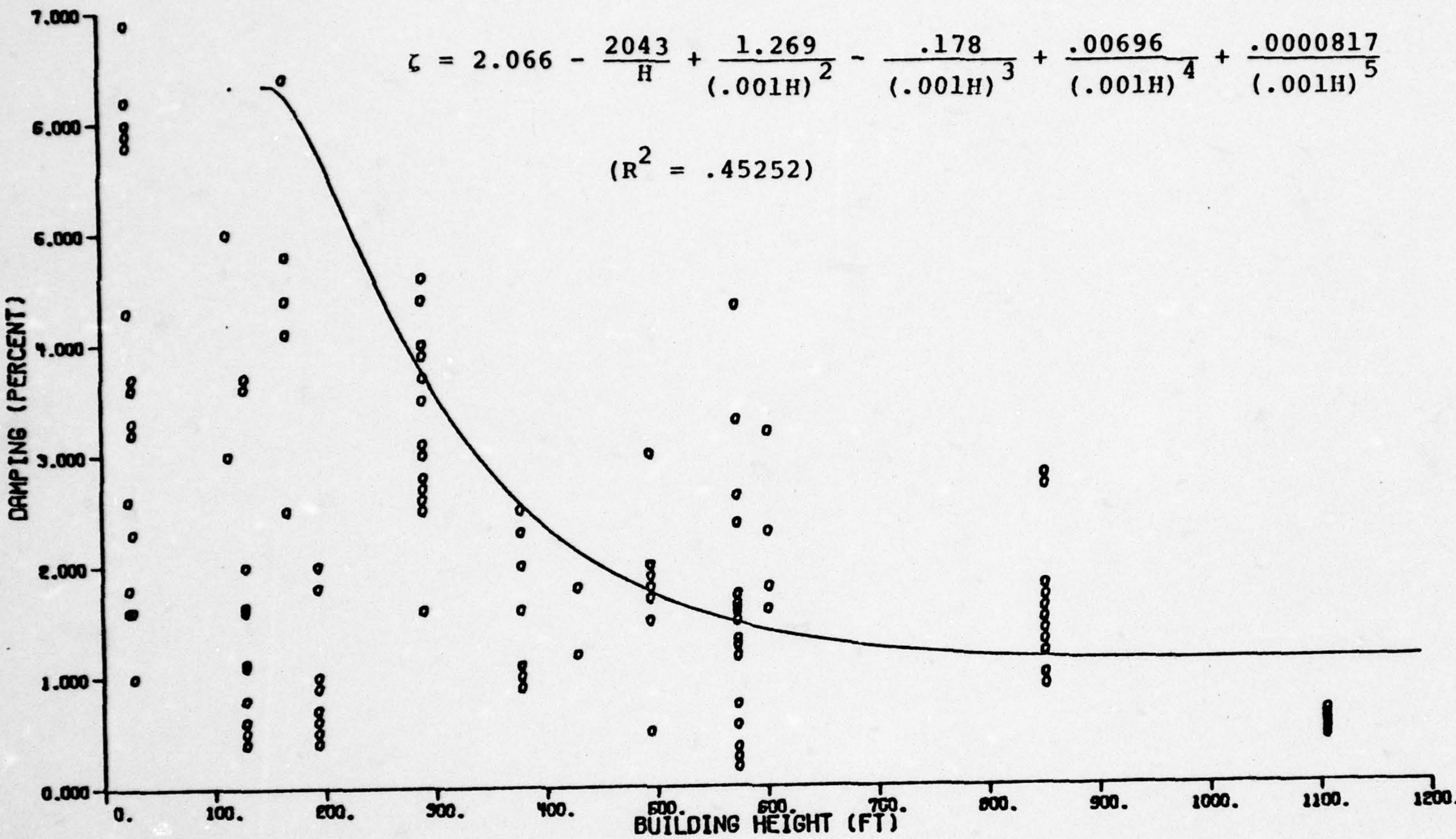

FIGURE 3.5
DAMPING FROM EQUATION 29

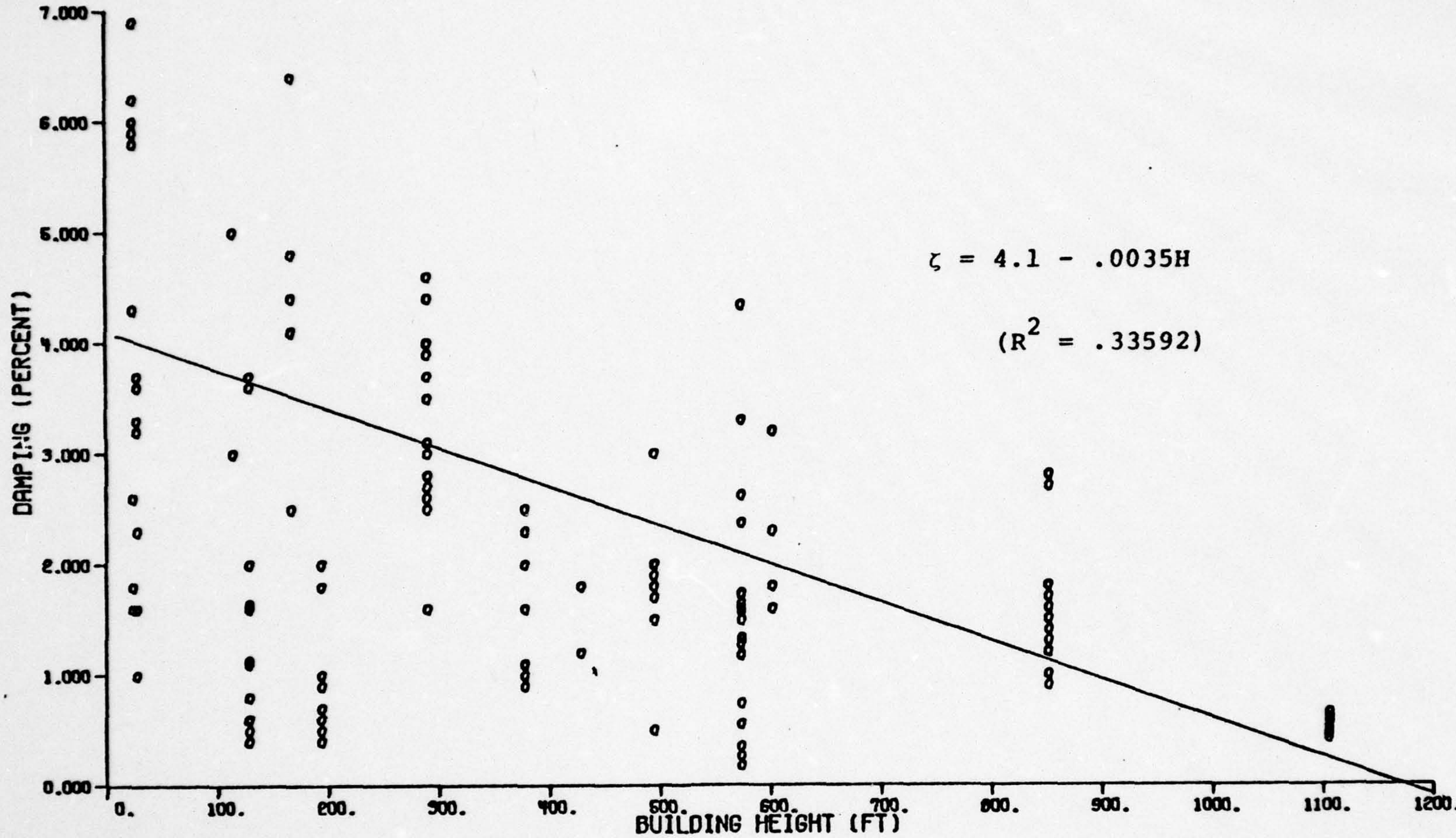

FIGURE 3.6
DAMPING FROM EQUATION 11

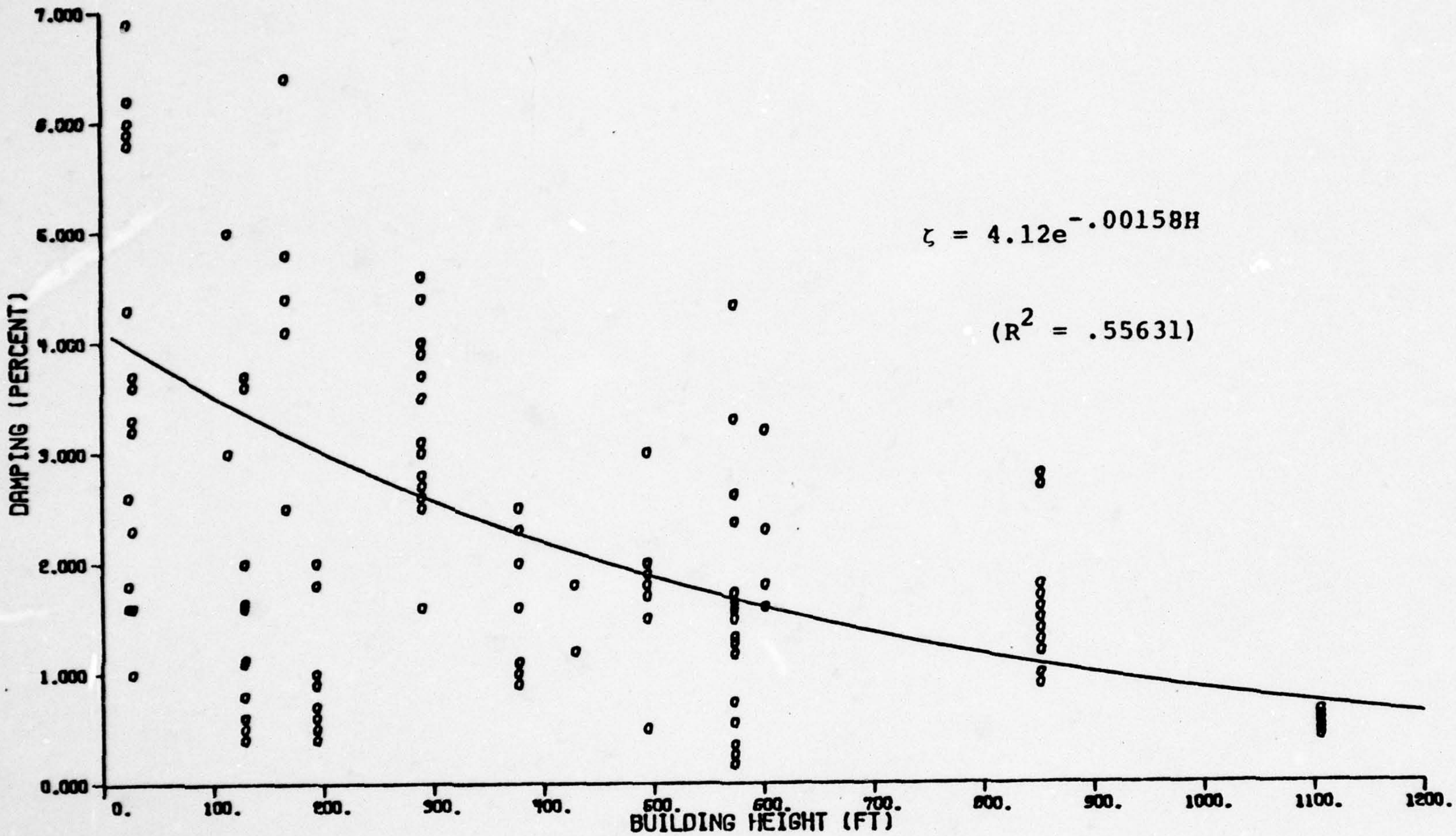

FIGURE 3.7
DAMPING FROM EQUATION 12

relationships tested the correlations with damping were very low, even when the mean damping values were used as input. The highest R^2 value obtained was 22.9% (for Eqn. 50). The relationship giving this level of correlation is shown in Fig. 3.8. Because of the low correlation value (obtained with mean values as input data) this relationship is unsatisfactory.

Two conclusions were drawn from these regression analyses. First, the generally low correlations indicated that building width was of secondary consequence in predicting damping values, particularly when compared to building height. Second, better correlations were obtained when building width was squared in the various relationships tried. Both of these conclusions became evident in the relationships which finally evolved using both building height and width. As will be seen, building width appears as a squared term modified by small coefficients compared to those modifying the building height terms. Its contribution to the determination of the predicted value of damping is minimal; however, its retention in the equation is necessary to obtain a higher correlation value.

To illustrate the type of relationships between damping and building width tried, Figs. 3.9, 3.10, 3.11 and 3.12 are presented. These graphs display Eqns. 48, 49, 57 and 61 respectively. Eqns. 48, 49 and 61 (Figs. 3.9,

AD-A054 438 ARMY MILITARY PERSONNEL CENTER ALEXANDRIA VA F/G 20/11

DEVELOPMENT OF AN EMPIRICAL RELATIONSHIP FOR THE PREDICTION OF --ETC(U)

MAY 78 T J RUSNAK

UNCLASSIFIED NL

2 OF 3
ADA
054438

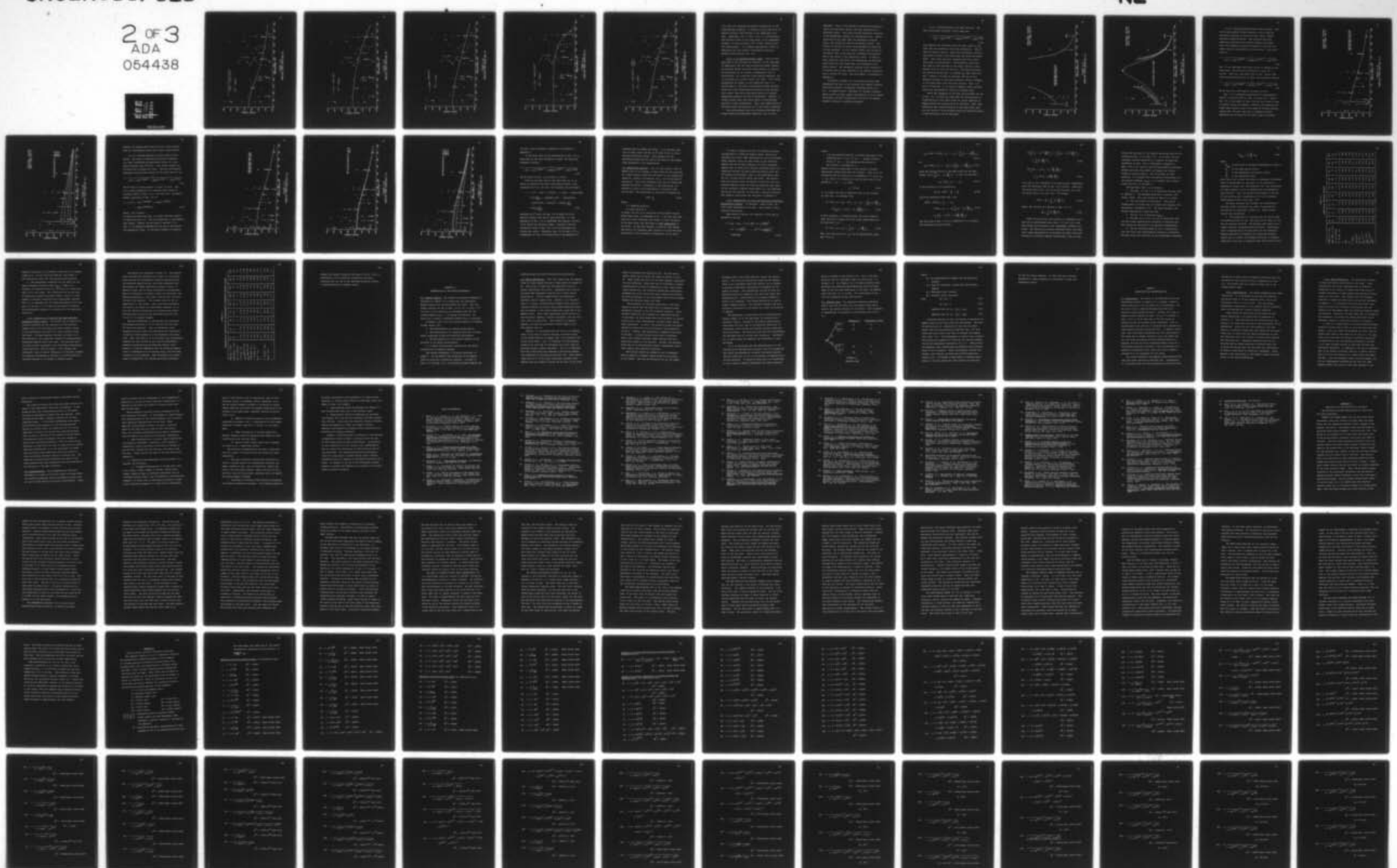

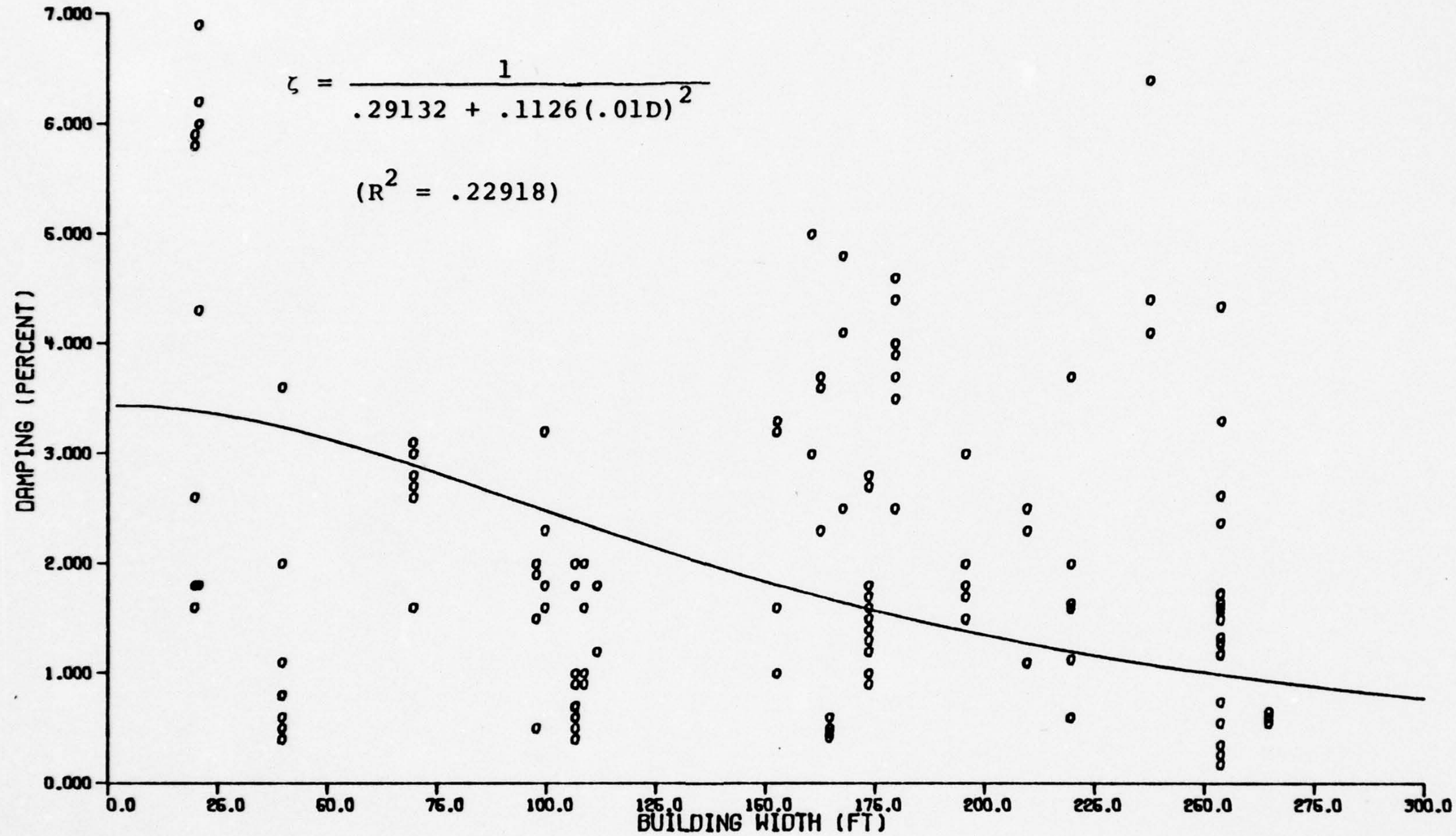

FIGURE 3.8
DAMPING FROM EQUATION 50

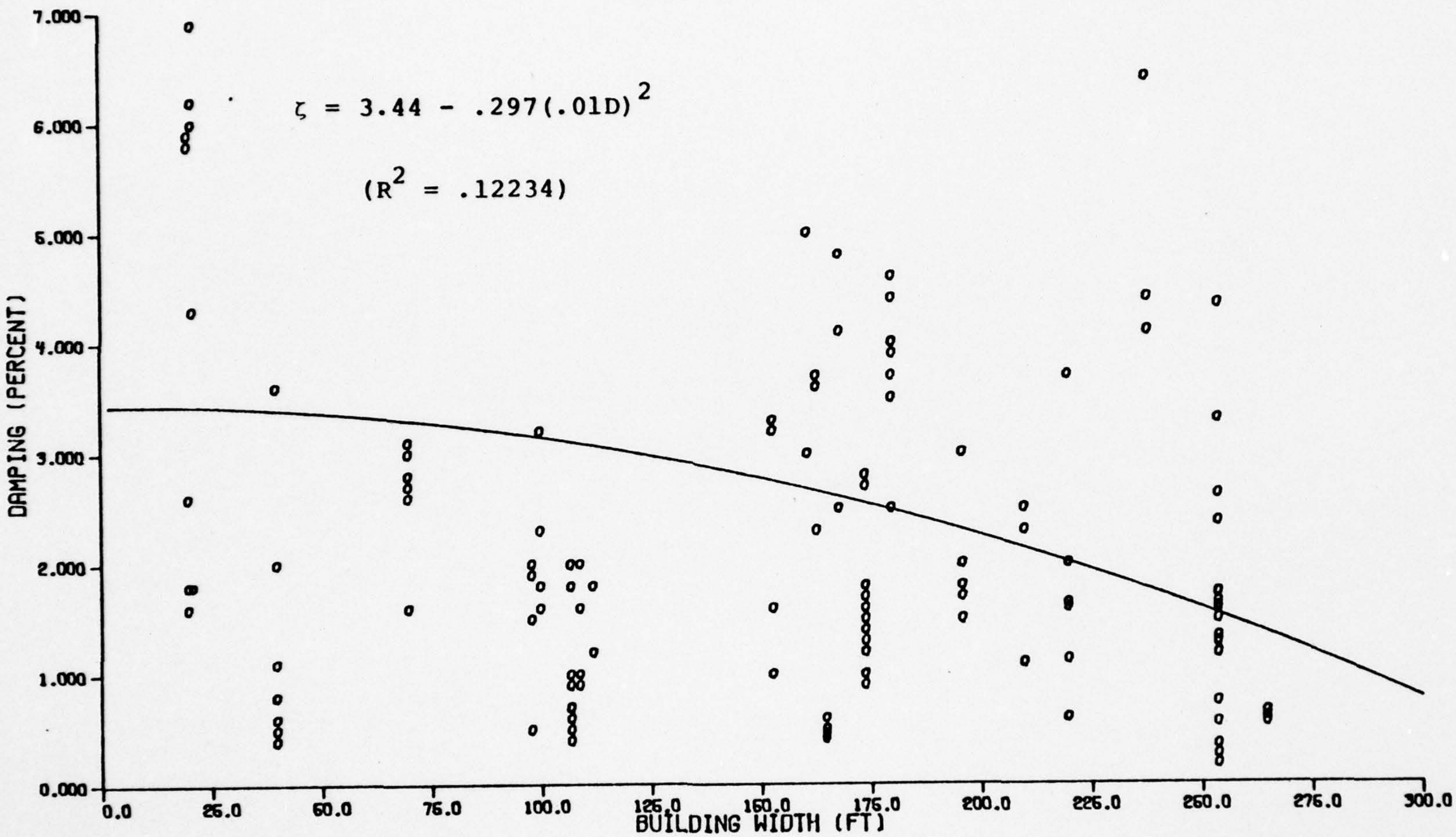

FIGURE 3.9
DAMPING FROM EQUATION 48

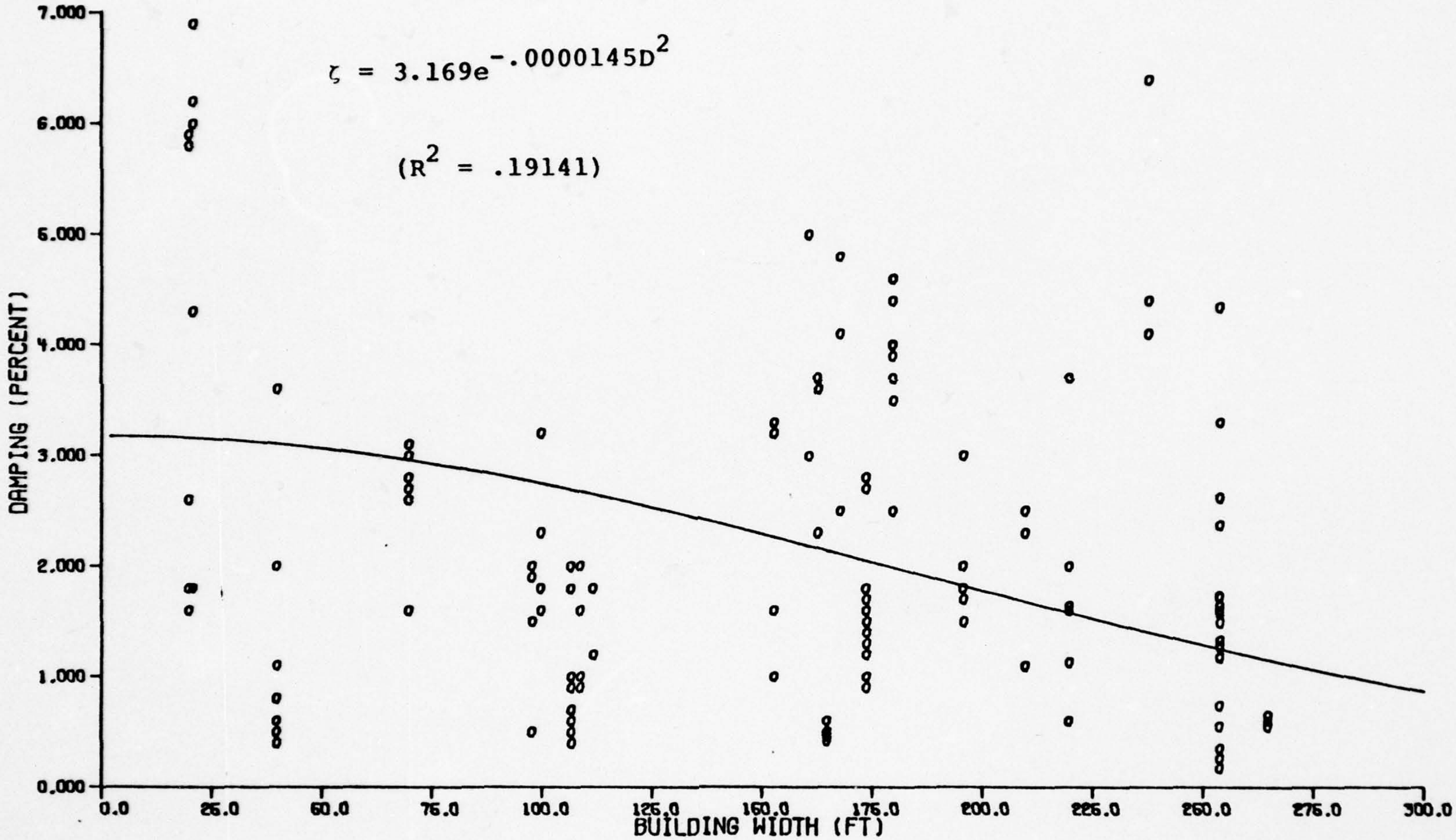

FIGURE 3.10
DAMPING FROM EQUATION 49

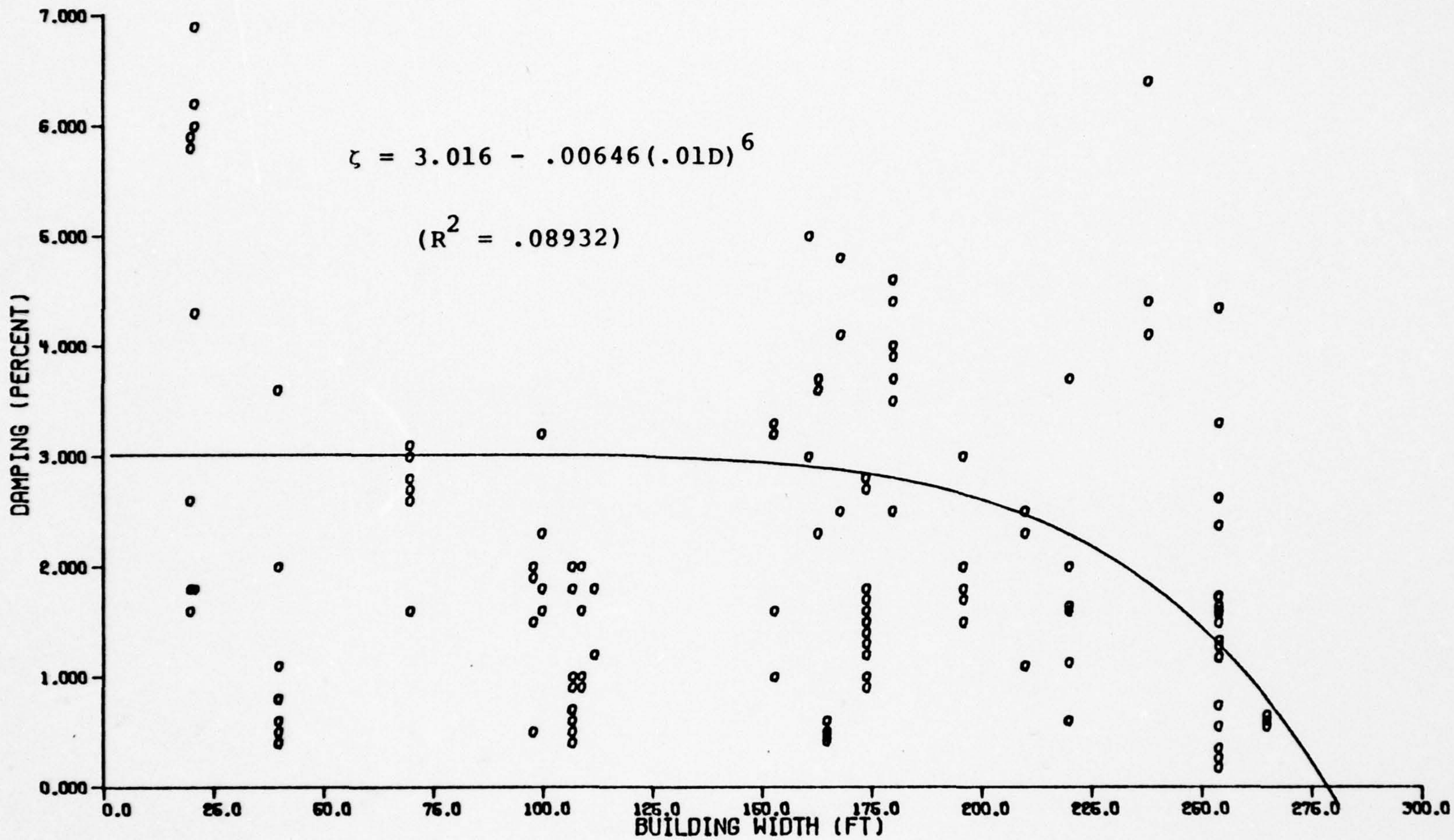

FIGURE 3.11
DAMPING FROM EQUATION 57

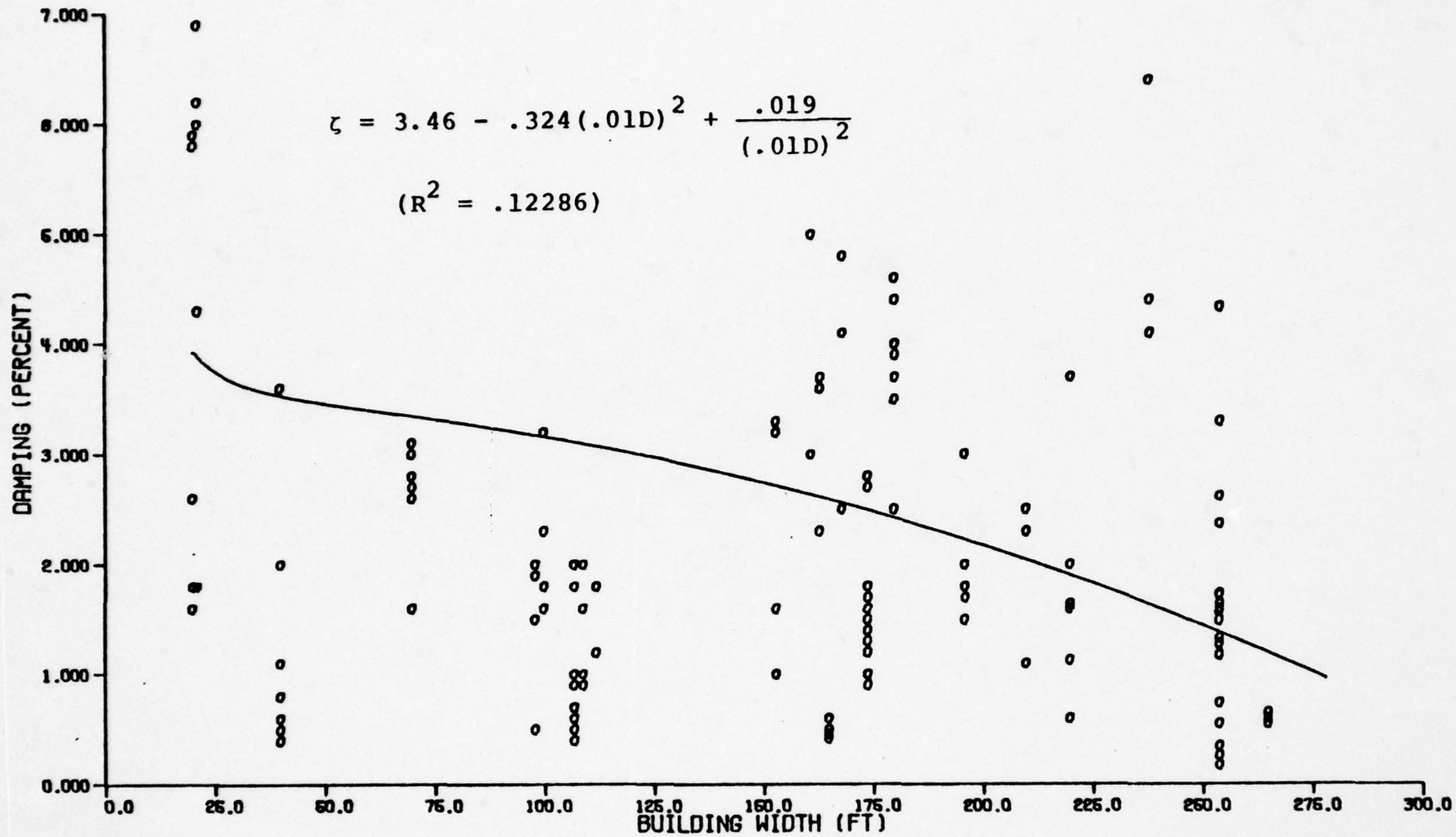

FIGURE 3.12
DAMPING FROM EQUATION 61

3.10, and 3.12) produced the highest correlations of the relationships attempted. It should be noted that they all contain building width-squared in the independent variable. Conversely, Eqn. 57 (Fig. 3.11) is a relationship with building width to the sixth power in the independent variable. A low correlation (R^2 = 8.93%) resulted from this relationship. It is merely presented as a means of comparison with the similar relationship containing building width-squared (Fig. 3.9).

3.3.3 ζ vs. Building Height, Width. From the work described in the previous two sections, it was reasonable to hypothesize that the best correlation between damping and building height and width would probably be obtained by considering (a) an inverse or exponential type of relationship, (b) a building width-squared component, and (c) dominance by building height over width. Using these presumptions as guides, it was determined that if a multiplicable or divisible relationship between building height and width existed which resulted in high correlation values, then this relationship would be a general homogeneous equation and thus be preferable. However, it became evident early that these types of relationships resulted in poor correlations. Thus, such combinations of building height and width are not in the "best" equations.

The relationships which are ultimately developed are called restricted homogeneous equations [56], or unit

dependent. Thus, it was decided to develop the equations using one measurement system, and then converting to a secondary system. This would provide equivalent equations in two measurement systems for international use. Since a large part of the input data was expressed in English units, this system was used as the primary system. Conversion to the Metric system of measurement was made and is also included. It will become evident that the use of the metric form of the equation is somewhat inconvenient due to the nature of the exponential terms. To obtain a more convenient expression, the methodology was developed again using the same input data, but expressed in the Metric system. The regression equation which resulted is of similar form to that obtained in the English system and with a similar R^2 value. This development is presented in Appendix D.

As stated in Chapter II, the Uniform Building Code establishes 160 feet as the dividing line between required structural systems in earthquake resistant design [23, 87]. It seemed logical, therefore, to consider relationships in each of these ranges independently so as to obtain the highest possible correlations, and thus, the highest possible accuracy in predicting damping.

3.3.3.1 Building Heights Less Than 160 Feet. The best relationship obtained in this range was:

$$\zeta = \frac{1}{.682 + .455e^{(.01H)^2} + .00213e^{(.01D)^2} - .683e^{(.01H)}} \tag{3-3}$$

This equation was developed using the mean values of the input data and produced a very high correlation. (The R^2 value is equal to 96.1%.) While this correlation value is very good it results from input data sets which are inadequate. Only seven sets were located which fell within this range of consideration. Unfortunately, these data sets were at both extremes of the range, leaving a void between about 30 feet and 100 feet. The high correlation was obtained because Eqn. 3-3 matched the input data very well. However, as might be expected, the use of this equation resulted in very high predicted values of damping in the range where input data were lacking. Figs. 3.13 and 3.14 show Eqn. 3-3 in plots of damping versus building height for representative values of building width.

While the inadequacy of the data set precludes the use of Eqn. 3-3, it should be noted that the consideration of concentrating on this lower range for future endeavors in damping prediction would seem to be justified. Thus, when additional data become available in the range where they are now lacking, a more accurate prediction equation having a high correlation can be developed.

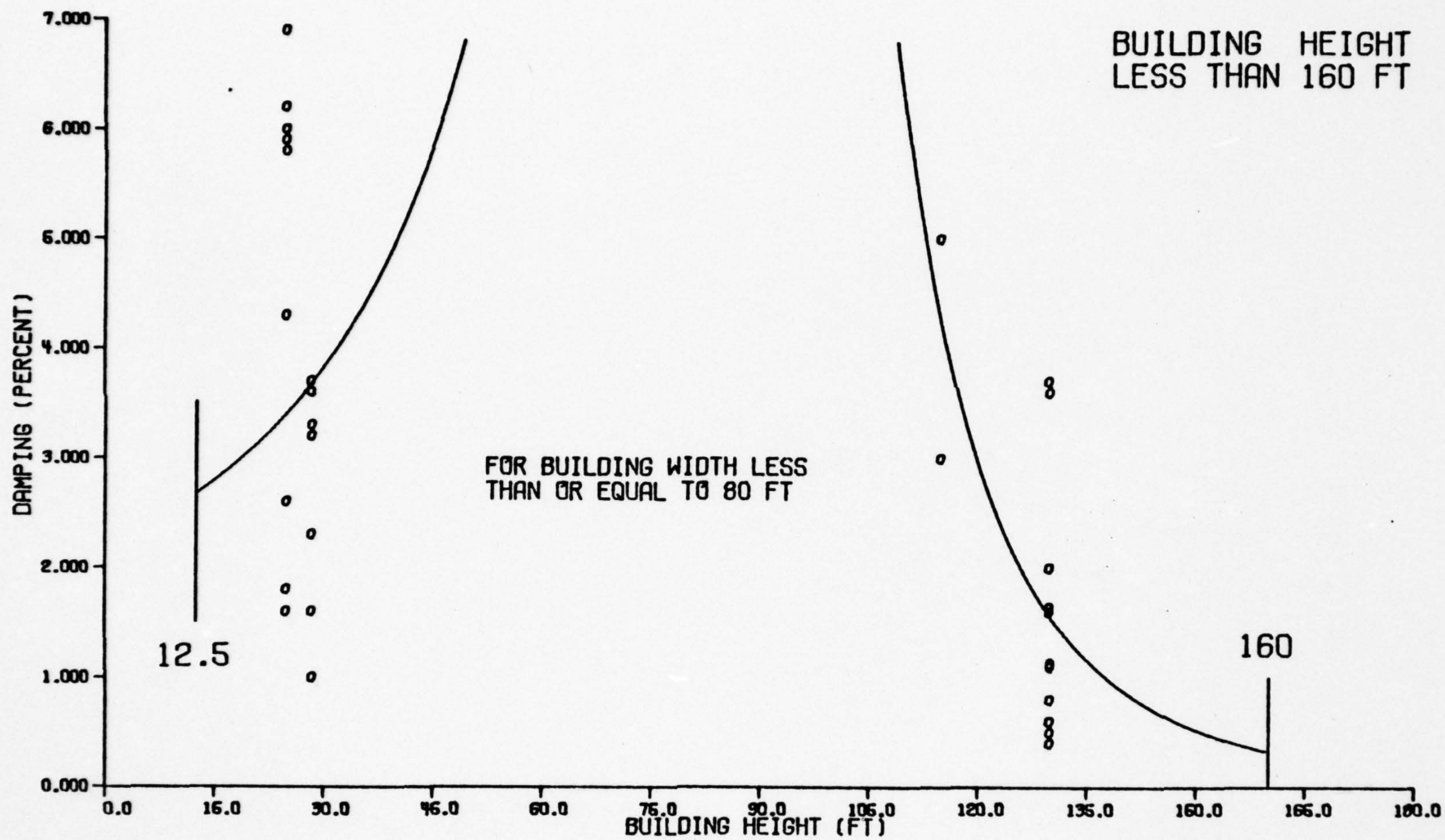

FIGURE 3.13
DAMPING FROM EQUATION 3-3

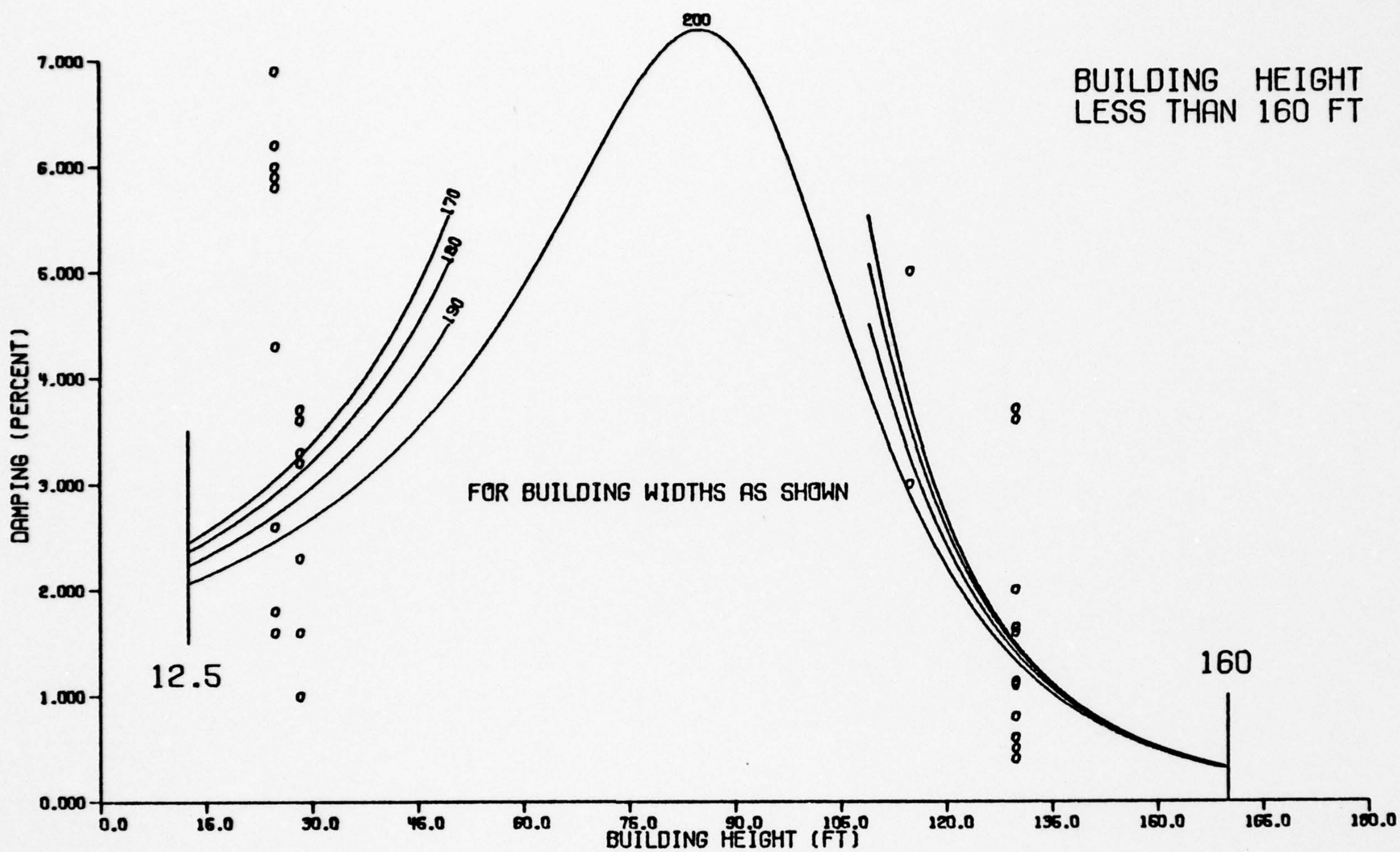

FIGURE 3.14
DAMPING FROM EQUATION 3-3

3.3.3.2 Building Heights Greater Than 160 Feet. Most of the experimental studies reported in the literature have been conducted on relatively tall, steel, moment-resistant framed buildings. The available data more completely represents the possible heights and widths. Thus, the regression equation developed is valid for the entire range of consideration in this section. This equation is:

$$\zeta = \frac{1}{-.196 + .562e^{(.001H)^2} + .000522e^{(.01D)^2} - .014e^{(.01D)}} \tag{3-4}$$

Eqn. 3-4 was developed using mean values of damping as the input data. The resulting correlation is high (R^2 = 91.17%). When the same basic form of Eqn. 3-4 was used with all the available data as input, the following resulted:

$$\zeta = \frac{1}{-.168 + .425e^{(.001H)^2} + .000715e^{(.01D)^2} + .0223e^{(.01D)}} \tag{3-5}$$

The R^2 value for this equation is equal to 30.4%.

Eqn. 3-4 is presented graphically for representative values of building width in Figs. 3-15 and 3-16. Either Eqn. 3-4 or the graphs of Figs. 3-15 and 3-16 could be used to predict values for damping. However, this equation and these graphs pertain only to the range of building heights greater than 160 feet, and since no adequate similar expression can be found for the lower range of building

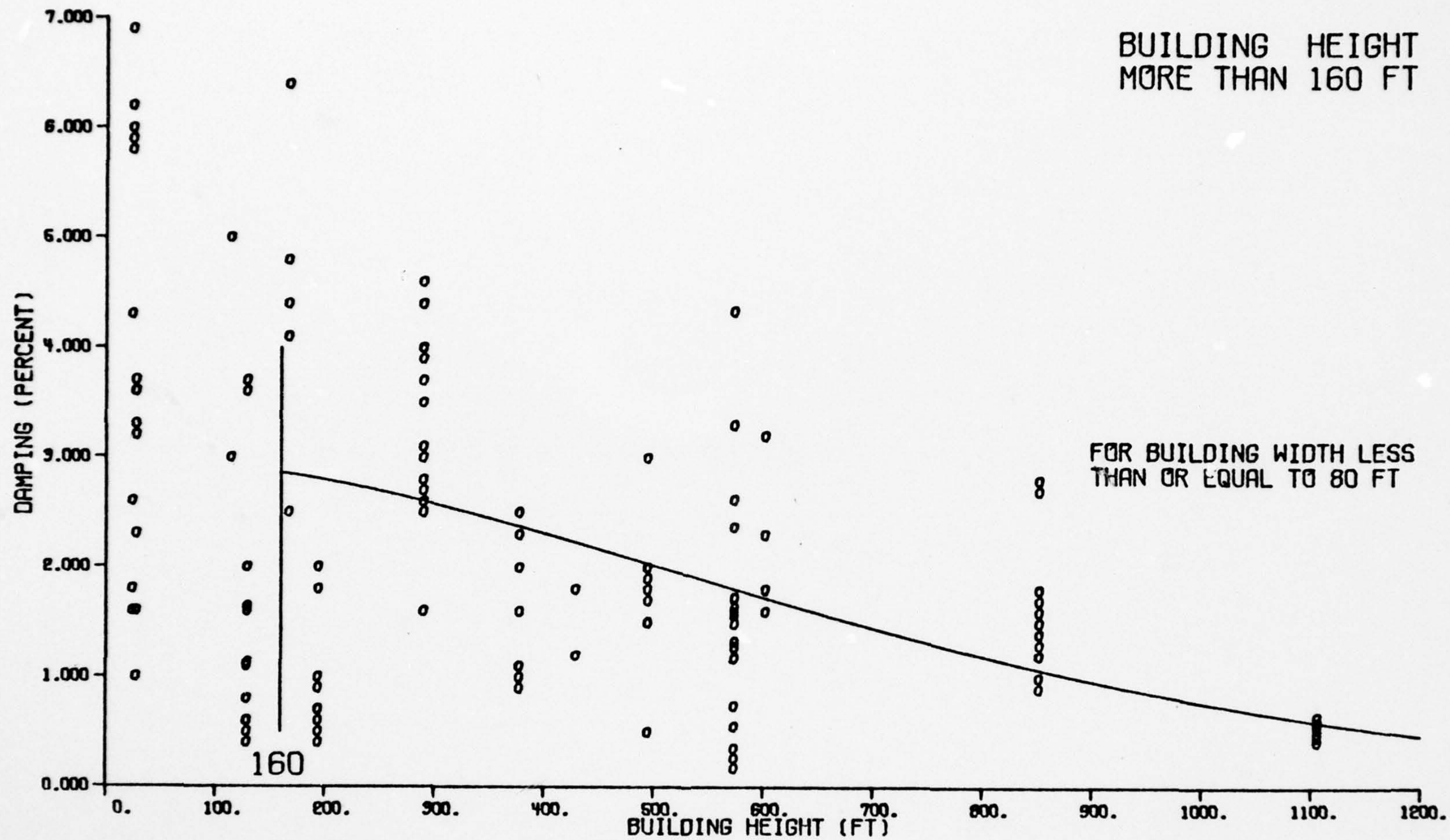

FIGURE 3.15
DAMPING FROM EQUATION 3-4

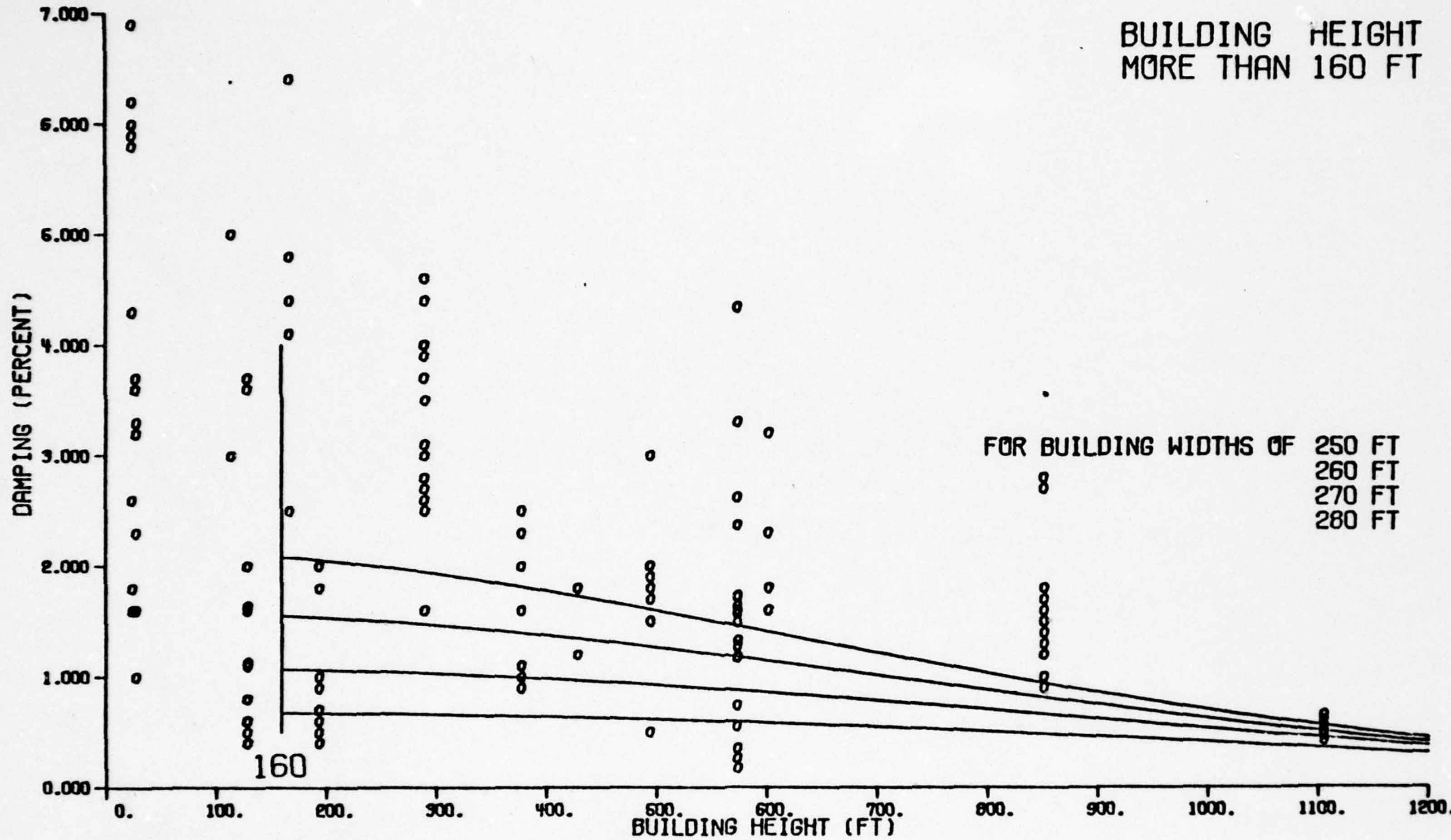

FIGURE 3.16
DAMPING FROM EQUATION 3-4

heights, no further effort will be given to the development of a relationship based upon height classification.

3.3.3.3 Building Heights in Entire Range of Data Values. The range of applicability herein is between 12.5 feet, considered the approximate height of a one-story structure, and 1200 feet. This range includes all the data sets available for input. The best relationship developed using the mean values for the input data set is:

$$\zeta = \frac{1}{-.155 + .597e^{(.001H)^2} + .00041e^{(.01D)^2} - .078e^{(.001H)}} \tag{3-6}$$

The R^2 value for this equation is equal to 84.2%. Eqn. 3-6 is shown graphically for representative values of building widths in Figs. 3-17, 3-18, and 3-19. The Metric system equivalent of Eqn. 3-6 is:

$$\zeta = [-.155 + .597e^{(.00328H)^2} + .00041e^{(.0328D)^2} - .078e^{(.00328H)}]^{-1} \tag{3-7}$$

where: H,D in meters.

It should be noted that Eqn. 3-7 yields identical results to those from Eqn. 3-6. The only difference is the measurement system. However, as was noted in section 3.3.3, Eqn. 3-7 is somewhat cumbersome to use due to the form of the exponential terms. If the Metric system is selected

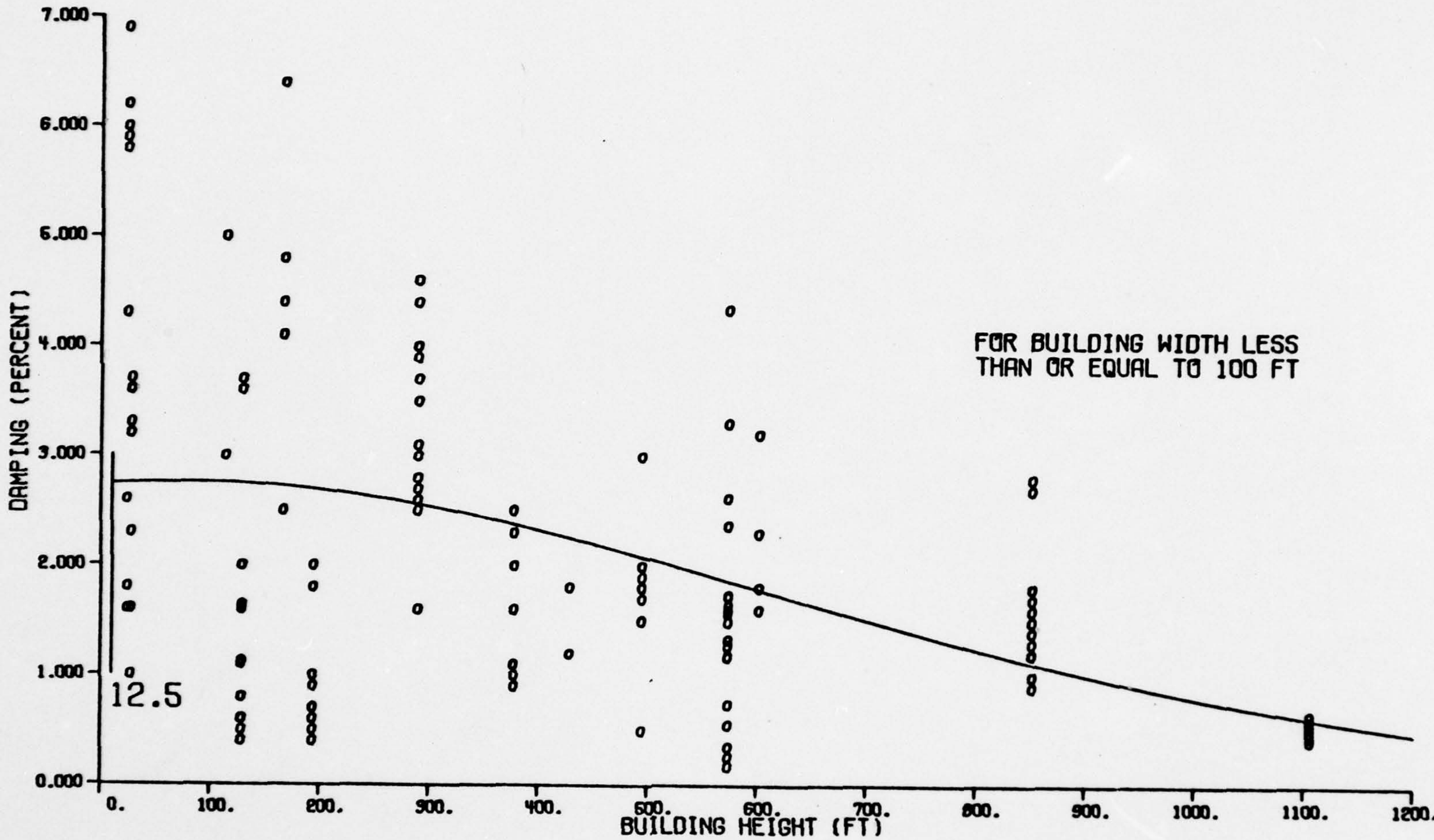

FIGURE 3.17
DAMPING FROM EQUATION 3-6

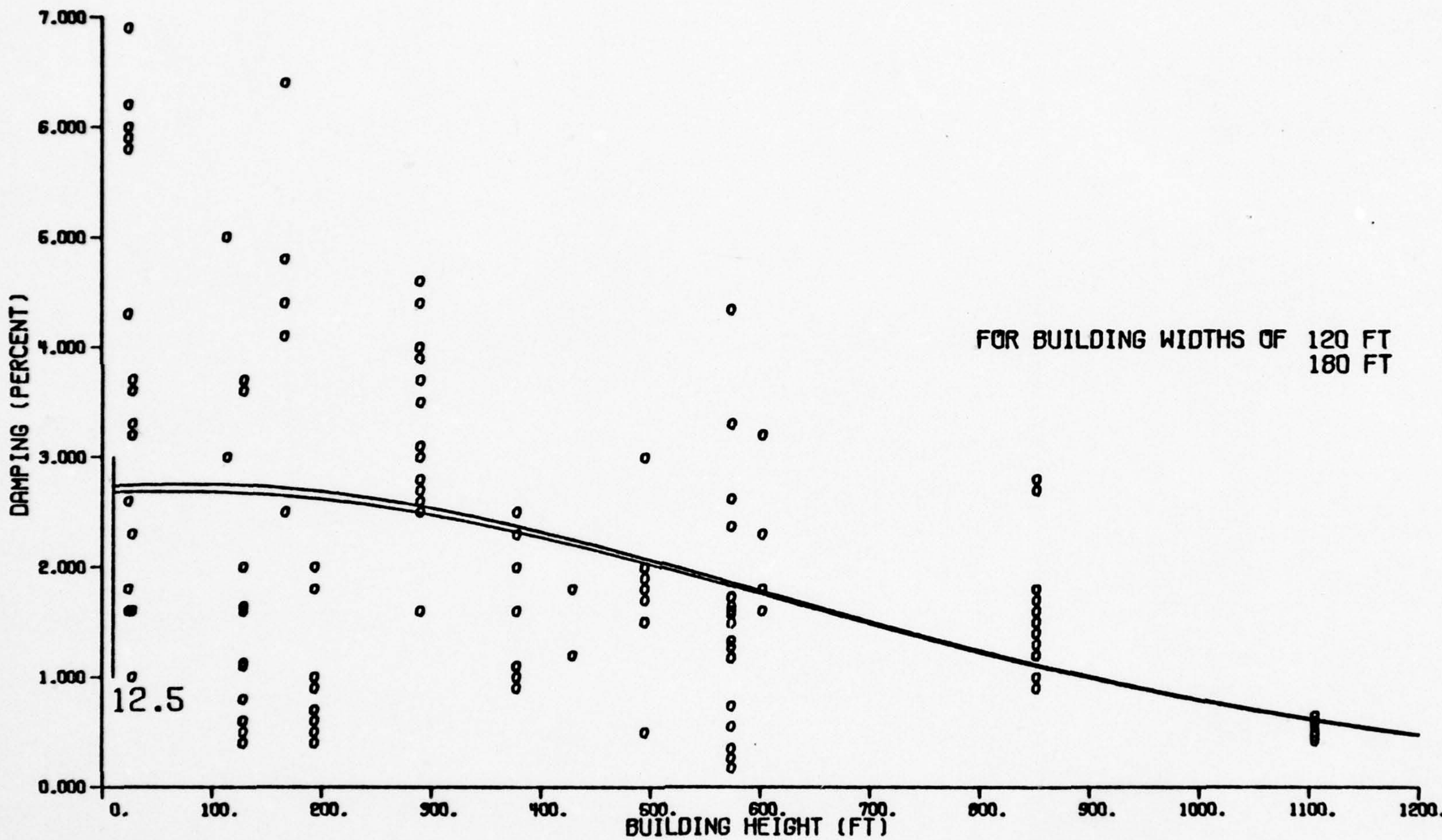

FIGURE 3.18
DAMPING FROM EQUATION 3-6

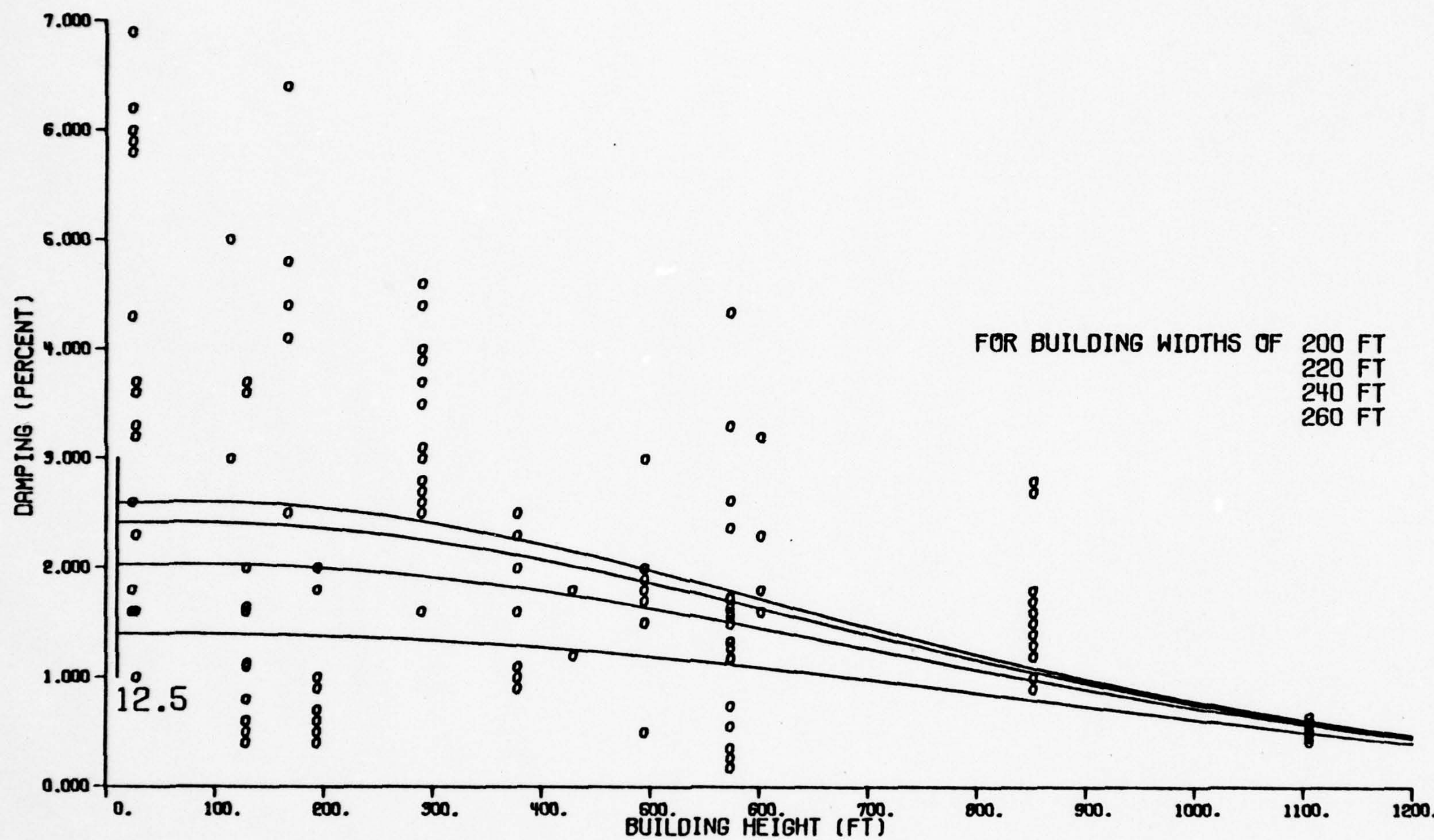

FIGURE 3.19
DAMPING FROM EQUATION 3-6

for use, a more convenient expression is developed in Appendix D.

If the basic form of the relationship in Eqn. 3-6 is used with all the data available as input, the following expression results:

$$\zeta = \frac{1}{.227 + .51e^{(.001H)^2} + .000956e^{(.01D)^2} - .204e^{(.001H)}} \tag{3-8}$$

The R^2 value for Eqn. 3-8 is equal to 22.24%.

With all the data used in the input data set in an effort to determine the best relationship without a preconceived notion of its form, the following was developed:

$$\begin{aligned}\zeta = &- 13.5 + .024H - 1.85(H/D) - 5.7(D/H) - 217816(1/HD)\\ &+ 9777\left(\frac{1}{H+D}\right) + .000000049(H^2D) - .000035(H^2+D)\\ &+ .00377(H^2/D) + 422(D/H^2) + 4195825\left(\frac{1}{H^2D}\right)\\ &- 69136\left(\frac{1}{H^2+D}\right)\end{aligned} \tag{3-9}$$

Although the R^2 value for Eqn. 3-9 is equal to 61.5%, which is greater than the R^2 value from Eqn. 3-8, the expression of Eqn. 3-9 is cumbersome and lengthy, and thus is not suited for practical usage. Because of the low correlation value of Eqn. 3-8, it is not desirable for further use either. Therefore, Eqn. 3-6 (or Eqn. 3-7) is recommended for use in the prediction of the damping of a

building from its height and width. It is the best equation of those tried, and has an R^2 value which is within the high correlation range. This equation and the associated graphs will be used as the basis of the methodology developed in this dissertation.

3.4 Sensitivity Analysis. Eqn. 3-6 will yield a value of damping that is an average, or mean value for the structure as a whole without regard for the nature of its composition (material, system or structural, etc.), or for the mode of excitation. Given this predicted value and its associated standard deviation, a statement of the uncertainty, expressed in terms of the coefficient of variation (COV), can be made. The coefficient of variation is defined as:

$$\mathrm{COV} = \frac{\sigma}{\bar{x}} \qquad (3\text{-}10)$$

where:

σ = standard deviation

$\bar{x}$ = mean value of x.

In words, the COV is an indication of how "good" the predicted mean value is considered to be. A low COV (say less than 15% or 20%) indicates that there is little variation in the mean value, and thus there is less uncertainty in its value. On the other extreme, a high COV (say greater than 80% or so) indicates wide variation in $\bar{x}$ and thus more uncertainty in the estimation (prediction) of its value.

In order to examine the COV's of building responses corresponding to predicted damping values, sensitivity analyses using first order approximation will be performed. These analyses relate the mean values of the predicted damping and the building response, and their variances. Another form of sensitivity analysis performed herein is a comparison between the mean predicted damping value and the maximum (and minimum) value in the experimental data set for a given building height and width. The results from this analysis show the amount of variation that the observed damping values are from the predicted mean value. In both analyses, response displacement to a low amplitude excitation was used and, to this end, a spectral displacement-damping relationship was developed in Appendix C.

3.4.1 Determination of Means and Variances of Building Displacement Response. To determine these values, the first order approximation was used. This concept is discussed briefly herein.

Using Taylor's Series, any function B = B(x) may be expanded as follows

$$B = B(x) = B(a) + B'(a)\,\frac{x-a}{1} + B''(a)\frac{(x-a)^2}{2}$$

$$+ B'''(a)\frac{(x-a)^2}{3!} + \cdots + B^{(n-1)}(a)\frac{(x-a)^{n-1}}{(n-1)!}$$

$$+ \text{remainder} \qquad (3\text{-}11)$$

where:

a is any quantity whatever, so chosen that none of the expression $B(a)$, $B'(a)$, $B''(a)$, ... became infinite.

$B'(a)$, $B''(a)$, ... are successive derivatives of the function B evaluated at a.

Taylor's Series is applicable to any function including those which contain more than one variable. Thus, if it is considered that the function to be expanded is $B = B(x_1, x_2, \ldots x_n)$, and if it is desired to use the mean value in the expansion, μ, μ_2, ... μ_n, where,

$$\mu_i \equiv E[x_i] \tag{3-12}$$

(μ_i is simply the mean or expected value of the variable x_i) then Eqn. 3-11 becomes [89]:

$$B = B(x_1, x_2 \ldots x_n) = B(\mu_1, \mu_2, \ldots \mu_n) + \sum_{i=1}^{n} (x_i - \mu_i) \frac{\partial B}{\partial x_i}\bigg|_{\mu_i}$$

$$+ \frac{1}{2} \sum_{i}\sum_{j} (x_i - \mu_i)(x_j - \mu_j) \frac{\partial^2 B}{\partial x_i \partial x_j}\bigg|_{\mu} + \ldots \tag{3-13}$$

If this expansion is truncated after the first summation term, the result becomes the first order approximation of the function B, or:

$$B = B(\mu_1, \mu_2, \ldots \mu_n) + \sum_{i=1}^{n} (x_i - \mu_i) \frac{\partial B}{\partial x_i}\bigg|_{\mu_i} \tag{3-14}$$

Thus, the mean value of B, μ_B, can be determined by using Eqn. 3-12, or:

$$\mu_B \equiv E[B] = E[B(\mu_1, \mu_2, \ldots \mu_n) + \sum_{i=1}^{n} (x_i - \mu_i)\frac{\partial B}{\partial x_i}\Big|_{\mu_i}] \tag{3-15}$$

or,

$$\mu_B = E[B(\mu_1, \mu_2, \ldots \mu_n)] + E[\sum_{i=1}^{n} (x_i - \mu_i)\frac{\partial B}{\partial x_i}\Big|_{\mu_i}] \tag{3-16}$$

Since the expected value of the mean values are the mean values, and $E(\sum_{i=1}^{n} (x_i - \mu_i) \frac{\partial B}{\partial x_i}\Big|_{\mu}] = 0$, Eqn. 3-16 becomes:

$$\mu_B = B(\mu_1, \mu_2, \ldots \mu_n) \tag{3-17}$$

If the variance of B is defined as:

$$\text{Var } B \equiv E[B^2] - \mu_B^2 = \sigma_B^2 \tag{3-18}$$

σ_B^2 can be determined using Eqn. 3-14:

$$\begin{aligned} E[B^2] = E[B^2(\mu_1, \mu_2, \ldots \mu_n) \\ + 2B(\mu_1, \mu_2, \ldots \mu_n) \sum_{i=1}^{n} (x_i - \mu_i) \frac{\partial B}{\partial x_i}\Big|_{\mu_i} \\ + \sum_i \sum_j (x_i - \mu_i)(x_j - \mu_j)\frac{\partial B}{\partial x_i} \frac{\partial B}{\partial x_j}\Big|_{\mu}] \end{aligned} \tag{3-19}$$

The last term of Eqn. 3-19 is a combination of a variance and covariance term as follows:

$$E\left[\sum_{i=1}^{n}(x_i - \mu_i)^2 \left(\frac{\partial B}{\partial x_i}\right)^2\Big|_\mu\right] = \sum_{i=1}^{n}[(x_i - \mu_i)^2]\left(\frac{\partial B}{\partial x_i}\right)^2\Big|_\mu$$

$$= \sum_{i=1}^{n}\sigma_i^2 \left(\frac{\partial B}{\partial x_i}\right)^2\Big|_\mu \qquad (3\text{-}20)$$

$$E\left[\sum_i \sum_j (x_i - \mu_i)(x_j - \mu_j) \frac{\partial B}{\partial x_i}\frac{\partial B}{\partial x_j}\Big|_\mu\right]$$

$$= \sum_i \sum_j \mathrm{cov}(x_i, x_j)\frac{\partial B}{\partial x_i}\frac{\partial B}{\partial x_j}\Big|_\mu \qquad (3\text{-}21)$$

If x_i and x_j are considered to be statistically independent, then the covariance term of Eqn. 3-21 vanishes. Realizing the first term of Eqn. 3-19 to be μ_B^2 (from Eqn. 3-17) and the second term to be zero, Eqn. 3-19 becomes:

$$E[B^2] = \mu_B^2 + \sum_{i=1}^{n} \sigma_i^2 \left(\frac{\partial B}{\partial x_i}\right)^2\Big|_\mu \qquad (3\text{-}22)$$

Hence, the variance of B defined in Eqn. 3-17 is:

$$\sigma_B^2 = \sum_{i=1}^{n}\sigma_i^2 \left(\frac{\partial B}{\partial x_i}\right)^2\Big|_\mu \qquad (3\text{-}23)$$

Thus, the mean value and variance of a dependent variable can be approximated using Eqns. 3-17 and 3-23 if the mean values and variances of the independent variables are known. The sensitivity analyses performed herein use these first order approximations to determine the mean values and variances of building response displacements from the mean

values and variances of the damping value predicted for the building by Eqn. 3-6 (or Eqn. 3-7). To do this, the displacement response spectrum for a typical low amplitude earthquake is used. This is developed in Appendix C. Eqns. C-12, C-13, and C-14 are the relationships developed between spectral displacement and damping for various ranges of building period. For the purpose of these analyses, it is assumed that the spectral displacement for zero percent damping, $S_{d(0\%)}$, is a constant and is determined from Fig. C.2 for any T.

The procedure, then, is as follows:

1. Use Eqns. 3-6 (or 3-7) to determine the mean value of damping, $\bar{\zeta}$. The standard deviation is constant, and equals .48421. Thus the variance of damping is .23446.

2. Use some method to determine T. This can be accomplished in several ways to include code formulas [87], measurement, assumptions, etc. For these analyses, the average experimental values are used.

3. Use Fig. C.2 to determine $S_{d(0\%)}$.

4. Use Eqn. C-12, C-13, or C-14 in conjunction with the first order approximation technique to determine the mean values and variances of the spectral displacements.

5. Use the following equation [16] in conjunction with the first order approximation technique to determine the mean values and variances of the displacement responses:

$$\vec{x}_{n_{max}} = \vec{\Phi}_n \frac{L_n}{M_n^*} S_{d_n} \qquad (3\text{-}24)$$

where:

$\vec{x}_{n_{max}}$ is the vector of maximum displacements of mode n;

$\vec{\Phi}_n$ is the shape factor vector;

L_n is the earthquake participation factor

M_n^* is the generalized mass

While there are at least three ways to determine the maximum value of displacement at any point in the structure as reported by Clough [16], and Stockdale [74], for the purpose of these analyses it will be assumed that the fundamental mode controls. Thus, the maximum displacement at the top of the building under consideration will be the maximum displacement found by using Eqn. 3-24.

The above procedure was followed for representative building heights throughout the range of applicability. The results are tabulated in Table 3.4. These results contain two revelations:

1. The coefficient of variation for the entire range of building heights is low. The worst COV is equal to .440 for the 60-story building. The general trend seems to be a higher COV with increasing building heights. Numerically, this is expected since the mean value for the predicted damping essentially decreases with increasing building height and, of course, the standard deviation is constant. Physically, this also is expected since there would be more

TABLE 3.4

SENSITIVITY ANALYSIS RESULTS

Bldg Ht, H (ft)	25	25	130	130	168	168	291	291	853
Bldg Wdth, D (ft)	20	21	40	220	168	238	70	180	174
No. of stories	2	2	9	9	12	12	22	22	60
$\bar{\zeta}$, fm Eqn. (%)	2.75	2.75	2.75	2.40	2.70	2.10	2.55	2.50	1.10
σ_ζ	.484	.484	.484	.484	.484	.484	.484	.484	.484
COV	.176	.175	.177	.202	.181	.235	.190	.194	.440
σ^2_ζ	.234	.234	.234	.234	.234	.234	.234	.234	.234
T (sec)	.449	.872	.500	.413	.930	1.04	2.5	2.6	1.48
$S_{d(0\%)}$ (in.)	.172	.304	.190	.154	.322	.356	.80	.83	.492
$\bar{S}_d$ (in.)	.065	.190	.119	.061	.203	.238	.599	.624	.370
$\sigma^2_{S_d}$ $(10)^{-5}$	1.41	7.04	2.78	1.55	8.32	14.86	48.5	53.7	67.2
$\bar{x}_{max}$ (in.)	.077	.225	.146	.075	.291	.341	.776	.809	.689
$\sigma^2_{x_{max}}$ $(10)^{-5}$	1.97	9.85	4.21	2.35	17.0	30.5	81.5	90.2	233
COV	.058	.044	.044	.065	.045	.051	.037	.037	.070

expected variations in the damping values due to the higher complexities of the structural make-up, thus there is more uncertainty about the value predicted by equation.

2. The displacement responses are all small for the type earthquake excitation used ($\bar{x}_{max}$ in Table 3.4). Further, the resulting COV's are also very low, being less than 7.0% in all cases. This indicates that for the type of sensitivity analysis performed herein, there is a high degree of certainty surrounding the displacement response. Thus, it is concluded that the predicted damping value from Eqn. 3-6 (or Eqn. 3-7) is good for accurately estimating the displacement response of a building to a low amplitude excitation.

<u>3.4.2 Comparison of Predicted and Experimentally-Determined Damping Values</u>. The second type of sensitivity analysis performed was the comparison of the predicted damping value with the highest and lowest damping values in the experimental data set for a given building height and width. The same procedure outlined in section 3.4.1 was followed in this comparison, except the experimentally-determined damping values were used. This was done twice for each building considered, with the highest experimental value used first, then the lowest. This analysis was performed to get an idea of the spread, or variation, between the response displacements, and thus to see how sensitive building response is to changes in damping values.

The results are tabulated in Table 3.5. Two observations are made when analyzing this table: (1) the differences between the displacement responses determined from the predicted damping values, and those determined from the highest and lowest experimental damping values, in absolute terms, and (2) these differences in percentages. When the differences in absolute terms are considered, the maximum difference is .129 inches (from the 291 foot high, 180 foot wide building). The average value for all 18 comparisons is .048 inches. Thus, even when considering the overall low values for displacement response, it is felt the absolute differences are tolerable and reflect favorably upon the use of the developed equations (Eqn. 3-6 or 3-7) to predict damping.

When the differences in percentages are considered, the maximum difference is 53.3% (for the 130 foot high, 220 foot wide building). This is considered a more important statistic than just considering the differences in absolute terms because it is not dependent upon magnitude. Thus, the value of 53.3% indicates that displacement response can vary as much as 50% from the displacement response calculated from the predicted damping value. However, it must be remembered that the predicted damping value is considered to be an average value, and thus some variance is to be expected. When considering the overall range of comparisons, the average percentage difference

TABLE 3.5

COMPARISON OF PREDICTED AND EXPERIMENTALLY-DETERMINED DAMPING VALUES

Bldg Ht, H (ft)	25	25	130	130	168	168	291	291	853
Bldg Wdth, D (ft)	20	21	40	220	168	238	70	180	174
No. of stories	2	2	9	9	12	12	22	22	60
$\bar{\zeta}$ fm Eqn. (%)	2.75	2.75	2.75	2.40	2.70	2.10	2.55	2.50	1.10
ζ_{max}(exp'm'l)(%)	6.90	6.00	3.70	2.00	6.40	4.80	4.40	4.60	2.80
ζ_{min}(exp'm'l)(%)	1.80	1.60	0.40	0.50	4.10	2.50	1.60	1.60	0.90
$\bar{x}$ fm mean (in.)	.077	.225	.146	.075	.291	.341	.776	.809	.689
x fm max (in.)	.056	.177	.135	.080	.221	.272	.714	.680	.570
diff. (in.)	.021	.048	.011	.005	.070	.069	.062	.129	.119
%	27.1	21.3	7.5	6.7	24.0	20.2	8.0	15.9	17.3
x fm min. (in.)	.089	.254	.199	.115	.258	.327	.874	.842	.711
diff. (in.)	.012	.028	.053	.040	.033	.014	.098	.033	.022
%	15.1	12.7	36.3	53.3	11.3	4.1	12.6	4.1	3.2

between the extreme values and the mean is 16.7%. This is considered to be an excellent correlation, and also indicates that the use of the developed equations results in good predictions of damping values.

CHAPTER IV

PRESENTATION OF THE DESIGN METHODOLOGY

4.1 General Remarks. The method for estimating damping as presented in Chapter III is based upon the correlation between damping and building height and width. This procedure involves the use of Eqns. 3-6 or 3-7, or Figs. 3.17, 3.18 and 3.19 for obtaining an estimated value for the viscous damping ratio, ζ, in design calculations. By using this approach a reasonable damping value is obtained.

In general, there are four distinct phases to a dynamic seismic design [79]:

1. The establishment of a design ground motion.
2. The determination of a damping value and a risked-based, acceptable stress and distortion performance.
3. The determination of the dynamic response of the building to the design ground motion.
4. A stress and distortion analysis for the forces generated by the dynamic response.

This design methodology is initially pertinent in phase 2. Its use enables the estimation of the damping ratio by utilizing a prediction equation. As shown in Figs. 3.17 through 3.19, a relationship between damping and

building height and width definitely can be obtained.

4.2 Design Methodology. Teal [79] states that the damping value for steel moment-resistant frames might be assumed as 5%. This value is based upon the expectation that inelastic deformation will occur. Apparently this value is one which many engineers currently use in their design calculations. Private communications from prominent engineers tend to support this. However, it is believed that if a strong, large-amplitude dynamic force excites a structure beyond the elastic range energy mechanisms which are not present in the elastic behavioral range add to the damping level. Since these mechanisms include failure of non-structural elements, yielding of members, and the like, they cannot be quantified. Their addition to damping, however, can make the equivalent viscous damping ratio even greater than 5%.

However, it is believed that the use of a 5% damping value is too high in elastic analyses, and would result in the underestimation of damage that a low intensity excitation could cause. Figs. 3.17 through 3.19 show damping values to be less than 3% throughout the entire range of building heights, widths considered. This is in agreement with the values which were adopted by the Nuclear Regulatory Commission as reported by Haviland [35]. These values range from 2% to 7% for steel structures depending upon whether they are welded or bolted and how near to the yield

point the stresses are expected to be. For low stress levels (below 50% of yield) the range of values is 2% to 4%. These values may still be too high, however, especially for tall buildings. While data was not available to permit classification by type of connections of the steel structures studied here, the following methodology nevertheless provides more exact values than those reported by Haviland by taking advantage of the relationship which exists between damping and building height and width.

This procedure is primarily applicable in the early stages of design when one needs only to establish those parameters required to use the developed equations. Basic building dimensions will normally be established quickly in any design as these depend upon such variables as capital restrictions, space requirements, building usage, and/or owner preference. In short, the building height and widths should be dictated by both architectural and engineering criteria. However, some engineering judgements would have to be made. A design engineer would need to determine that a steel moment-resistant frame comprises the main structural system for the building. Further, the building would have to be free-standing without supplemental structural support from adjacent structures.

The building should be founded on soil of adequate bearing capacity to support design loads so that piling is not needed. This was the condition for all the sample

buildings used in the input data set, except the Hancock Center. Soil-structure interaction affecting the damping value is not considered explicitly herein, and is assumed to provide a negligible contribution to damping for the sample buildings. This methodology can thus be used for buildings which are founded on soil that have these same characteristics. Extrapolation to buildings founded on piles is not endorsed. This method should not be used to predict damping whenever the engineer considers the soil-structure interaction in his design as a major contribution to damping.

The methodology is applicable only to buildings with regular shapes; it is not applicable to buildings with reentrant corners. Because of the stress concentrations associated with this type of configuration additional reinforcement, which alters the relevant dynamic properties, must be provided. The data base from which this methodology was developed did not include such structures. Consequently, no basis exists for applying the methodology to such buildings.

If it is determined that the characteristics of the building being designed are consistent with the assumptions upon which the methodology is based, the design engineer can use either Eqn. 3-6 or 3-7 to predict the damping ratio for his building. It should be noted that it is sufficient to use a value of damping determined from these equations

which is rounded to the nearest 0.1%. This is the best precision one can reasonably expect by using Figs. 3.17 through 3.19. For example, for a 20-story building which satisfies the conditions described above and with height equal to 250 feet and width equal to 180 feet, the damping ratio from Eqn. 3-6 is 2.559%. It is sufficient to use 2.6% for subsequent design calculations.

4.3 Decision Tree. The regression equations developed herein also form the basis for a procedure which can be used in the dynamic analysis of structures. This procedure, or methodology is presented as the decision-tree of Fig. 4.1:

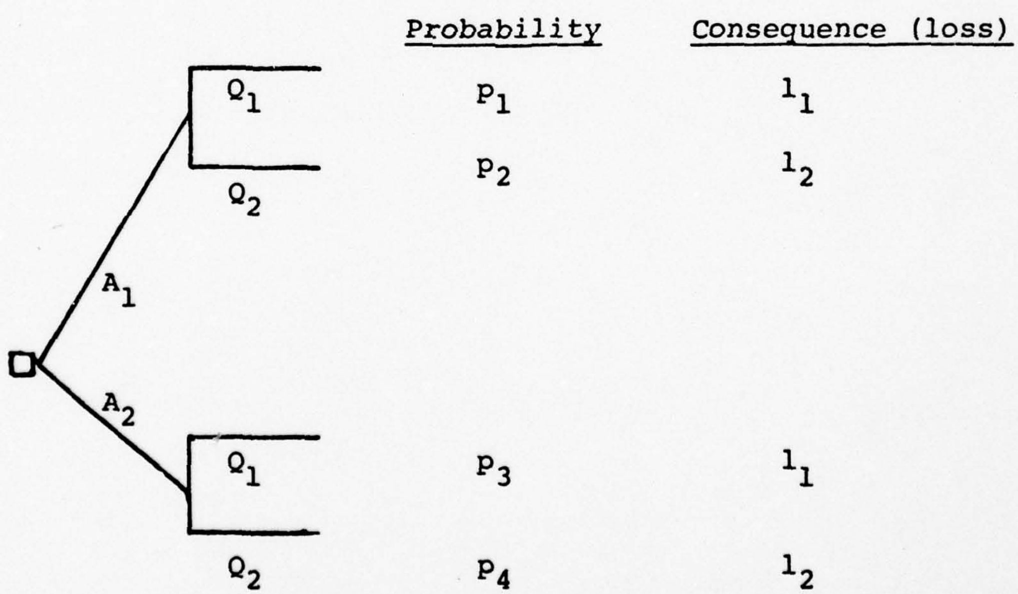

FIGURE 4.1

DECISION TREE

where:

A_1 = No experimentation needed; use the prediction equation

A_2 = Test the structure, collect data and estimate damping

Q_1 = Estimated value "correct"

Q_2 = Estimate value "incorrect"

Note:

$$p_1 + p_2 = 1 \tag{4-1}$$

$$p_3 + p_4 = 1 \tag{4-2}$$

$$\text{Expected loss for } A_1 = p_1 l_1 + p_2 l_2 \tag{4-3}$$

$$\text{Expected loss for } A_2 = p_3 l_1 + p_4 l_2 \tag{4-4}$$

A decision whether to test a structure to determine its damping value can be made using this methodology. The basis of this decision is a comparison of the loss one would expect from using the prediction equations (Eqn. 4-3) with those from using actual test data to estimate the damping ratio (Eqn. 4-4). This assessment of relative loss involves the subjective assignment of values to the various probabilities and consequences depicted in Fig. 4.1. These values are dependent upon circumstances surrounding each structure which is to be aanlyzed. These circumstances include time factors, cost factors, building and occupancy importance factors, etc. No attempt is made herein to develop guidelines, or limiting values for these factors as such work

is left for future endeavor. At this time any consistent evaluation of these parameters is sufficient to make this methodology useful.

CHAPTER V

CONCLUSIONS AND RECOMMENDATIONS

5.1 Conclusions. The extent of the applicability of the methodology derived in Chapter III is limited. However, since objectivity is at the basis of its development, its use will result in damping determinations which are consistent among design engineers. Further, the limit of damping values predicted by Eqns. 3-6 or 3-7 is shown in Figs. 3.17-3.19 to be less than 3% for all values of building height and building width considered. This is significantly less than the 5% presently being assumed for steel moment-resistant structures [79]. It appears, therefore, that this design methodology may have application in the broad area of damage estimation since the damage due to a low level excitation would be underestimated by a designer who uses 5% as the estimated damping value for a steel moment-resistant structure. This is presented as a possible consideration only, since the topic of damage estimation is not considered in this study.

For taller buildings, the damping values predicted are less than those reported by Haviland [35]. Consequently, it is believed that the values presented by Haviland could

be used as an upper limit for damping predictions when the intensity of the excitation force is expected to be low, i.e., low enough such that induced stresses are in the linear-elastic range.

5.1.1 Applicability. The design methodology has range limitations. It is proposed for use when the expected excitation force is of low intensity level, such as for earthquake tremors or wind forces. Thus this design methodology is applicable in its present form to structures which are designed for linearly-elastic responses.

Other conditions which must be satisfied for this design methodology to be applicable are presented in section 4.2. These restrictions are predicated upon the nature of the input data set used in the development of the methodology. While this will be discussed in the next section, it should be noted that such conditions are stipulated only to insure that the design methodology is used for structures which are "similar" to those which comprise the input data set. Reasonable extrapolations will no doubt be made by design engineers in certain cases, but it should be obvious that such decisions will necessarily be based to some degree on subjective judgements. Consequently, such usage would to some degree, negate the objectivity of the design methodology.

5.1.2 Data Availability. Two conclusions relating to data availability were drawn in this study. First, considerable additional experimentation is needed on structures with a variety of height and width ratios if further refinements of these empirically-derived relationships are to be made. Even though there are problems inherent in conducting these tests, as has been discussed in Chapter I, it is believed this study shows that test results can be used to develop relationships that are effective and dependable means for predicting damping values of buildings. Obviously, the more tests that are conducted and documented, the better the relationship that can be developed insofar as prediction accuracy is concerned.

A total of 16 experiments on 14 steel-framed buildings ranging in height from 25 feet to 1107 feet have been used herein. Since only these few buildings over this range of heights were tested, gaps exist in the data set. The type result that such gaps can produce in empirical deviations is exemplified by the relationships developed in section 3.3.3.1 when building heights of less than 160 feet were considered separately. In addition to the lack of repeated data on the shorter buildings, there is a similar lack of data on the tall buildings, e.g., those taller than about 600 feet. Only two buildings taller than this height, the 853 foot TRANSAMERICA BUILDING and the 1107 foot JOHN HANCOCK CENTER, were found to have been reported in the

open literature as having been tested to determine dynamic properties.

The second conclusion which has been drawn concerns the nature of the experimental data that is reported. It has become evident that inconsistencies exist in the amount and type of experimental results that are reported. These inconsistencies hamper subsequent research of the type conducted herein. If the design methodology using empirically-derived relationships is to be refined/improved beyond its current state, the conditions for its use as mentioned in section 4.2 must be more precisely defined. This can only be achieved if the results of forced vibration generator tests and ambient tests are couched in similar and consistent parameters. While it would be presumptuous to expect that the form of reporting test results should be standardized, it is not unrealistic to expect that the results from experiments which are similar in intent and design should be similar in content also. The detailed literature search conducted as a part of this study revealed that such similarities and consistencies do not now exist in the open literature.

5.2 Recommendations. The recommendations which are developed as a result of this work relate to future vibration testing procedures, future refinements of this work, and use of these empirically-derived relationships. These

areas of concern are not independent as the recommendation pertaining to the use of these equations (methodology) is a function of the extent and nature of future-related work done of this type.

Future endeavors directed toward refinements of this work should be considered. In the absence of simple theoretical determinations for the viscous damping ratio of buildings, empirical determinations can be used. These empirical relationships, however, are only as good and exact as the input data set used in their derivation. Thus, the following recommendations are made in connection with the conduct and reporting of vibration experiments:

1. More experimentation on actual steel-framed buildings should be performed. Especially, tests should be conducted on several buildings with heights of between 30 and 100 feet, between 200 and 300 feet, and greater than 600 feet. (These reflect the gaps in the data which exist presently.)

2. Results of such experiments should include, as a minimum, the following:

a. A complete description to include name, location, height, widths, number of stories, typical story height, number of bays in direction considered, type of structural system, shape, type of foundation, non-structural elements (in linear feet or equivalent), secondary or additional structural elements (in linear feet or equivalent),

type of floor system, type of connections, type of fire-proofing, nature of occupancy (office, apartment, etc.), and any special members included in the design to resist design loads and thus affect the dynamic properties of the building (like grade beams, permanent interior partition walls, etc.).

b. Method of measuring damping values (bandwidth, logarithmic decrement, etc.); a description of this method should be included, especially if unique, or not widely known.

c. Modal information to include frequencies, periods, damping values and measured mode shapes for both translational and torsional modes.

d. Mass or weight (design dead load) presented by floors as in a lumped mass system.

The following recommendations are made in connection with the conduct of future-related work based upon these experiments:

1. The basic analytical relationship should be refined to include factors for nonmeasurable features like shape, foundation type, type of connections, amount and type of non-structural elements, amount and type of fire-proofing, type of floor system, occupancy type, and special structural members included.

2. The effect of building width should be reexamined and relative importance evaluated. Since damping appears to

be weakly correlated to this parameter, it might be more important to include width effects in some other form, like number of bays, for example.

3. Relationships should be developed for damping in each translational mode and in the torsional mode.

4. Relationships should be developed for buildings with heights less than 160 feet separate from those greater than 160 feet. Since existing structures reflect different design philosophies for these two ranges of height, separate relationships may produce better correlations for estimating the damping parameter.

Finally, a long-term goal is reflected in the following recommendation which is made in connection with the use of these empirically-derived relationships. As mentioned in the introduction to this section, this recommendation has as a basis the realization of future-related work as just described: The empirically-derived relationships could be incorporated in seismic design and/or analysis procedures which use response to earthquake excitation as a basis. An example is the use of the earthquake response spectra to analyze the response of a structure to an earthquake of certain intensity.

LIST OF REFERENCES

1. Bathe, K. J., Wilson, E. L., and Peterson, F. E., "SAP IV - Structural Analysis Program for Static and Dynamic Response of Linear Systems," Report No. EERC 73-11, Earthquake Engineering Research Center, Univ. of California, Berkeley, Calif., 1973.

2. Beliveau, J. G., "Identification of Viscous Damping in Structures from Modal Information," J. Appl. Mech. Trans., ASME, v. 43, Ser. E., n. 2, June 1976, pp. 335-339.

3. Benfer, N. A., and Coffman, J. E., eds., San Fernando, California, Earthquake of February 9, 1971, Environmental Research Laboratories, National Oceanic and Atmospheric Administration, U.S. Department of Commerce, U.S. Government Printing Office, Washington, D.C., 1973.

4. Benya, J. S., A Forced Vibration Study of a Steel Framed Building, M.Sc. Thesis, School of Engineering, University of California, Los Angeles, Calif., 1967.

5. Berg, G. V., "Designing for Earthquakes," Contemporary Steel Design, American Iron and Steel Institute, New York, N.Y., v.2, n.3, 11 pgs.

6. Blevins, R. D., Flow-Induced Vibration, Van Nostrand Reinhold Company, New York, N.Y., 1977.

7. Blume, J. A., "A Machine for Setting Structures and Ground into Forced Vibration," Bull. Seism. Soc. Am., v.25, n.1, 1935, pp. 361-379.

8. Blume, J. A., "Motion and Damping of Buildings Relative to Seismic Response Spectra," Bull. Seism. Soc. Am., v.60, n.1, 1970, pp. 231-259.

9. Blume, J. A., and Assoc., Engineers, "A Compilation of Measured Damping Values of Structures and Structural Elements," report prepared for Westinghouse, Feb., 1970.

10. Bouwkamp, J. G., "Dynamics of Full Scale Structures," Applied Mechanics in Earthquake Engineering, W.D. Iwan (ed.), ASME, New York, N.Y., 1974, pp. 99-134.

11. Bouwkamp, J. G., "Research on the Structural Damping of Steel Trussed and Framed Multistory Building," Third World Conference on Earthquake Engineering, v.III, New Zealand, 1965, pp. IV-112 - IV - 122.

12. Bouwkamp, J. G., and Blohm, J. K., "Dynamic Response of a Two-story Steel Frame Structure," Bull. Seism. Soc. Am., v.56, n.6, 1966, pp. 1289-1303.

13. Caravani, P., and Thomson, W. T., "Frequency Response of a Dynamic System With Statistical Damping," AIAA Journal, v.11, n.2, Feb., 1973, pp. 170-173.

14. Caravani, P., and Thomson, W. T., "Identification of Damping Coefficients in Multidimensional Linear Systems," J. Appl. Mech., June 1974, pp. 379-382.

15. Chen, S. J. H., Methods of System Identification In Structural Engineering, M. Sc. Thesis, School of Engineering, Purdue University, West Lafayette, Ind., 1976.

16. Clough, R. W., "Earthquake Response of Structures," Earthquake Engineering, R. L. Wiegel (coordinating ed.), Prentice-Hall, Inc., Englewood Cliffs, N.J., 1970.

17. Clough, R. W., and Li, F. L-Y., "The Dynamic Behavior of a First-Story Girder of a Three-Story Steel Frame Subjected to Earthquake Loading," Earthquake Engineering Research Center, Report No. EERC 75-35, College of Engineering, University of California, Berkeley, Calif., 1975.

18. Clough, R. W., and Penzien, J., Dynamics of Structures, McGraw-Hill, Inc., New York, N.Y., 1975.

19. Clough, R. W., and Tang, D. T., "Earthquake Simulator Study of a Steel Frame Structure, Vol. I: Experimental Results," Earthquake Engineering Research Center, Report No. EERC 75-6, College of Engineering, University of California, Berkeley, Calif., 1975.

20. Cook, R. D., Concepts and Applications of Finite Element Analysis, John Wiley & Sons, Inc., New York, N.Y., 1974.

21. Corotis, R. B., and Vanmarcke, E. H., "Time-Dependent Spectral Content of System Response," J. Engr. Mech. Div., ASCE, v.101, n.EM5, Oct. 1975, pp. 623-637.

22. Davenport, A. G., Hogan, M., and Vickery, B. J., "An Analysis of Records of Wind Induced Building Motion and Column Strain Taken at the John Hancock Center (Chicago)," BWLT-10-1970, The University of Western Ontario, London, Canada, 1970.

23. Degenkolb, H. J., "Earthquake Forces on Tall Structures," Bethlehem Steel Co., 25 pgs.

24. Degenkolb, H. J., Dean, R. G., and Wyllie, L. A., Jr. "Earthquake Resistant Design of Structures Seminar," Reprint of lecture notes from presentation to the New York Metropolitan Section of the American Society of Civil Engineers in Mar. and Apr. 1971.

25. Foutch, D. A., "A Study of the Vibrational Characteristics of Two Multistory Buildings," Earthquake Engineering Research Laboratory, EERL 76-03, California Institute of Technology, Pasadena, Calif., 1976.

26. Gallo, M. P., and Ang, A. H -S., "Evaluation of Safety of Reinforced Concrete Buildings to Earthquakes," Report No. UILU-ENG-76-2018, Civil Engineering Studies, University of Illinois, Urbana-Champaign, Ill., 1976.

27. Gersch, W., "On the Achievable Accuracy of Structural System Parameter Estimates," J. Sound Vib., v.34, n.1, May 1974, pp. 63-79.

28. Gersch, W. and Foutch, D. A., "Least Squares Estimates of Structural System Parameters Using Covariance Function Data," IEEE Trans. Automatic Control, AC-19, 1974, pp. 898-903.

29. Gersch, W., Nielsen, N. N. and Akaike, H., "Maximum Likelihood Estimation of Structural Parameters from Random Vibration Data," J. Sound Vib., v.31, n.3, 1973, pp. 295-308.

30. Hanson, R. D., " Static and Dynamic Tests of a Full Scale Steel Frame Structure," Earthquake Engineering Research Laboratory, California Institue of Technology, Pasadena, Calif., 1965.

31. Hart, G. C. and Collins, J. D. "Study of Modeling of Substructure Damping Matrices," SAE preprint, n. 720813 for meeting Oct. 2-5, 1972, pp. 2408-2416.

32. Hart, G. C. and Vasudevan, R., "Earthquake Design of Buildings: Damping," J. of the Structural Div., ASCE, n.ST1, Jan. 1975, pp. 11-29.

33. Hart, G. C. and Yao, J. T. P., "System Identification In Structural Dynamics," J. Engr. Mech. Div., ASCE, v.103, n.EM6, Dec. 1977, pp. 1089-1104.

34. Hasselman, T. K., "Method for Constructing a Full Modal Damping Matrix from Experimental Measurements," AIAA Journal, v.10, n.4, Apr. 1972, pp. 526-527.

35. Haviland, R., "A Study of the Uncertainties in the Fundamental Translational Periods and Damping Values for Real Buildings," Report No. R76-12, Massachusetts Institute of Technology, Department of Civil Engineering, Cambridge Mass., Feb. 1976.

36. Hobbs, G. K., "Methods for Modeling and Analyzing Viscoelastically Damped Structures," ASME Pap. 71-Vibr.-36, Sep. 8-10 1971, 8 pgs.

37. Hudson, D. E., "Dynamic Tests of Full Scale Structures," Earthquake Engineering, R. L. Wiegel (coordinating ed.), Prentice-Hall, Inc., Englewood Cliffs, N.J., 1970.

38. Hudson, D. E., "Resonance Testing of Full Scale Structures," J. Engr. Mech. Div., ASCE, v.90, n.EM3, June 1964, pp. 1-9.

39. Hudson, D. E., "Dynamic Tests of Full Scale Structures," J. Engr. Mech. Div., ASCE, v.103, n.EM6, Dec. 1977, pp. 1141-1157.

40. Hudson, D. E., "Synchronized Vibration Generators for Dynamic Tests of Full-Scale Structures," Earthquake Engineering Research Laboratory, California Institute of Technology, Pasadena, Calif., 1962.

41. Ibanez, P., "Identification of Dynamic Parameters of Linear and Nonlinear Structural Models from Experimental Data," Journal of Nuclear Engineering and Design, v.25, 1973, pp. 30-41.

42. Ibanez, P., "Methods for the Identification of Dynamic Parameters of Mathematical Structural Models from Experimental Data," Journal of Nuclear Engineering and Design, v.27, 1974, pp. 209-219.

43. Jennings, P. C., Matthiesen, R. B. and Hoerner, J. B., "Forced Vibrations of a Tall Steel-Frame Building," Int. J. of Earthquake Engineering and Structural Dynamics, v.1, n.2, Oct.-Dec. 1972, pp. 107-132.

44. Jennings, P. C., Matthiesen, R. B., and Hoerner, J. B., "Forced Vibration of a 22-Story Steel Frame Building," Earthquake Engineering Research Laboratory, EERL 71-01, California Institute of Technology, Pasadena, Calif., 1971.

45. Kanai, K., and Yoshizawa, S., "On the Period of Damping of Vibration in Actual Buildings," Bull. Earthquake Res. Inst., University of Tokyo, v.39, part 3, Sep. 1961.

46. Keightley, W. O., "Vibration Tests of Structures," Earthquake Engineering Research Laboratory, California Institute of Technology, Pasadena, Calif., 1961.

47. Lew, H. S., Leyendecker, E. V., and Dikkers, R. D., Engineering Aspects of the 1971 San Fernando Earthquake, Building Science Series 40, Building Research Division, Institute for Applied Technology, National Bureau of Standards, U.S. Department of Commerce, U.S. Government Printing Office, Washington, D.C., 1971.

48. Lazan, B. J., Damping of Materials and Members in Structural Mechanics, Pergamon Press, Inc., New York, N.Y., 1968.

49. Lazan, B. J., "Energy Dissipation Mechanisms in Structures with Particular Reference to Material Damping," Structural Damping, J. E. Ruzicka (ed.), ASME, N.Y., 1959, pp. 1-34.

50. Lazan, B. J., and Goodman, L. E., "Material and Interface Damping," Shock and Vibration Handbook, v.11, C. M. Harris and C. E. Crede (eds.), McGraw-Hill Book Co., Inc., New York, N.Y., 1961, pp. 36-1- 36-46.

51. Matzen, V. C., and McNiven, H. D., "Identification of the Energy Absorption Characteristics of an Earthquake Resistant Structure: Identification of Parameters from Shaking Table Experiments," ASCE-EMD Specialty Conf., UCLA Extension, Mar. 30-31 1976, pp. 330-341.

52. McGuire, W., Steel Structures, Prentice-Hall, Inc., Englewood Cliffs, N.J., 1968.

53. McNiven, H. D., and Matzen, V. C., "Identification of the Energy Absorption Characteristics of an Earthquake Resistant Structure: Description of the Identification Method," ASCE-EMD Specialty Conf., UCLA Extension, Mar. 1976, pp. 402-411.

54. Merritt, R. G., "Equivalent Viscous Damping of Elasto-Plastic Systems Under Sinusoidal Loading," Tech. Rpt., Dept. of the Army, Construction Engineering Research Laboratory, Champaign, Ill., May 1977, 31 pgs.

55. Morrone, A., "Damping Values of Nuclear Power Plant Components," Condensation of a Westinghouse Nuclear Energy Systems Report, WCAP-7921, same title, Nov. 1972.

56. Murphy, G., Similitude In Engineering, The Ronald Press Company, New York, N.Y., 1950.

57. Newmark, N. M., "Current Trends In the Seismic Analysis and Design of High-Rise Structures," Earthquake Engineering, R. L. Wiegel (coordinating ed.), Prentice-Hall, Inc., Englewood Cliffs, N.J., 1970.

58. Nie, N., Brent, D. H., and Hull, C. H., Statistical Package for the Social Sciences, McGraw-Hill Book Company, New York, N.Y., 1970.

59. Nielsen, N. N., "Dynamic Response of Multistory Buildings," Earthquake Engineering Research Laboratory, California Institute of Technology, Pasadena, Calif., 1964.

60. Nielsen, N. N., "Vibration Tests of a Nine-Story Steel Frame Building," J. Engr. Mech. Div., ASCE, v.92, n.EM1, Feb. 1966, pp. 81-110.

61. NSF-UCEER Conference on Earthquake Engineering Research, Mar. 10-11, 1967, report, California Institute of Technology, Pasadena, Calif., 1967.

62. Petrovski, J., Stephen, R. M., Gartenbaum, E., and Bouwkamp, J. G., "Dynamic Behavior of a Multistory Triangular-Shaped Building," Earthquake Engineering Research Center, Report No. EERC 76-3, College of Engineering, University of California, Berkeley, Calif., 1976.

63. Plunkett, R., "Measurement of Damping," Structural Damping, J. E. Ruzicka (ed.), ASME, N.Y., 1959, pp. 117-131.

64. Raggett, J. D., "Estimating Damping of Real Structures," J. of the Structural Div., ASCE, n.ST9, Sep. 1975, pp. 1823-1835.

65. Rea, D., Bouwkamp, J. G., and Clough, R. W., "The Dynamic Behavior of Steel Frame and Truss Buildings," AISI Bull., n.9, Apr. 1968.

66. Rea, D., Clough, R. W., Bouwkamp, J. G., and Vogel U., "Damping Capacity of a Model Steel Structure," Earthquake Engineering Research Center, Report No. EERC 69-14, College of Engineering, University of California, Berkeley, Calif., 1969.

67. Richardson, M., and Potter, R., "Viscous Vs. Structural Damping in Modal Analysis," 46th Shock and Vibration Symposium, San Diego, Calif., Oct. 1975.

68. Rodeman, R., Estimation of Structural Dynamic Model Parameters, Ph.D. Thesis, School of Engineering, Purdue University, West Lafayette, Ind., 1974.

69. Schiff, A. J., "Identification of Large Structures Using Data From Ambient and Low Level Excitations," System Identification of Vibrating Structures, ASME, Winter Meeting, New York, N.Y., 1972.

70. Seismic Design for Buildings, Department of the Army, (TM5-809-10), Navy (NAV FAC P-355), and Air Force (AFM 88-3, Chap. 13), Apr. 1973.

71. Shannon, R. D., A Forced Vibration Study of a Completed Five-Story Steel Frame Building, M. Sc. Thesis, School of Engineering, University of California, Los Angeles, Calif., 1969.

72. Stephen, R. M. Bouwkamp, J. G., Clough, R. W., and Penzien, J., "Structural Dynamic Testing Facilities at the University of California, Berkeley," Earthquake Engineering Research Center, Report No. EERC 69-8, College of Engineering, University of California, Berkeley, Calif., 1969.

73. Stephen, R. M., Hollings, J. P., and Bouwkamp, J. G., "Dynamic Behavior of a Multistory Pyramid-Shaped Building," Earthquake Engineering Research Center, Report No. EERC 73-17, College of Engineering, University of California, Berkeley, Calif., 1974.

74. Stockdale, W. K., "Modal Analysis Methods in Seismic Deisgn for Buildings," Tech. Rpt. n. M-132, Dept. of the Army, Construction Engineering Research Laboratory, Champaign, Ill., June 1975, 36 pgs.

75. Sweet, A. L., Schiff, A. J., and Kelley, J. W., "Identification of Structural Parameters Using Low-Amplitude Impulsive Loading," Journal of Acoustical Society of America, v.57, n.5, May 1975, pp. 1128-1137.

76. Tall, L., Beedle, L. S., Galambos, T. V. (eds.), Structural Steel Design, The Roland Press Company, New York, N.Y., 1964.

77. Tanaka, T., Yoshizawa, S., Osawa, Y., and Morishita, T., "Period and Damping of Vibration in Actual Buildings During Earthquakes," Bull. Earthquake Res. Inst., University of Tokyo, v.47, part 6, Nov. 1969, pp. 1073-1092.

78. Taoka, G. T., Hogan, M., Khan, F. R., and Scanlan, R. W., "Ambient Response Analysis of Some Tall Structures," J. of the Structural Div., ASCE, n.ST1, Jan. 1975, pp. 49-65.

79. Teal, E. J., "Seismic Design Practice for Steel Buildings," Engineering J. Am. Steel Construction, v.12, n.4, 4th Quarter 1975, pp. 101-151.

80. Thomson, W. T., Calkins, T., and Caravani, P., "A Numerical Study of Damping," J. of Earthquake Engineering and Structural Dynamics, v.3, 1974, pp. 98-103.

81. Torkamani, M. A. M., and Hart, G. C., "Building System Identification Using Earthquake Date," Rpt. No. UCLA-ENG-7507, Mechanics and Structures Department, School of Engineering and Applied Science, University of California, Los Angeles, Calif., Jan. 1975.

82. Torres, M. R., and Mote, C. D., Jr., "Expected Equivalent Damping Under Random Excitation," J. of Engineering for Industry, ASME, Series B, v.91, Nov. 1969, pp. 967-974.

83. Trifunac, M. D., "Ambient Vibration Test of a Thirty-nine Story Steel Frame Building," Earthquake Engineering Research Laboratory, EERL 70-02, California Institute of Technology, Pasadena, Calif., 1970.

84. Trifunac, M. D., "Comparisons Between Ambient and Forced Vibration Experiments," Earthquake Engineering and Structural Dynamics, n.1, 1972, pp. 133-150.

85. Trifunac, M. D., "Wind and Microtremor Induced Vibrations of a Twenty-two Story Steel Frame Building," Earthquake Engineering Research Laboratory, EERL 70-01, California Institute of Technology, Pasadena, Calif., 1970.

86. Uchida, N., Aoyagi, T., Kawamura, M., and Nakagawa, K., "Vibration Test of a Steel Frame Having Precast Concrete Panels," Fifth World Conference on Earthquake Engineering, Rome, Italy, June 25-29, 1973, pp. 1167-1176.

87. Uniform Building Code, 1976 Edition.

88. Ward, H. S., and Crawford, R., "Wind Induced Vibrations and Building Modes," Bull. Seism. Soc. Am., v.56, n.6, 1966, pp. 793-813.

89. Yao, J. T. P., C. E. 574 class notes on Introduction to Structural Reliability, School of Engineering, Purdue University, West Lafayette, Ind., 1977.

90. Yao, J. T. P., Omid'varan, C., Gurpinar, A., and Hulsbos, C. L., "Seismic Design of Building Structures," Tech. Rpt. n. 5-10, Dept. of the Army, Construction Engineering Research Laboratory, Champaign, Ill., Jul. 1972, 144 pgs.

Appendix A

Description of Buildings Used in Analysis

The following building descriptions are taken from the cited references.

CENTURY CITY THEME TOWERS [62] are twin multi-story structures, forty-four stories in height above the plaza level, and six underground parking levels, located in Los Angeles, California. The dynamic tests were performed on the South Tower during November, 1974 and March, 1975. The height of the building is 575 feet above the plaza level. It has an equilateral triangular floor plan with sides of 254 feet. The steel frame structure consists of core triangular frames with three corner columns connected by deep beams at the second floor of the building. Steel framing for the building core, similar to that for the lower floors, extends from the second floor to the roof. The exterior walls are constructed as three identical moment-resistant frames with twenty-three bays of 10 feet 2 inches. A deep steel girder covering the top two floors is rigidly connected to all three exterior frames. Thus, the structural system consists of the equilateral triangular core and exterior moment-resistant frames connected at each floor with shear-end-connected beams. The reinforced concrete floor slabs in the core part are 4 1/2 inches deep; the composite exterior slabs are 4 1/2 inches in depth over 18 gage steel deck. The core frame columns are rolled sections of W14

shape, and the core sections are in general rolled sections, mostly wide flange shape varying from W12 to W36. Exterior columns consist of standard W series sections and built-up sections. Exterior frame spaced beams are built-up girders with a constant depth of four feet and differing plate thicknesses. Deep exterior beams at the top of the building and at the second floor level are also built-up sections with depths of twenty-eight feet and seven feet, respectively. The structural steel used in the building for both the beams and the columns is A36 and A50, the latter (high strength steel) being used in general in the lower floors. Below the ground level the structural system consists of reinforced concrete elements forming peripheral core walls with a thickness of 20 inches and core reinforced concrete columns connected to rigid slabs at each parking level. The corner columns are also reinforced concrete members with dimensions at the lowest level of 20 by 20 feet. The core part of the building rests on a triangular shaped mat eight feet thick. The top of the mat is located about 66 feet below the plaza level. The corner columns rest on individual foundation mats with thicknesses of 14 feet and plan dimensions of about 40 x 45 feet for the north and 40 x 49 feet for the south columns. The foundation mat is placed in a silty sand layer.

The TRANSAMERICA BUILDING [73] is a multi-story pyramid-shaped steel structure, 60 stories in height,

located in San Francisco, California. The 853 foot high building has a square plan, 174 x 174 feet, and consists of a two-story high ground floor, a triangularly shaped tubular space truss around the perimeter between the 2nd and 5th floor levels, and above this level a moment-resistant frame with the exterior walls sloping inward at an approximate ratio of 1 to 11. The upper 10 stories consist of an open-framed pyramid shaped structure which will not be occupied. On the east and west sides of the building, starting just below the 30th floor, shafts project from the building which contain elevators on the east side and a stairwell and duct shaft on the west side. The main exterior frame geometry consists of single columns, extending through three below-ground floors and resting directly on a nine foot thick reinforced concrete mat. The columns extend to the 2nd floor level where they meet the sloping pryamidal columns. The 5th floor level is the apex of four columns which fan out in a pyramidal fashion while having their base on the 2nd floor. On the perimeter of the building these sloping pyramidal columns form a network of three dimensional space frames between the 5th and 2nd floor levels. The main N-S and E-W frames are the same from the 5th floor up; however, starting between the 29th and 30th floor up to the 50th floor, shafts project from the building on the east and west sides. The main exterior columns slope inward from the 5th floor level at an

approximate ratio of 1 to 11. The building stiffness is provided by the conventional rigid frame system above the 5th floor and below the 2nd floor, with the three dimensional space frames in between. This gives the overall structure a mixed system of flexible portion (below the 2nd floor), rigid portion (between 2nd and 5th floors), and flexible portion (above the 5th floor). A system of 4 "K" braces are introduced in the first story, symmetrically placed within the building, stiffening this story and making it compatible with the stiff system between the 2nd and 5th floors. The building interior moment-resistant framing consists of four frames in each direction up to the 17th floor, and two frames in each direction from the 17th floor to the 45th floor. The columns are fabricated square box sections varying in outside dimensions from 30 inches at the Plaza level to 18 inches at the top of the building. The main framing beams are rolled section varying from W36 to W14. The structural steel for both beams and columns is A36 and A572 grade 42, the latter high strength steel being used for the lower floors up to the 5th floor. Underground, the beam and column steel is encased in concrete. The exterior of the building is faced with a reinforced concrete precast stone paneling. This paneling is structurally attached to the building frame and extends to the 50th floor. Over the upper 10 stories the columns are faced with precast stone elements; the

space between the columns is covered with an aluminum louvered paneling. The paneling is structurally attached using clip angles on the lower section and rods on the upper section.

The MAIN EAST BUILDING [65] and its service tower are one of twin facilities comprising the Medical Center complex at the University of California in San Francisco. An elevator tower serves all buildings in the complex through a connecting corridor. The East Building is 195 feet (15 stories) high, and its outside plan dimensions are 107 x 107 feet. This building is one story shorter than the West Building. The steel columns of the moment-resistant steel frames are placed 10 feet in from the perimeter of the building at on-center spacings of 30 feet 1 1/2 inches, 33 feet 4 inches, and 30 feet 1 1/2 inches along each side. The reinforced slabs were cast in place using lightweight concrete. Although the buildings were designed as free standing structures, there are two types of non-structural connections which exist on every floor level at points of access from one building to another. First, bellows-type aluminum ducts run the whole height of the buildings for weatherproofing purposes; secondly, in order to permit traffic between buildings, steel plates bolted to ledges on the service tower and to the floor slabs of the connecting corridor span the gap to the East Building, where they rest freely on the floor slabs. Structural connections between

the East Building and its service tower are present at the ground floor level, and at the foundation level. These connections consist of reinforced concrete beams and slabs. The mechanical service tower and elevator towers are constructed of vertical steel trusses stiffened by encasing them entirely in concrete. The height of both towers is approximately 200 feet. The elevator tower is 30 x 30 feet, and the service tower 20 x 36 feet in plan. The central section of each mechanical service tower is occupied by a stairwell, and the spaces on either side of the stairwell by piping and ventilation ducts. The elevator tower contains six elevator shafts. It serves both main buildings through a connecting corridor which leads into corridors around the central core of each main building.

The RALPH M. PARSONS COMPANY WORLD HEADQUARTERS [25] is a steel-frame structure located in Pasadena, California. The headquarters consists of three buildings. Two identical four-story satellite structures are located to the north-east and northwest of the main building. The main structure has a large four-story portion at the south end and a 12-story tower that is roughly octagonal in shape on the north side. The tower is approximately 168 feet high and 168 x 238 feet in plan. Separation joints are provided at the satellite end of the walkway joining the central building to the satellite structures. This separation joint is 2 inches wide at the 2nd floor level and 5 inches wide at the

3rd, 4th, and 5th floor levels. The lateral loads are resisted by full moment-resisting steel frames. The girders of all frames in the structure not designed as moment-resisting have shear end connections and were designed to carry only gravity loads. The foundation system is composed of individual spread footings with pedestals beneath each column. The bottoms of the footings beneath the tower columns of the moment-resisting frames are 14 feet below the finished floor levels of the 1st floor; those beneath the columns of the four story portion are seven feet below this level. Grade beams are also provided along the column lines of the moment-resisting frames. These measure 5 feet by 3 feet beneath the tower, and 3 feet by 2 feet 3 inches for the others.

The CENTRAL ENGINEERING BUILDING [9, 55, 59, 60] located on the California Institute of Technology campus in Pasadena, California, is a 9-story steel frame building, 220 x 40 feet in plan. The floor slabs are 5 inch reinforced lightweight concrete slabs. The 10th floor contains room for heavy equipment. At the time when most of the steady-state vibration tests were performed, the weight of each of the floors above the 2nd floor, except for the 10th, was estimated from construction drawings to be approximately 920 kips. The 10th floor was estimated to have a weight of 1640 kips. The steel-frame was designed to carry all loads. At the final stage of construction, wire mesh and plaster

were used on the inside of the columns to complete the fireproofing of the steel columns. The building is characterized by the very rigid girders in the long E-W direction. The welded girders are attached to the columns by high strength bolts. The girders have a depth of 6 feet 6 inches, typical top and bottom chords are 8 inch channels. The welded trusses in the short N-S direction are attached to the columns by high strength bolts. The typical truss has a depth of 3 feet 4 inches, top chords consisting of two 5 inch by 3 inch angles, and bottom chords consisting of two 6 inch by 3 1/2 inch angles. The beams in the long E-W direction are W12 x 27. Staircases are located at the ends of the building. The staircase sections are attached to the building by expansion joints; they add no appreciable stiffness to the building. The floor slabs had voids to accommodate air conditioning ducts and elevators; these can be assumed to have a negligible effect on the vibrational characteristics of the building.

The UNION BANK BUILDING [83] in the city of Los Angeles rises for 42 stories (536 feet) from the second basement level to the roof, with 39 stories (496 feet) above the plaza level. The tower is of rectangular cross section, 14 by 7 bays, or 196 x 98 feet. The typical story height above the 11th floor is 12 feet 1 inch. Three levels of parking together with a plaza level 302 x 514 feet surround the lower four stories of the central tower. The main

entrance and lobby are on the plaza level. The 2nd through 39th floors are occupied by offices; the 1st and 2nd basements and the street level are used for parking, storage, office services, rental area, truck loading and mechanical equipment. The air handling equipment occupies the 39th floor. The structural steel frames are moment-resistant for vertical and lateral loads for the full height of the tower. Shear walls are provided from the 2nd basement level to the 2nd floor. Typical floor construction consists of lightweight concrete over steel beams of seven feet spacing. The tower is structurally separated from the parking structure by a joint allowing two inches of differential horizontal movement. Spread footings are continuous under the exterior columns of the tower and in the transverse direction under the shear core. Individual spread footings support interior columns.

The SAN DIEGO GAS AND ELECTRIC COMPANY office complex [43, 44, 85] occupies a city block in downtown San Diego, California. The complex consists of two buildings: a 22-story tower and a 2-story U-shaped building. The two story building envelops the tower on three sides but is structurally separated from the tower by three inch seismic joints. Together, the buildings have over 325,000 square feet of floor space and are occupied by nearly 1000 employees. The 291 foot tower is approximately 180 x 70 feet in plan. The structural system is a moment-resistant,

ductile steel-frame supporting 21 floor levels and a roof above grade, and two levels below. There are seven frames aligned E-W and three frames in the N-S direction. Girders join the columns in both directions, and intermediate beams, which support the floor system, are framed into the girders in the N-S direction. The girders and beams are rolled shapes, whereas the columns are 24 inch built-up sections. The framing changes at the top two levels of the structure, but is essentially symmetrical. A36 steel is used throughout. The typical floor system for the office portions of the tower consists of cellular steel decking intermittently welded to the structural frame. The decking is topped with approximately 2 inches of concrete. Five-inch reinforced concrete slabs cast over the floor beams are used in areas where the loading is heavier, and a reinforced concrete slab, composite with the floor system, is used to support the heavy mechanical equipment on the 20th and 21st floors. All steel framing below the 1st floor of the structure is encased in reinforced concrete. Above this level, fireproofing is achieved by metal lath and plaster facing on the columns, and by a sprayed layer of Zonolite plaster on the beams, girders and undersides of the steel decking of the floors. The fireproofing undoubtedly contributes to the stiffness of the structure, especially for small displacements. The interior walls of the building are of 4 inch and 6 inch metal lath and plaster

construction, the latter thickness being used for the walls which surround the elevator cores. Although these asymmetrically located walls are not structural, they may influence the structural response. The exterior curtain walls are also nonstructural and consist mainly of glass and lightweight metal panels. All four sides of the tower are faced with precast, reinforced concrete fins which are attached to the structural frame at each floor level. These fins, which measure approximately 6 inches by 18 inches by 27 feet each, contribute substantially to the mass and stiffness of the tower. Their function, however, is architectural. Another architectural feature involves the 2-story columns on the lowest levels of the north portion of the tower. The columns are encased in reinforced concrete and covered with a ceramic veneer. There are additional dummy columns of reinforced concrete between the actual columns. The foundation conditions were relatively favorable permitting the use of spread footings with dimensions varying from 14 to 22 feet.

The JOHN HANCOCK CENTER [22, 78] in Chicago is a 100-story steel-framed tower of multiple use, comprising apartments, office, parking and commercial space. Although rectangular in cross section, its sides are tapered with constant slopes, so that the base plan dimensions of 265 x 165 feet are linearly reduced to 160 x 100 feet at the roof level. The height from plaza to roof is 1107 feet.

Lateral loads are resisted by an exterior diagonal truss system. Regularly spaced exterior columns are interconnected with diagonal truss members to form a sloped rigid tube, cantilevered from the ground and extending to the roof. Though not a structure with a steel moment-resisting frame, the results of these tests were included in this study because this structure was the largest steel frame structure tested. Further, it is felt that at the height of approximately 1000 feet the difference in damping values between a full moment-resisting structural frame and a diagonal truss system would not be large, thus the diagonal truss should yield a good approximation for damping of a similarly configured moment-resisting frame.

The CANADIAN IMPERIAL BANK OF COMMERCE BUILDING [88] is located in Montreal, Canada. It is 603 feet tall with plan dimensions of 140 x 100 feet, or seven bays by four bays. There are 44 stories above ground level, with a typical story height of 12 feet 5 inches. It has a three floor substructure, 245 x 185 feet in plan. The building is founded on bedrock 48 feet below street level. The footings are designed for 25 tons/square foot bearing capacity. The structure's main lateral load-carrying system is a structural steel moment-resisting frame with high tensile bolted field connections. Lower column sections are composed of 320-pound core sections, with cover plates up to seven inches thick and 28 inches wide. Typical floor construction

consists of corrugated metal deck units supported by purlins and topped by reinforced concrete. The curtain wall is constructed of precast concrete faced with slate. Exterior columns and framing adjacent to internal shafts are fireproofed in concrete, while other internal framing has sprayed asbestos fireproofing. The structure is used as an office building with nonstructural internal partitions. There is a reinforced concrete core for the elevator shaft.

The CIL HOUSE [88] is located in Montreal, Canada. The structure is 430 feet tall with dimensions in plan of 168 x 112 feet, or six bays by three bays. There are 34 floors above ground level, with a typical story height of 11 feet 8 3/4 inches. It has a substructure which is four floors in depth, and is founded on bedrock. The lateral load resisting system of the structure is a structural steel moment-resisting frame with welded connections, and welding fabrication was used to manufacture the columns. Flange plates up to 28 x 7 1/4 inches, and web plates up to 17 x 5 inches were used. The floor system is concrete slabs formed-in-place for the basements, the ground and mechanical floors, and the roof. Elsewhere, the floors are constructed of 3 inch steel decking with a 2 1/2 inch concrete fill. The curtain walls are lightweight aluminum construction supported by steel outriggers. The beams and columns in areas with concrete slabs are fireproofed with

concrete. In the other areas, the steel is fireproofed with sprayed asbestos. The structure is used as an office building with some permanent lightweight slag aggregate block partitions and a reinforced concrete core for the elevator.

The TOKYO KAIJO BUILDING [9, 55] located in Tokyo, Japan, was a seven story steel framed structure about 115 feet in height, with a U-shaped plan of about 161 x 290 feet. The structure was composed of built-up small members, brick masonry curtain walls, concrete beams and slab floors and pumice concrete fireproofing. The building was damaged by the 1923 earthquake, and was old and in need of repair when tested. Evidently this condition state influenced the damping value determinations. The building was demolished in 1966 or 1967.

The SANWA TOKYO BUILDING [86] was modeled by a full size two-story steel framed structure. Since the model was full sized, it is taken as a test of a two story structure, rather than as a test of the 25-story building (100 meters, or approximately 328 feet tall) it represents. A description of this model, then, follows. The frame has two concrete floor slabs, each 6.3 x 6.0 meters (approximately 21 x 20 feet) in size, supported by square tubular steel columns. The center of gravity was made to coincide with the center or rigidity. Thus the frame is believed to have identical natural periods and modes of vibration with

respect to the longitudinal, transverse and diagonal directions. To one side of the two bay structure which has a floor height of 3.84 meters (about 12 feet 6 inches) and a span of 3.15 meters (approximately 10 feet), six column-covering panels, four beam-covering panels and steel windows were fastened, all similar to the actual building (Sanwa Building). Vertical joints between the panels covering columns and beams were approximately 1 inch (25 mm) wide and horizontal joints between the panels covering upper and lower columns were approximately 3/4 inches (20 mm) wide and all joints were caulked. Each column-covering panel weighed 2.8 tons and the beam covering panel, 1.5 tons. The primary purpose of the test was to obtain design data on the precast concrete panels for the actual building. However, the two-story test structure was designed with actual dimensions in mind, and it contained full-size structural and nonstructural members. Thus, it is felt that the results of the forced vibration generator test are admissible as valid data for a two-story steel frame structure.

The new TITLE INSURANCE AND TRUST BUILDING [12] in Oakland, California is a typical rectangular two-story, welded, steel rigid frame building. Reinforced concrete-block walls on two adjacent exterior faces act as shear walls. These two rigid concrete-block walls shifted the center of rotation to a point near the intersection of the

walls. The dynamic system that resulted was one in which torsion about the center of rotation was the primary motion. The two-story structure has an estimated total weight of 5600 kips. The plan dimensions are 153 x 163 feet, and the story heights are 14.5 feet and 14 feet respectively.

The ALCOA BUILDING [43, 44, 62, 85, 88] in San Francisco, California is a 27 story, rectangular steel framed building. It is 379 feet in height and has plan dimensions of 210 x 109 feet. The building's structural system includes diagonal bracing throughout the height. The floors are reinforced concrete slabs [10]. Though this structure has additional rigidity in the diagonal bracing, it is still considered an appropriate structure to include in this study, since the damping values obtained from the forced vibration generator experiments seem to fit in nicely with those from tests on steel moment-resistant frame buildings of approximately the same heights.

Appendix B

Building Height and Width Regression Equations

This appendix contains a list of regression equations for predictions of damping developed in this research. It includes equations containing building height only, building width only, and combinations of building height and width. Where the mean values were used, annotations indicating this are made. These values are the means of the data available for one particular value of height, or width, or combination. Where no annotation occurs, all of the data was used to develop the regression equation. The following notation pertains to this appendix:

ζ = % of critical damping ratio,

H = Building height, feet

D = Building width, feet

H1 = 0.001H, feet   H2 = 0.01H, feet

H3 = 0.001H, meters   H4 = 0.01H, meters

D1 = 0.01D, feet   D2 = 0.01D, meters

D3 = 0.01D, meters   D4 = 0.001D, meters

A, B, C, E, F, G, I, J, K, L, M, N = Regression equation constants (while these letters are used repeatedly, they represent a specific constant in any particular equation)

R^2 = Correlation statistic (representation of the goodness of fit of the developed equation with

the input data; the higher the R^2, the better the predictor capability of the equation), in $\frac{\text{percent}}{100}$ [58]

<u>Equations Involving Building Height</u> (35 regressions run):

1. $\zeta = A + BH$ ($R^2 = .19530$)

2. $\zeta = e^A e^{BH}$ ($R^2 = .22782$)

3. $\zeta = \frac{1}{A + BH}$ ($R^2 = .10827$)

4. $\zeta = A + BH^2$ ($R^2 = .16948$)

5. $\zeta = e^A e^{BH^2}$ ($R^2 = .22601$)

6. $\zeta = \frac{1}{A + BH^2}$ ($R^2 = .11931$)

7. $\zeta = A + B\sqrt{H}$ ($R^2 = .18083$)

8. $\zeta = e^A e^{B\sqrt{H}}$ ($R^2 = .20482$)

9. $\zeta = \frac{1}{A + B\sqrt{H}}$ ($R^2 = .09462$)

10. $\zeta = e^A e^{BH} e^{CH^2}$ ($R^2 = .23234$)

11. $\zeta = A + BH$ ($R^2 = .33592$) (Mean values used)

12. $\zeta = e^A e^{BH}$ ($R^2 = .55631$) (Mean values used)

13. $\zeta = \frac{1}{A + BH}$ ($R^2 = .61528$) (Mean values used)

14. $\zeta = A + BH^2$ ($R^2 = .28000$) (Mean values used)

15. $\zeta = e^A e^{BH^2}$ (R^2 = .54498) (Mean values used)

16. $\zeta = \dfrac{1}{A + BH^2}$ (R^2 = .74188) (Mean values used)

17. $\zeta = \dfrac{1}{A + B(H1)^2}$ (R^2 = .74188) (Mean values used)

18. $\zeta = A + B\sqrt{H}$ (R^2 = .31166) (Mean values used)

19. $\zeta = e^A e^{B\sqrt{H}}$ (R^2 = .49273) (Mean values used)

20. $\zeta = \dfrac{1}{A + B\sqrt{H}}$ (R^2 = .48745) (Mean values used)

21. $\zeta = \dfrac{1}{A + BH^3}$ (R^2 = .78033) (Mean values used)

22. $\zeta = \dfrac{1}{A + BH^4}$ (R^2 = .79185) (Mean values used)

23. $\zeta = \dfrac{1}{A + BH^5}$ (R^2 = .79513) (Mean values used)

24. $\zeta = \dfrac{1}{A + BH^6}$ (R^2 = .79491) (Mean values used)

25. $\zeta = \dfrac{1}{A + BH^5}$ (R^2 = .12113)

26. $\zeta = \ln(A + BH)$ (R^2 = .00938)

27. $\zeta = \ln(A + BH^2)$ (R^2 = .00897)

28. $\zeta = e^A e^{B(H2)}$ (R^2 = .05779)

29. $\zeta = A + B/H + C/H^2 + E/H^3 + F/H^4 + G/H^5$ (R^2 = .45252)

30. $\zeta = A + B/H^2 + C/H^3 + E/H^4 + F/H^5$ $(R^2 = .44093)$

31. $\zeta = A + B/H + C/H^2 + E/H^3 + F/H^4$ $(R^2 = .35943)$

32. $\zeta = A + B/H + C/H^3 + E/H^4 + F/H^5$ $(R^2 = .40522)$

33. $\zeta = A + B/H + C/H^2 + E/H^3 + F/H^5$ $(R^2 = .36505)$

34. $\zeta = A + B/H + C/H^2 + E/H^4 + F/H^5$ $(R^2 = .37667)$

35. $\zeta = A + B/H + C/H^2 + E/H^3$ $(R^2 = .18083)$

Equations Involving Building Width (26 regressions run):

36. $\zeta = A + BD$ $(R^2 = .10907)$

37. $\zeta = e^A e^{BD}$ $(R^2 = .12407)$

38. $\zeta = \dfrac{1}{A + BD}$ $(R^2 = .08387)$

39. $\zeta = A + BD^2$ $(R^2 = .12070)$

40. $\zeta = e^A e^{BD^2}$ $(R^2 = .14895)$

41. $\zeta = \dfrac{1}{A + BD^2}$ $(R^2 = .11712)$

42. $\zeta = A + B\sqrt{D}$ $(R^2 = .09521)$

43. $\zeta = e^A e^{B\sqrt{D}}$ $(R^2 = .10404)$

44. $\zeta = \dfrac{1}{A + B\sqrt{D}}$ $(R^2 = .06348)$

45. $\zeta = A + BD$ $(R^2 = .11516)$ (Mean values used)

46. $\zeta = e^{A} e^{BD}$ (R^2 = .17062) (Mean values used)

47. $\zeta = \frac{1}{A + BD}$ (R^2 = .18406) (Mean values used)

48. $\zeta = A + BD^2$ (R^2 = .12234) (Mean values used)

49. $\zeta = e^{A} e^{BD^2}$ (R^2 = .19141) (Mean values used)

50. $\zeta = \frac{1}{A + BD^2}$ (R^2 = .22918) (Mean values used)

51. $\zeta = A + B\sqrt{D}$ (R^2 = .10819) (Mean values used)

52. $\zeta = e^{A} e^{B\sqrt{D}}$ (R^2 = .15550) (Mean values used)

53. $\zeta = \frac{1}{A + B\sqrt{D}}$ (R^2 = .15485) (Mean values used)

54. $\zeta = A + BD^3$ (R^2 = .11690)

55. $\zeta = A + BD^4$ (R^2 = .10743)

56. $\zeta = A + BD^5$ (R^2 = .09762)

57. $\zeta = A + BD^6$ (R^2 = .08932)

58. $\zeta = A + B/D^3$ (R^2 = .04414)

59. $\zeta = A + B/D^4$ (R^2 = .04618)

60. $\zeta = A + B/D^5$ (R^2 = .04767)

61. $\zeta = A + BD^2 + C/D^2$ (R^2 = .12286)

Equations Involving Modifications to Building Height (3 regressions run):

62. $\zeta = A + [\frac{B}{.297 + 1.055(H1)^2}]$ ($R^2 = .21787$) (Mean values used)

63. $\zeta = A + B/(H1)^2$ ($R^2 = .04515$) (Mean values used)

64. $\zeta = A + B/(H1)^3$ ($R^2 = .04261$) (Mean values used)

Equations Involving Combinations of Building Height and Building Width (203 regressions run):

65. $\zeta = A + BD^2 + C/H + E/H^2 + F/H^3 + G/H^4 + I/H^5 + J/D^2$
($R^2 = .49637$)

66. $\zeta = A + BD^2 + C/H + E/H^2 + F/H^3 + G/H^4 + I/H^5$
($R^2 = .46165$)

67. $\zeta = A + B/H + C/H^2 + E/H^3 + F/H^4 + G/H^5 + I/D^2$
($R^2 = .46196$)

68. $\zeta = A + BD^2/H$ ($R^2 = .00005$)

69. $\zeta = A + BD^2/H^2$ ($R^2 = .00139$)

70. $\zeta = A + BD^2/H^3$ ($R^2 = .00141$)

71. $\zeta = A + BD^2/H^4$ ($R^2 = .00147$)

72. $\zeta = A + BD^2/H^5$ ($R^2 = .00155$)

73. $\zeta = A + BD^2(1/H^2 + 1/H^3 + 1/H^4 + 1/H^5)$ ($R^2 = .00139$)

74. $\zeta = A + BD^2/H^2 + CD^2/H^3 + ED^3/H^4 + FD^2/H^5$ ($R^2 = .07225$)

75. $\zeta = e^A e^{BD^2/H}$ ($R^2 = .00518$)

76. $\zeta = e^A e^{BD^3/H^5}$ $(R^2 = .01322)$

77. $\zeta = A + B/D^2H$ $(R^2 = .04777)$

78. $\zeta = A + B/D^2H^2$ $(R^2 = .04836)$

79. $\zeta = A + B/D^2H^3$ $(R^2 = .04851)$

80. $\zeta = A + B/D^2H^4$ $(R^2 = .00000)$

81. $\zeta = A + B/D^2H^5$ $(R^2 = .00000)$

82. $\zeta = e^A e^{B/D^2H}$ $(R^2 = .05286)$

83. $\zeta = e^A e^{B/D^2H^5}$ $(R^2 = .00000)$

84. $\zeta = A + B/D^2H + C/D^2H^2 + E/D^2H^3 + F/D^2H^4 + G/D^2H^5$

$(R^2 = .14636)$

85. $\zeta = A + B/D^2H + C/D^2H^2 + E/D^2H^3$ $(R^2 = .05709)$

86. $\zeta = A + B/D^2(1/H + 1/H^2 + 1/H^3 + 1/H^4 + 1/H^5)$

$(R^2 = .04779)$

87. $\zeta = A + B/D^2(1/H + 1/H^2 + 1/H^3)$ $(R^2 = .04779)$

88. $\zeta = A + B(D + 1/H)$ $(R^2 = .10906)$

89. $\zeta = A + B(D^2 + 1/H)$ $(R^2 = .12070)$

90. $\zeta = A + B(D + 1/H^2)$ $(R^2 = .10907)$

91. $\zeta = A + B(D^2 + 1/H^2)$ $(R^2 = .12070)$

92. $\zeta = A + B(D + 1/H^3)$ $(R^2 = .10907)$

93. $\zeta = A + B(D^2 + 1/H^3)$ $(R^2 = .12070)$

94. $\zeta = A + B(D + 1/H^4)$ $(R^2 = .10907)$

95. $\zeta = A + B(D^2 + 1/H^4)$ $(R^2 = .12070)$

96. $\zeta = A + B(D + 1/H^5)$ $(R^2 = .10907)$

97. $\zeta = A + B(D^2 + 1/H^5)$ $(R^2 = .12070)$

98. $\zeta = A + B(1/D + 1/H)$ $(R^2 = .06556)$

99. $\zeta = A + B(1/D^2 + 1/H)$ $(R^2 = .05979)$

100. $\zeta = A + B(1/D + 1/H^2)$ $(R^2 = .05198)$

101. $\zeta = A + B(1/D^2 + 1/H^2)$ $(R^2 = .04918)$

102. $\zeta = A + B(1/D + 1/H^3)$ $(R^2 = .05112)$

103. $\zeta = A + B(1/D^2 + 1/H^3)$ $(R^2 = .04387)$

104. $\zeta = A + B(1/D + 1/H^4)$ $(R^2 = .05109)$

105. $\zeta = A + B(1/D^2 + 1/H^4)$ $(R^2 = .04337)$

106. $\zeta = A + B(1/D + 1/H^5)$ $(R^2 = .05109)$

107. $\zeta = A + B(1/D^2 + 1/H^5)$ $(R^2 = .04335)$

108. $\zeta = A + BH + CD + E(HD) + FH/D + GD/H + I/HD + J/H+D$

$(R^2 = .41653)$

109. $\zeta = A + BH + CH/D + ED/H + F(H^2D) + G(H^2+D) + IH^2/D$

$+ JD/H^2 + K/H^2D + L/(H^2+D) + M/(HD) + N/(H+D)$

$(R^2 = .61462)$

110. $\zeta = A + BH^2 + CD^2 + E/(HD) + F/(H+D) + G/H^2D + I/(H^2+D)$

$+ J(HD^2) + KH/D^2 + LD^2/H + M/(HD^2) + N/(H+D^2)$

$(R^2 = .57273)$

111. $\zeta = A + BH + CD + E(HD) + F(H/D) + G(D/H) + I/(HD)$

$+ J/(H+D)$ $(R^2 = .43783)$

112. $\zeta = A + BH^2 + CD + E(H^2D) + F(H^2/D) + G(D/H^2)$

$+ I/(H^2D) + J/(H^2+D)$ $(R^2 = .26033)$

113. $\zeta = A + BH + CD^2 + E(HD^2) + F(H/D^2) + G(D^2/H) + I/(HD^2)$

$+ J/(H+D^2)$ $(R^2 = .49229)$

114. $\zeta = A + BH^2 + CD^2 + E(H^2D^2) + F(H^2/D^2) + G(D^2/H^2)$

$+ I/(H^2D^2) + J/(H^2+D^2)$ $(R^2 = .35860)$

115. $\zeta = A + B\sqrt{H} + CD + E(\sqrt{H}D) + F(\sqrt{H}/D) + G(D/\sqrt{H})$

$+ I/(\sqrt{H}D) + J/(\sqrt{H} + D^2)$ $(R^2 = .51643)$

116. $\zeta = A + BH + C\sqrt{D} + E(H\sqrt{D}) + F(H/\sqrt{D}) + G(\sqrt{D}/H)$

$+ I/(H\sqrt{D}) + J/(H+\sqrt{D}$ $(R^2 = .35893)$

117. $\zeta = A + B\sqrt{H} + C\sqrt{D} + E(\sqrt{H}\sqrt{D}) + F(\sqrt{H}/\sqrt{D}) + G(\sqrt{D}/\sqrt{H}$

$+ I/(\sqrt{H}\sqrt{D}) + J/(\sqrt{H} + \sqrt{D})$ $(R^2 = .48419)$

118. $\zeta = A + BH^2 + C\sqrt{D} + E(H^2\sqrt{D}) + F(H^2/\sqrt{D}) + G(\sqrt{D}/H^2)$

$+ I(H^2\sqrt{D} + J/(H^2+\sqrt{D})$ $(R^2 = .22660)$

119. $\zeta = A + B\sqrt{H} + CD^2 + E(\sqrt{H}D^2) + F(\sqrt{H}/D^2) + G(D^2/\sqrt{H})$

$+ I/(\sqrt{H}D^2) + J/(\sqrt{H}+D^2)$ $(R^2 = .50722)$

120. $\zeta = A + B(H/D) + C(D/H)$ $(R^2 = .13001)$

121. $\zeta = A + B\sqrt{H} + C(\sqrt{H}/D) + E(D/\sqrt{H}) + F/(\sqrt{H}+D)$

$(R^2 = .34289)$

122. $\zeta = A + BH + C\sqrt{D} + E(H/\sqrt{D}) + F(\sqrt{D}/H) + G/(H+\sqrt{D})$

$(R^2 = .23098)$

123. $\zeta = A + B\sqrt{H} + C\sqrt{D} + E(\sqrt{H}/\sqrt{D}) + F(\sqrt{D}/\sqrt{H}) + G/(\sqrt{H}\sqrt{D}$

$+ I/(\sqrt{H}+\sqrt{D})$ $(R^2 = .47398)$

124. $\zeta = A + B\sqrt{H} + C(H^2/D^2) + E\sqrt{D} + F(\sqrt{D}/\sqrt{H}) + G(\sqrt{H}/\sqrt{D})$

$(R^2 = .55871)$

125. $\zeta = A + B(D/H^2)$ $(R^2 = .00575)$

126. $\zeta = A + B(H/D^2)$ $(R^2 = .00125)$

127. $\zeta = A + B(H^2/D^2)$ $(R^2 = .10854)$

128. $\zeta = A + B(\sqrt{H}/D)$ $(R^2 = .00070)$

129. $\zeta = A + B/(\sqrt{H}+D)$ $(R^2 = .05109)$

130. $\zeta = A + B(\sqrt{D}/H)$ $(R^2 = .02643)$

131. $\zeta = A + B/(H+\sqrt{D})$ $(R^2 = .06938)$

132. $\zeta = A + B(\sqrt{H}/\sqrt{D})$ $(R^2 = .09196)$

133. $\zeta = A + B(\sqrt{D}/\sqrt{H})$ $(R^2 = .02296)$

134. $\zeta = \dfrac{1}{A + B(Hl)^2}$ $(R^2 = .76566)$ (Mean values used)

135. $\zeta = \dfrac{1}{A + B(Hl)^2 + C(Dl)}$ $(R^2 = .77856)$ (Mean values used)

136. $\zeta = A + \dfrac{B}{.315 + 1.16(Hl)^2}$ $(R^2 = .51618)$ (Mean values used)

137. $\zeta = A + \dfrac{B}{.315 + 1.16(Hl)^2} + Ce^{(Dl)^2}$ $(R^2 = .65517)$

(Mean values used)

138. $\zeta = A + \dfrac{B}{.315 + 1.16(Hl)^2} + Ce^{(Dl)^2} + Ee^{(Dl)}$

$(R^2 = .65716)$ (Mean values used)

139. $\zeta = A + \dfrac{B}{.315 + 1.16(Hl)^2} + Ce^{(Dl)^2} + Ee^{(Dl)} + F(Dl)^2$

$(R^2 = .68819)$ (Mean values used)

140. $$\zeta = A + \frac{B}{.315 + 1.16\,(Hl)^2} + Ce^{(Dl)^2} + Ee^{(Dl)} + F(Dl)^2 + G(Dl)$$ $(R^2 = .70093)$ (Mean values used)

141. $$\zeta = A + \frac{B}{.315 + 1.16(Hl)^2} + Ce^{(Dl)^2} + Ee^{(Dl)} + F(Dl)^2 + G(Dl) + H/(Dl)^2$$ $(R^2 = .73831)$ (Mean values used)

142. $$\zeta = A + \frac{B}{.315 + 1.16(Hl)^2} + C/(Dl)^2$$ $(R^2 = .51693)$ (Mean values used)

143. $$\zeta = \frac{1}{A + B(Hl)^2}$$ $(R^2 = .76566)$ (Mean values used)

144. $$\zeta = \frac{1}{A + B(Hl)^2 + C(Dl)^2}$$ $(R^2 = .78992)$ (Mean values used)

145. $$\zeta = \frac{1}{A + B(Hl)^2 + C(Dl)^2 + E(Dl)}$$ $(R^2 = .80652)$ (Mean values used)

146. $$\zeta = \frac{1}{A + B(Hl)^2 + C(Dl)^2 + E(Dl) + F/(Dl)^2}$$ $(R^2 = .82437)$ (Mean values used)

147. $$\zeta = \frac{1}{A + B(Hl)^2 + C(Dl)^2 + E(Dl) + F/(Dl)^2 + G/(Dl)}$$ $(R^2 = .83060)$ (Mean values used)

148. $\zeta = e^{A} e^{B(H1)}$ (R^2 = .57705) (Mean values used)

149. $\zeta = e^{A} e^{B(H1)} e^{C(D1)^2}$ (R^2 = .60141) (Mean values used)

150. $\zeta = e^{A} e^{B(H1)} e^{C(D1)^2} e^{E(D1)}$

(R^2 = .61272) (Mean values used)

151. $\zeta = e^{A} e^{B(H1)} e^{C(D1)^2} e^{E(D1)} e^{F/(D1)^2}$

(R^2 = .62702) (Mean values used)

152. $\zeta = e^{A} e^{B(H1)} e^{C(D1)^2} e^{E(D1)} e^{F/(D1)^2} e^{G/(D1)}$

(R^2 = .67817) (Mean values used)

153. $\zeta = e^{A} e^{B(H1)^2}$ (R^2 = .57392) (Mean values used)

154. $\zeta = e^{A} e^{B(H1)^2} e^{C(D1)^2}$ (R^2 = .59945) (Mean values used)

155. $\zeta = e^{A} e^{B(H1)^2} e^{C(D1)^2} e^{E/(D1)^2}$

(R^2 = .60522) (Mean values used)

156. $\zeta = e^{A} e^{B(H1)^2} e^{C(D1)^2} e^{E/(D1)^2} e^{F/(D1)}$

(R^2 = .66213) (Mean values used)

157. $\zeta = e^{A} e^{B(H1)^2} e^{C(D1)^2} e^{E/(D1)^2} e^{F/(D1)} e^{G(D1)}$

(R^2 = .67214) (Mean values used)

158. $$\zeta = \frac{1}{A + B(H1)^2 + C(D1)}$$

(R^2 = .77856) (Mean values used)

159. $$\zeta = \frac{1}{A + B(H1)^2 + C/(D1)^2}$$

(R^2 = .76699) (Mean values used)

160. $$\zeta = \frac{1}{A + B(H1)^2 + Ce^{(D1)}}$$

(R^2 = .79509) (Mean values used)

161. $$\zeta = \frac{1}{A + B(H1)^2 + Ce^{(D1)^2}}$$

(R^2 = .81257) (Mean values used)

162. $$\zeta = \frac{1}{A + B(H1)^2 + C\sqrt{D1}}$$

(R^2 = .77327) (Mean values used)

163. $$\zeta = \frac{1}{A + B(H1)^2 + Ce^{(D1)^2}}$$ (R^2 = .21278)

164. $$\zeta = \frac{1}{A + B(H1)^2 + Ce^{(D1)^2}}$$

(R^2 = .13695) (1^{st} mode only)

165. $$\zeta = \frac{1}{A + B(H1)^2 + Ce^{(D1)^2} + Ee^{(H1)^2}}$$

(R^2 = .84589) (Mean values used)

166. $$\zeta = \frac{1}{A + Be^{(H1)^2} + Ce^{(D1)^2}}$$

(R^2 = .84119) (Mean values used)

167. $$\zeta = \frac{1}{A + Be^{(H1)^2} + Ce^{(D1)^2} + Ee^{(H1)}}$$

(R^2 = .84187) (Mean values used)

168. $$\zeta = \frac{1}{A + Be^{(H1)}}$$ (R^2 = .72965) (Mean values used)

169. $$\zeta = \frac{1}{A + Be^{(H1)^2}}$$ (R^2 = .80519) (Mean values used)

170. $$\zeta = \frac{1}{A + Be^{(H1)} + Ce^{(D1)^2}}$$

(R^2 = .78729) (Mean values used)

171. $$\zeta = \frac{1}{A + Be^{(H1)^2} + C^{(D1)^2}}$$

(R^2 = .81872) (Mean values used)

172. $$\zeta = \frac{1}{A + Be^{(H1)^2} + C(D1)^2}$$

(R^2 = .82750) (Mean values used)

173. $$\zeta = \frac{1}{A + Be^{(H1)^2} + C/(D1)}$$

(R^2 = .80922) (Mean values used)

174. $$\zeta = \frac{1}{A + Be^{(Hl)^2} + C/(Dl)^2}$$

(R^2 = .80973) (Mean values used)

175. $$\zeta = \frac{1}{A + B(Hl)^2}$$ (R^2 = .13400) (1^{st} mode only)

176. $$\zeta = \frac{1}{A + B(Hl)^2 + Ce^{-(Dl)}}$$

(R^2 = .26248) (1^{st} mode only)

177. $$\zeta = \frac{1}{A + B(Hl)^2 + Ce^{-(Dl)} + E(Dl)}$$

(R^2 = .34692) (1^{st} mode only)

178. $$\zeta = \frac{1}{A + B(Hl)^2 + Ce^{-(Dl)} + E(Dl) + F/(Dl)^2}$$

(R^2 = .48966) (1^{st} mode only)

179. $$\zeta = \frac{1}{A + B(Hl)^2 + Ce^{-(Dl)} + E(Dl) + F/(Dl)^2 + Ge^{(Dl)}}$$

(R^2 = .61844) (1^{st} mode only)

180. $$\zeta = \frac{1}{A + B(Hl)^2}$$ (R^2 = .41715) (2^{nd} mode only)

181. $$\zeta = \frac{1}{A + B(Hl)^2 + Ce^{(Dl)}}$$

(R^2 = .47062) (2^{nd} mode only)

182. $$\zeta = \frac{1}{A + B(H1)^2 + Ce^{(D1)} + Ee^{-(D1)}}$$

(R^2 = .49846) (2^{nd} mode only)

183. $$\zeta = \frac{1}{A + B(H1)^2 + Ce^{(D1)} + Ee^{-(D1)} + F/(D1)^2}$$

(R^2 = .51289) (2^{nd} mode only)

184. $$\zeta = \frac{1}{A + B(H1)^2 + Ce^{(D1)} + Ee^{-(D1)} + F/(D1)^2 + G/(D1)}$$

(R^2 = .53364) (2^{nd} mode only)

185. $$\zeta = \frac{1}{A + B(H1)^2}$$

(R^2 = .20663) (1^{st} & 2^{nd} modes)

186. $$\zeta = \frac{1}{A + B(H1)^2 + Ce^{-(D1)}}$$

(R^2 = .24366) (1^{st} & 2^{nd} modes)

187. $$\zeta = \frac{1}{A + B(H1)^2 + Ce^{-(D1)} + E(D1)^2}$$

(R^2 = .31755) (1^{st} & 2^{nd} modes)

188. $$\zeta = \frac{1}{A + B(H1)^2 + Ce^{-(D1)} + E(D1)^2 + F/(D1)^2}$$

(R^2 = .39270) (1^{st} & 2^{nd} modes)

189. $$\zeta = \frac{1}{A + B(H1)^2 + Ce^{-(D1)} + E(D1)^2 + F/(D1)^2 + G/(D1)}$$

(R^2 = .47498) (1^{st} & 2^{nd} modes)

190. $$\zeta = \frac{1}{A + B(H1)^2 + Ce^{(H1)^2}}$$

(R^2 = .26681)(1st mode only)

191. $$\zeta = \frac{1}{A + B(H1)^2 + Ce^{(H1)^2} + E/(D1)}$$

(R^2 = .32720)(1st mode only)

192. $$\zeta = \frac{1}{A + B(H1)^2 + Ce^{(H1)^2} + E/(D1) + F/(D1)^2}$$

(R^2 = .45389)(1st mode only)

193. $$\zeta = \frac{1}{A + B(H1)^2 + Ce^{(H1)^2} + E/(D1) + F/(D1)^2 + G(D1)}$$

(R^2 = .63657)(1st mode only)

194. $$\zeta = [A + B(H1)^2 + Ce^{(H1)^2} + E/(D1) + F/(D1)^2 + G(D1) + Ie^{(D1)^2}]^{-1}$$

(R^2 = .70371)(1st mode only)

195. $$\zeta = [A + B(H1)^2 + Ce^{(H1)^2} + E/(D1) + F/(D1)^2 + G(D1) + Ie^{(D1)^2} + Je^{(H1)}]^{-1}$$

(R^2 = .71778)(1st mode only)

196. $\zeta = [A + B(Hl)^2 + Ce^{(Hl)^2} + E/(Dl) + F/(Dl)^2 + G(Dl) + Ie^{(Dl)^2} + Je^{(Hl)} + Ke^{(Dl)}]^{-1}$

(R^2 = .71952)(1st mode only)

197. $\zeta = \dfrac{1}{A + B(Hl)^2}$ (R^2 = .34551)($H \leq 160'$)

198. $\zeta = \dfrac{1}{A + B(Hl)^2 + Ce^{(Hl)}}$

(R^2 = .39074)($H \leq 160'$)

199. $\zeta = \dfrac{1}{A + B(Hl)^2 + Ce^{(Hl)} + E/(Dl)^2}$

(R^2 = .41000)($H \leq 160'$)

200. $\zeta = \dfrac{1}{A + B(Hl)^2 + Ce^{(Hl)} + E/(Dl)^2 + F(Dl)^2}$

(R^2 = .41585)($H \leq 160'$)

201. $\zeta = \dfrac{1}{A + B(Hl)^2 + Ce^{(Hl)} + E/(Dl)^2 + F(Dl)^2 + Ge^{(Dl)^2}}$

(R^2 = .41673)($H \leq 160'$)

202. $\zeta = \dfrac{1}{A + B(Hl)^2}$ (R^2 = .17840)($H > 160'$)

203. $\zeta = \dfrac{1}{A + B(Hl)^2 + Ce^{(Dl)^2}}$

(R^2 = .30282)($H > 160'$)

204. $$\zeta = \frac{1}{A + B(Hl)^2 + Ce^{(Dl)^2} + Ee^{(Hl)}}$$

$(R^2 = .31080)(H > 160')$

205. $$\zeta = \frac{1}{A + B(Hl)^2 + Ce^{(Dl)^2} + Ee^{(Hl)} + Fe^{(Hl)^2}}$$

$(R^2 = .34016)(H > 160')$

206. $$\zeta = \frac{1}{A + B(Hl)^2 + Ce^{(Dl)^2} + Ee^{(Hl)} + Fe^{(Hl)^2} + Ge^{(Dl)}}$$

$(R^2 = .34434)(H > 160')$

207. $$\zeta = [A + B(Hl)^2 + Ce^{(Dl)^2} + Ee^{(Hl)} + Fe^{(Hl)^2} + Ge^{(Dl)} + I(Dl)]^{-1}$$

$(R^2 = .34442)(H > 160')$

208. $$\zeta = [A + B(Hl)^2 + Ce^{(Dl)^2} + Ee^{(Hl)} + Fe^{(Hl)^2} + Ge^{(Dl)} + I(Dl) + J/(Dl)]^{-1}$$

$(R^2 = .34512)(H > 160')$

209. $$\zeta = \frac{1}{A + Be^{(Hl)^2} + Ce^{(Dl)^2} + E(Hl)^2 + Fe^{(Hl)}}$$

$(R^2 = .86126)$ (Mean values used)

210. $$\zeta = \frac{1}{A + Be^{(Hl)^2} + Ce^{(Dl)^2} + E(Hl)^2 + Fe^{(Hl)} + Ge^{(Dl)}}$$

$(R^2 = .86163)$ (Mean values used)

211. $\zeta = [A + Be^{(Hl)^2} + Ce^{(Dl)^2} + E(Hl)^2 + Fe^{(Hl)} + Ge^{(Dl)}$
$+ I(Dl)]^{-1}$

(R^2 = .86358) (Mean values used)

212. $\zeta = [A + Be^{(Hl)^2} + Ce^{(Dl)^2} + E(Hl)^2 + Fe^{(Hl)} + Ge^{(Dl)}$
$+ I(Dl) + J/(Dl)^2]^{-1}$

(R^2 = .87000) (Mean values used)

213. $\zeta = [A + Be^{(Hl)^2} + Ce^{(Dl)^2} + E(Hl)^2 + Fe^{(Hl)} + Ge^{(Dl)}$
$+ I(Dl) + J/(Dl)^2 + K/(Dl)]^{-1}$

(R^2 = .87753) (Mean values used)

214. $\zeta = \dfrac{1}{A + Be^{(Hl)^2} + Ce^{(Dl)}}$

(R^2 = .83182) (Mean values used)

215. $\zeta = \dfrac{1}{A + B(Hl)^2 + C/(Dl)}$

(R^2 = .76692) (Mean values used)

216. $\zeta = \dfrac{1}{A + Be^{(Hl)} + Ce^{(Dl)}}$

(R^2 = .76015) (Mean values used)

217. $\zeta = \dfrac{1}{A + Be^{(Hl)} + C(Dl)}$ (R^2 = .74050) (Mean values used)

218. $$\zeta = \frac{1}{A + Be^{(Hl)} + C/(Dl)^2}$$

(R^2 = .72994) (Mean values used)

219. $$\zeta = \frac{1}{A + Be^{(Dl)^2}}$$

(R^2 = .62810) (Mean values used)

($H \leq 160'$)

220. $$\zeta = \frac{1}{A + Be^{(Dl)^2} + Ce^{(Hl)^2}}$$

(R^2 = .77609) (Mean values used)

($H \leq 160'$)

221. $$\zeta = \frac{1}{A + Be^{(Dl)^2} + Ce^{(Hl)^2} + Ee^{(Hl)}}$$

(R^2 = .92069) (Mean values used)

($H \leq 160'$)

222. $$\zeta = \frac{1}{A + Be^{(Dl)^2} + Ce^{(Hl)^2} + Ee^{(Hl)} + F/(Dl)^2}$$

(R^2 = .99712) (Mean values used)

($H \leq 160'$)

223. $$\zeta = \frac{1}{A + Be^{(Dl)^2} + Ce^{(Hl)^2} + Ee^{(Hl)} + F/(Dl)^2 + Ge^{(Dl)}}$$

(R^2 = .99975) (Mean values used)

($H \leq 160'$)

224. $$\zeta = \frac{1}{A + Be^{(H2)^2} + Ce^{(D1)^2} + Ee^{(H2)}}$$

(R^2 = .96086) (Mean values used)

($H \leq 160'$)

225. $$\zeta = \frac{1}{A + Be^{(H1)^2}}$$

(R^2 = .87556) (Mean values used)

($H > 160'$)

226. $$\zeta = \frac{1}{A + Be^{(H1)^2} + Ce^{(D1)^2}}$$

(R^2 = .90947) (Mean values used)

($H > 160'$)

227. $$\zeta = \frac{1}{A + Be^{(H1)^2} + Ce^{(D1)^2} + Ee^{(D1)}}$$

(R^2 = .91174) (Mean values used)

($H > 160'$)

228. $$\zeta = \frac{1}{A + Be^{(H1)^2} + Ce^{(D1)^2} + Ee^{(D1)} + F/(D1)^2}$$

(R^2 = .91343) (Mean values used)

($H > 160'$)

229. $$\zeta = \frac{1}{A + Be^{(H1)^2} + Ce^{(D1)^2} + Ee^{(D1)} + F/(D1)^2 + G(H1)^2}$$

($H > 160'$)(R^2 = .91414) (Mean values used)

230. $$\zeta = [A + Be^{(H1)^2} + Ce^{(D1)^2} + Ee^{(D1)} + F/(D1)^2 + G(H1)^2 + Ie^{(H1)}]^{-1}$$

(R^2 = .97765) (Mean values used)

(H > 160')

231. $$\zeta = [A + Be^{(H1)^2} + Ce^{(D1)^2} + Ee^{(D1)} + F/(D1)^2 + G(H1)^2 + Ie^{(H1)} + J(D1)]^{-1}$$

(R^2 = .97795) (Mean values used)

(H > 160')

232. $$\zeta = \frac{1}{A + Be^{(H1)^2} + Ce^{(D1)^2} + Ee^{(H1)}}$$

(R^2 = .91042) (Mean values used)

(H > 160')

233. $$\zeta = \frac{1}{A + Be^{(H1)^2} + Ce^{(D1)^2} + Ee^{(H1)}}$$

(R^2 = .84187) (Mean values used)

234. $$\zeta = \frac{1}{A + Be^{(H2)^2} + Ce^{(D1)^2} + Ee^{(H2)}}$$

(R^2 = .84056) (Mean values used)

235. $$\zeta = \frac{1}{A + Be^{(H2)^2} + Ce^{(D1)^2} + Ee^{(H2)}}$$

(R^2 = .89896) (Mean values used)

(H > 160')

236. $$\zeta = \frac{1}{A + Be^{(H2)^2} + Ce^{(D1)^2} + Ee^{(H2)}}$$

(R^2 = .40704) (H $\leq$ 160')

237. $$\zeta = \frac{1}{A + Be^{(H2)^2} + Ce^{(D1)^2} + Ee^{(H2)}}$$

(R^2 = .92781) (1^{st} mode only)

(H $\leq$ 160')

238. $$\zeta = \frac{1}{A + Be^{(H1)^2} + Ce^{(D1)^2} + Ee^{(D1)}}$$

(R^2 = .30439) (H > 160')

239. $$\zeta = \frac{1}{A + Be^{(H1)^2} + Ce^{(D1)^2} + Ee^{(D1)}}$$

(R^2 = .67740) (1^{st} mode only)

(H > 160')

240. $$\zeta = \frac{1}{A + Be^{(H3)^2} + Ce^{(D2)^2} + Ee^{(D2)}}$$

(R^2 = .74847) (Mean values used)

($H \leq 49$ mtrs)

241. $$\zeta = \frac{1}{A + Be^{(H4)^2} + Ce^{(D2)^2} + Ee^{(D2)}}$$

(R^2 = .75237) (Mean values used)

($H \leq 49$ mtrs)

242. $$\zeta = \frac{1}{A + Be^{(H3)^2} + Ce^{(D3)^2} + Ee^{(D3)}}$$

(R^2 = .80864) (Mean values used)

($H \leq 49$ mtrs)

243. $$\zeta = \frac{1}{A + Be^{(H4)^2} + Ce^{(D3)^2} + Ee^{(D3)}}$$

(R^2 = .81100) (Mean values used)

($H \leq 49$ mtrs)

244. $$\zeta = \frac{1}{A + Be^{(H3)^2} + Ce^{(D3)^2} + Ee^{(H3)}}$$

(R^2 = .90434) (Mean values used)

($H \leq 49$ mtrs)

245. $$\zeta = \frac{1}{A + Be^{(H4)^2} + Ce^{(D3)^2} + Ee^{(H4)}}$$

(R^2 = .91204) (Mean values used)

($H \leq 49$ mtrs)

246. $$\zeta = \frac{1}{A + Be^{(H4)^2} + Ce^{(D2)^2} + Ee^{(H4)}}$$

(R^2 = .97149) (Mean values used)

($H \leq 49$ mtrs)

247. $$\zeta = \frac{1}{A + Be^{(H3)^2} + Ce^{(D4)^2} + Ee^{(H3)}}$$

(R^2 = .97658) (Mean values used)

($H \leq 49$ mtrs)

248. $$\zeta = \frac{1}{A + Be^{(H4)^2} + Ce^{(D2)^2} + Ee^{(H4)}}$$

(R^2 = .97644) (Mean values used)

($H \leq 49$ mtrs)

249. $$\zeta = \frac{1}{A + Be^{(H3)^2} + Ce^{(D3)^2} + Ee^{(H3)}}$$

(R^2 = .91151) (Mean values used)

($H > 49$ mtrs)

AD-A054 438 ARMY MILITARY PERSONNEL CENTER ALEXANDRIA VA F/G 20/11

DEVELOPMENT OF AN EMPIRICAL RELATIONSHIP FOR THE PREDICTION OF --ETC(U)

MAY 78 T J RUSNAK

UNCLASSIFIED NL

3 OF 3
ADA
054438

END
DATE
FILMED
6-78
DDC

250. $$\zeta = \frac{1}{A + Be^{(H4)^2} + Ce^{(D3)^2} + Ee^{(H4)}}$$

(R^2 = .92154) (Mean values used)

(H > 49 mtrs)

251. $$\zeta = \frac{1}{A + Be^{(H4)^2} + Ce^{(D2)^2} + Ee^{(H4)}}$$

(R^2 = .90462) (Mean values used)

(H > 49 mtrs)

252. $$\zeta = \frac{1}{A + Be^{(H3)^2} + Ce^{(D2)^2} + Ee^{(H3)}}$$

(R^2 = .87178) (Mean values used)

(H > 49 mtrs)

253. $$\zeta = \frac{1}{A + Be^{(H4)^2} + Ce^{(D3)^2} + Ee^{(D3)}}$$

(R^2 = .89009) (Mean values used)

(H > 49 mtrs)

254. $$\zeta = \frac{1}{A + Be^{(H3)^2} + Ce^{(D3)^2} + Ee^{(D3)}}$$

(R^2 = .91092) (Mean values used)

(H > 49 mtrs)

255. $$\zeta = \frac{1}{A + Be^{(H4)^2} + Ce^{(D2)^2} + Ee^{(D2)}}$$

(R^2 = .87704) (Mean values used)

(H > 49 mtrs)

256. $$\zeta = \frac{1}{A + Be^{(H3)^2} + Ce^{(D4)^2} + Ee^{(D4)}}$$

(R^2 = .88317) (Mean values used)

(H > 49 mtrs)

257. $$\zeta = \frac{1}{A + Be^{(H3)^2} + Ce^{(D2)^2} + Ee^{(D2)}}$$

(R^2 = .88602) (Mean values used)

(H > 49 mtrs)

258. $$\zeta = \frac{1}{A + Be^{(H1)^2} + Ce^{(D1)^2} + Ee^{(D1)}}$$

(R^2 = .84181) (Mean values used)

259. $$\zeta = \frac{1}{A + Be^{(H2)^2} + Ce^{(D1)^2} + Ee^{(D1)}}$$

(R^2 = .83215) (Mean values used)

260. $$\zeta = \frac{1}{A + Be^{(H3)^2} + Ce^{(D4)^2} + Ee^{(H3)}}$$

(meters) (R^2 = .80655) (Mean values used)

261. $$\zeta = \frac{1}{A + Be^{(H3)^2} + Ce^{(D4)^2} + Ee^{(D4)}}$$

(R^2 = .81048) (Mean values used)

(meters)

262. $$\zeta = \frac{1}{A + Be^{(H3)^2} + Ce^{(D2)^2} + Ee^{(H3)}}$$

(R^2 = .81073) (Mean values used)

(meters)

263. $$\zeta = \frac{1}{A + Be^{(H3)^2} + Ce^{(D2)^2} + Ee^{(D2)}}$$

(R^2 = .81327) (Mean values used)

(meters)

264. $$\zeta = \frac{1}{A + Be^{(H4)^2} + Ce^{(D4)^2} + Ee^{(D4)}}$$

(R^2 = .82680) (Mean values used)

(meters)

265. $$\zeta = \frac{1}{A + Be^{(H4)^2} + Ce^{(D2)^2} + Ee^{(D2)}}$$

(R^2 = .82926) (Mean values used)

(meters)

266. $$\zeta = \frac{1}{A + Be^{(H4)^2} + Ce^{(D4)^2} + Ee^{(H4)}}$$

(R^2 = .84800) (Mean values used)

(meters)

267. $$\underline{\underline{\zeta = \frac{1}{A + Be^{(H4)^2} + Ce^{(D2)^2} + Ee^{(H4)}}}}$$

(R^2 = .85084) (Mean values used)

(meters)

Note: Underlined equations 233 and 267 are selected.

Appendix C

Development of Spectral Displacement vs Damping Relationship

To use the first order approximation of the mean value and variance of the spectral displacement, an analytical relationship between spectral displacement and damping must exist. For the type of low-amplitude earthquake force or wind force which is considered herein, a correlation between these two random variables is developed.

The spectral velocity, or spectral pseudo-velocity, is defined [16] as the maximum value of the response function, $\underline{X(t)}$; where $\underline{X(t)}$ denotes the integral in the Duhamel expression for earthquake response of a damped structure (with at-rest initial conditions):

$$\underline{X(t)} = \int_0^t \ddot{x}_g(\tau) e^{-\zeta\omega(t-\tau)} \sin\omega(t-\tau)\,d\tau \qquad \text{(C.1)}$$

where: $\ddot{x}_g(\tau)$ = ground acceleration

ζ = equivalent viscous damping ratio

ω = natural frequency

Thus, spectral velocity, denoted by S_v, is:

$$S_v \doteq X_{max} = \left[\int_0^t \ddot{x}_g(\tau) e^{-\zeta\omega(t-\tau)} \sin\omega(t-\tau)\,d\tau\right]_{max} \qquad \text{(C.2)}$$

And, spectral displacement, S_d, is the ratio of spectral velocity to the circular frequency:

$$S_d \equiv \frac{S_v}{\omega} \qquad \text{(C.3)}$$

Spectral velocity, for any given earthquake input and for specified damping ratios, can be determined as a function of structure period, T. This has been done by others for earthquake records of various intensities. The resulting curves are rough and exhibit sharp changes in direction. These irregularities are due to "local resonances in the ground motion record," and are not significant for general usage. Thus, these curves may be "smoothed" by averaging spectral velocity response for several different earthquake motions and then normalizing to a standard intensity. The result is an average velocity response spectrum for a specified earthquake intensity level. Then by using the relationship, Eqn. C-3, and a similar relationship between spectral acceleration, S_a, and spectral velocity:

$$S_a \equiv \omega S_v \tag{C-4}$$

average displacement and average acceleration response spectra can be developed. It should be noted that because of these interrelationships, if any one of the three - spectral displacement, spectral velocity, spectral acceleration - is known, the other two can be derived. A combined earthquake response spectrum for a given earthquake intensity level can be constructed in convenient format using tripartite paper. Such a spectrum for a low intensity earthquake level is depicted in Fig. C.1.

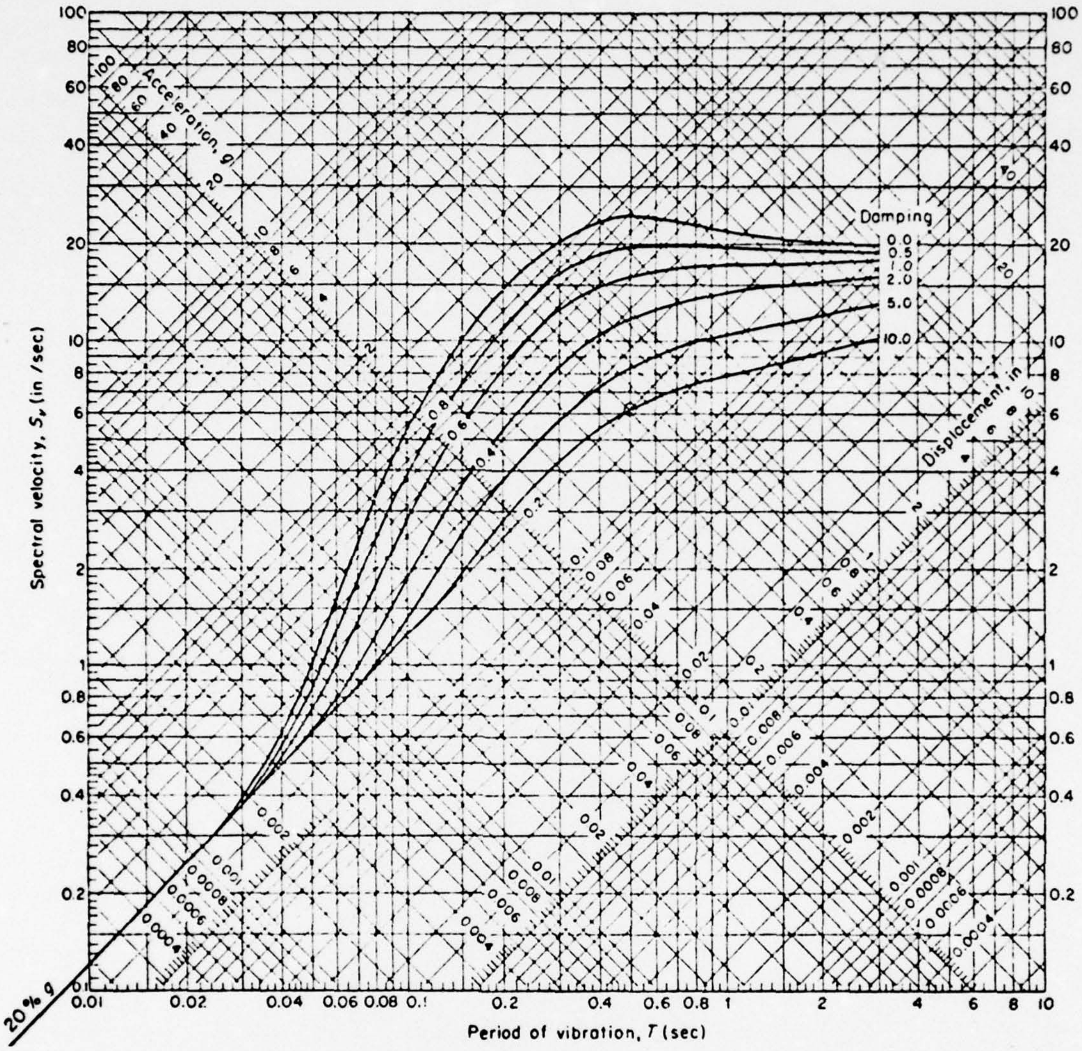

FIGURE C.1
COMBINED EARTHQUAKE RESPONSE SPECTRA

From: Wiegel, EARTHQUAKE ENGINEERING, Prentice-Hall, Inc., 1970. Reproduced by permission of Prentice-Hall, Inc., Englewood Cliffs, N.J.

Earthquake response spectra are valuable because they provide a measure of structure response to the earthquake force (or lateral motion of similar intensity). Fig. C.1 shows that a single point is plotted on the graph from the known period and damping of a structure. This point, then, represents values for spectral displacement, spectral velocity, and spectral acceleration. The response of a single-degree-of-freedom system can be determined directly using these spectral values. Moreover, certain characteristics of the responses of a multi-degree-of-freedom system can be determined by using these spectral values in conjunction with the generalized coordinate approach.

For purposes of developing a spectral displacement versus damping relationship, Fig. C.2 is derived from Fig. C.1. However, using Fig. C.1 to calculate the base shear force, which represents the total earthquake force acting in the structure, results in a value which is larger than that which would be calculated using the seismic design provisions of the Uniform Building Code [87] for a building in Seismic Zone 3. Consequently, the earthquake force of Fig. C.1 is too strong for use in this sensitivity analysis. In order to obtain response spectra for an earthquake of sufficiently low intensity to be consistent with the assumptions made, the spectral displacements shown in Fig. C.2 have been reduced by a factor of 10. The presumption herein is that while the intensity may differ, the overall

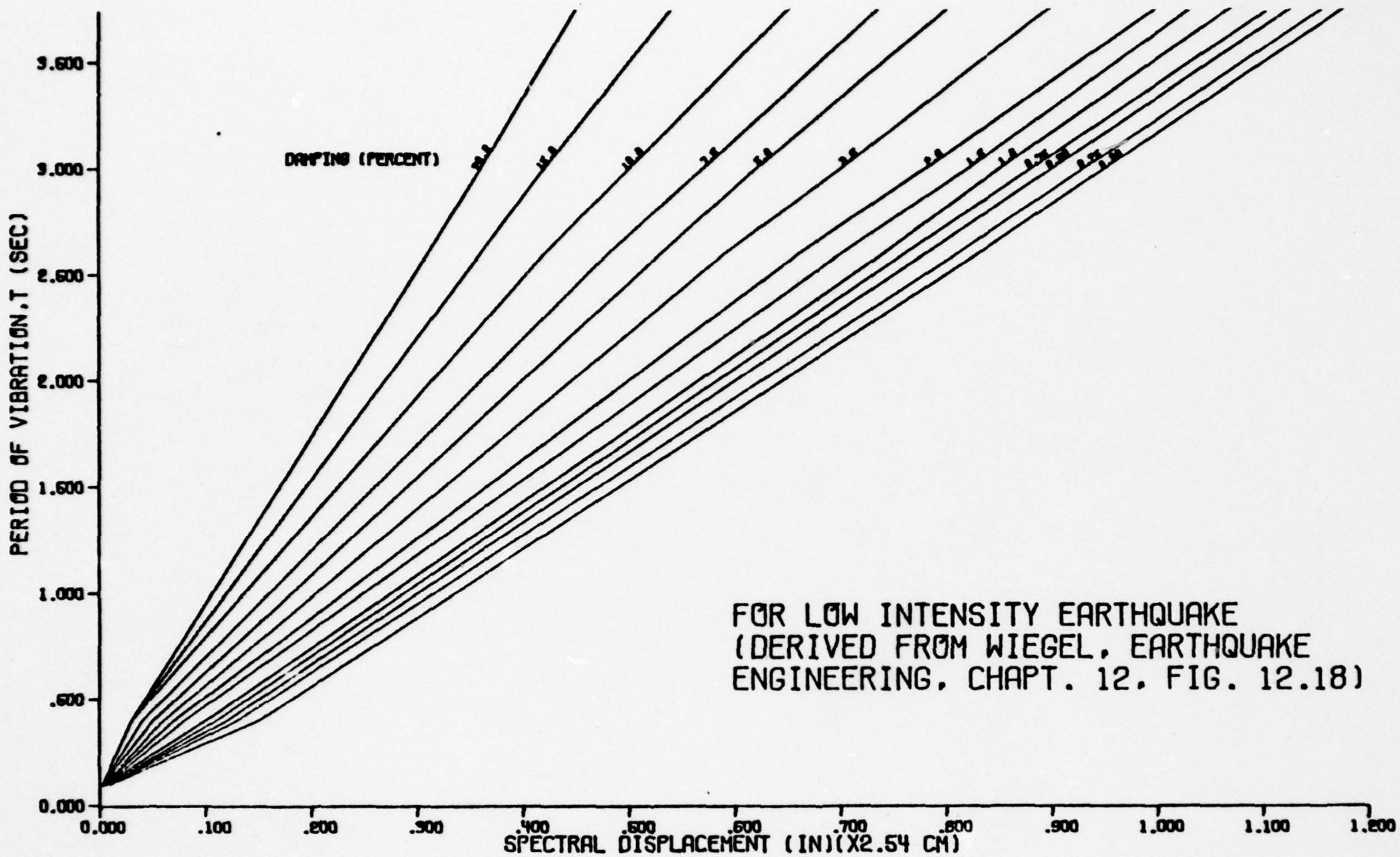

FIGURE C.2
DISPLACEMENT RESPONSE SPECTRUM

shapes of the response spectra are generally similar. Since this is an attempt to merely establish a reasonably low intensity earthquake function, it is felt this assumption is acceptable.

Fig. C.3 is a graph of spectral displacement (normalized to displacement values of an undamped system) versus damping which is derived from Fig. C.2. Each curve in Fig. C.3 represents a constant value of the period of vibration, T. These curves are shown for T = 0.1, 0.5, 1.5, and 4.0 seconds. It should be noted that Figs. C.2 and C.3 are simply two ways of depicting the relationship that exists among spectral displacement, period, and damping. While Fig. C.3 is in itself useful, a relationship between spectral displacement and damping, <u>for a constant value of T</u>, is sought. Mathematically, this relationship is expressed in a normalized relation as:

$$S_d | S_{d(0\%)} = f(\zeta) \qquad T, \text{ constant} \tag{C-5}$$

While the shapes of the four curves in Fig. C.3 differ from each other, the overall trend indicates that either an exponential or an inverse relationship would best approximate the function which is sought.

The REGRESSION subroutine of the Statistical Program for the Social Sciences (SPSS) [58] was used to establish this relationship. The basic concept of this subroutine is to produce the linear relationship which will correlate as

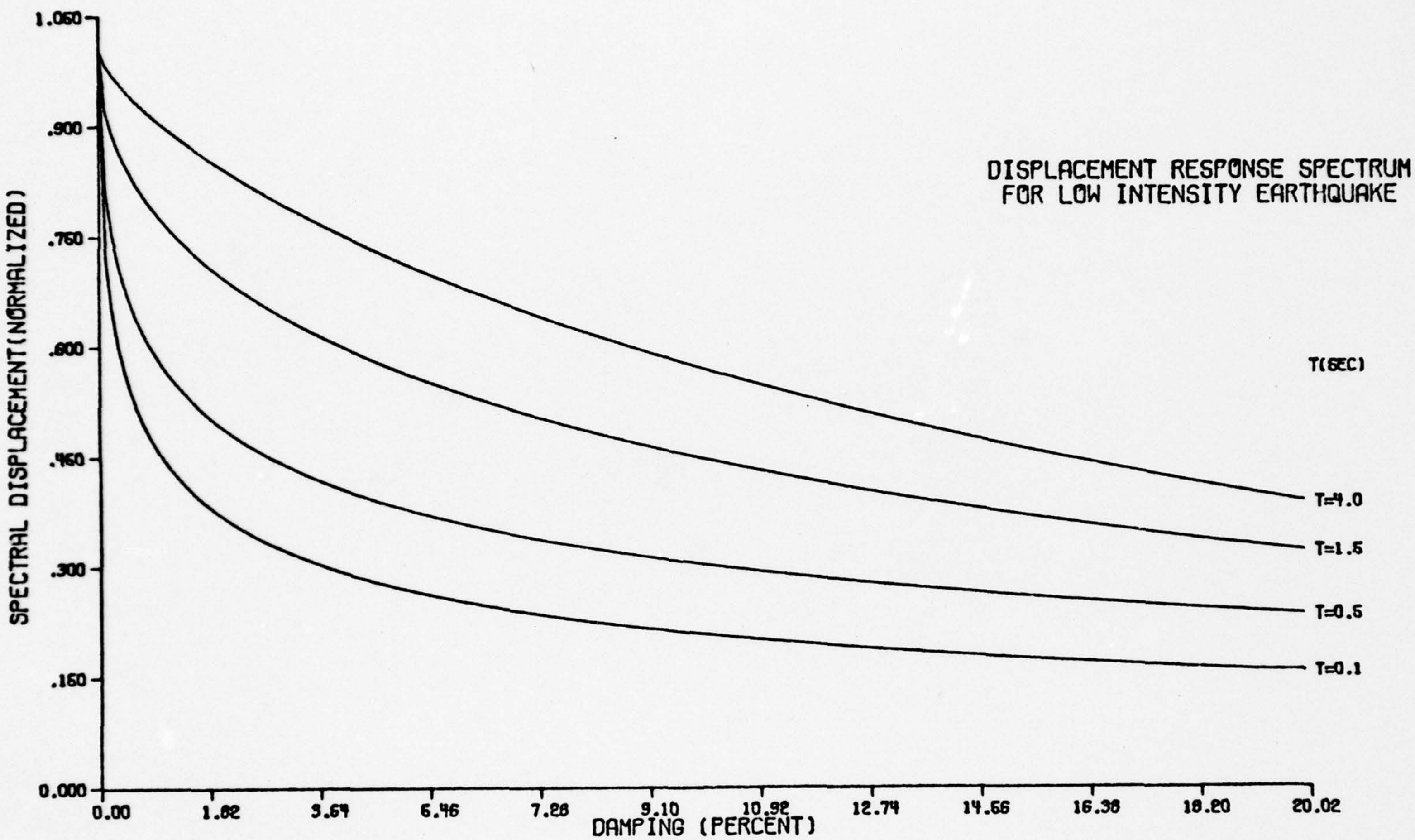

FIGURE C.3
SPECTRAL DISPLACEMENT VS DAMPING

highly as possible the independent variable with the dependent variable. The measure of this correlation is the R^2 statistic which indicates the amount of the error which is explained by the established linear relationship. In order to use the linear regression technique for the exponential and inverse relationships, the independent variables were transformed as shown in Eqns. C-7 and C-9 below.

Output of interest from this regression analysis subroutine are the R^2 statistic, the regression coefficients, and the scattergram depicting this relationship between the independent and dependent variables. For an exponential relationship, the following equation is used:

$$S_d | S_{d(0\%)} = Ae^{B\zeta^C} \qquad \text{(C-6)}$$

which can also be expressed as:

$$\ell n(S_d | S_{d(0\%)}) = A + B\zeta^C \qquad \text{(C-7)}$$

For an inverse relationship, the following is used:

$$S_d | S_{d(0\%)} = \frac{1}{A + B\zeta^C} \qquad \text{(C-8)}$$

or,

$$\frac{1}{S_d | S_{d(0\%)}} = A + B\zeta^C \qquad \text{(C-9)}$$

In each of the above equations:

A, B are the regression coefficients,

c is the exponent of ζ, varied external to the computer program to obtain the best correlation; 1, 2 and 1/2 are values which are used.

Noting from Fig. C.3 the wide variation in curves, it might be anticipated that a single relationship between variables would be insufficient in that the correlation obtained would be unsatisfactory even for a first order approximation. The regression equation for the entire range of T was developed resulting in the following exponential relationship:

$$\ell n(S_d/S_{d(0\%)}) = .05 - .268\zeta^{1/2} \qquad \text{(C-10)}$$

or,

$$S_d/S_{d(0\%)} = 1.05e^{-.268\zeta^{1/2}} \qquad \text{(C-11)}$$

This is shown as the solid line in Fig. C.4. It should be noted that the curve varies significantly from the extreme curves of T = 4 sec and T = 0.1 sec (dashed lines in Fig. C.4) especially in the lower range of damping ($\zeta < 10\%$) which is of primary interest.

To establish relationships which more accurately represent spectral displacement in the range of interest, equations describing the relationship between $S_d|S_{d(0\%)}$ and ζ for ranges of T are developed. The selection of these range values is necessarily arbitrary; however, there are limiting conditions. On the one extreme, an infinite number

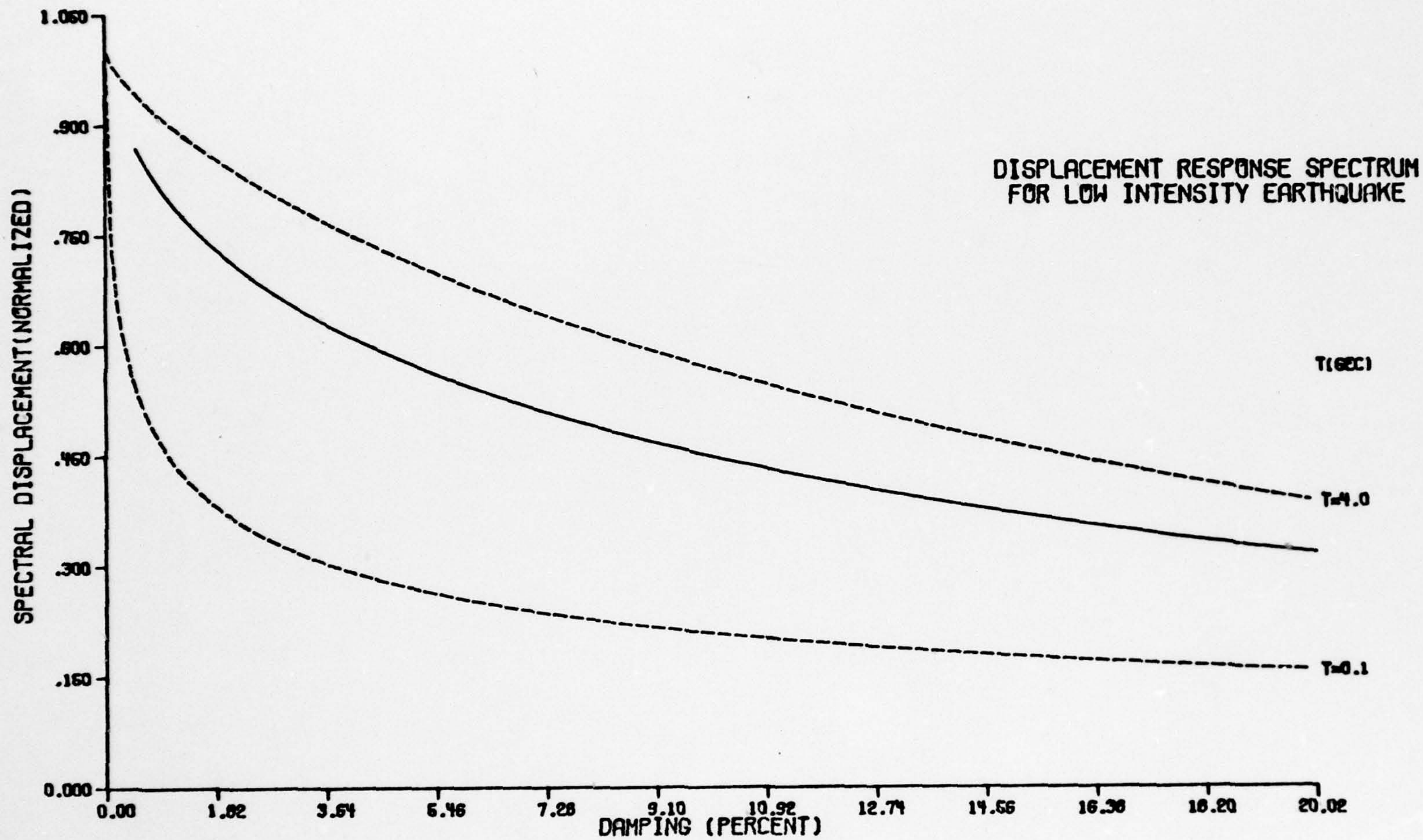

FIGURE C.4
SPECTRAL DISPLACEMENT VS DAMPING

of curves can be developed, each based upon a discrete value for T. While this yields the most accurate of all possible alternatives, it is not practical. Neither is the other extreme as depicted in Fig. C.4. Criteria, then, must be selected so that appropriate ranges of T values can be selected objectively.

It seems reasonable to assume that the R^2 statistic is an appropriate criterion to use. If, for a given range of T any developed regression equation has an R^2 value of 90% or better, then for the same reasons as presented in Chapter III, this range will be considered to be adequate for the purposes of this sensitivity analysis. Accordingly, the following ranges of T with corresponding regression equations and R^2 statistics were determined:

Range	Regression Equation	R^2	
$.1 \leq T < .5$	$S_d \mid S_{d(0\%)} = \dfrac{1}{.911 + 1.033\zeta^{1/2}}$	.94082	(C-12)
$.5 \leq T < 1.5$	$S_d \mid S_d(0\%) = 1.035e^{-.3036\zeta^{1/2}}$	.94147	(C-13)
$1.5 \leq T \leq 4.0$	$S_d \mid S_{d(0\%)} = 1.104e^{-.2426\zeta^{1/2}}$	.97020	(C-14)

It should be noted that while the best relationships turn out to be inverse for the lower range of T and exponential for the higher ranges, the best correlation in all cases occurs when $\zeta^{1/2}$ is used for the dependent variable. The above relationships are shown on Figs. C.5, C.6, and C.7

for ranges of T of $.1 \leq T < .5$, $.5 \leq T < 1.5$, and $1.5 \leq T \leq 4.0$ respectively. As is seen in these figures, the regression equations provide a better correlation between the variables in the appropriate ranges than the regression line in Fig. C.4 does over the entire range of T. Consequently, these are the equations which are used in the sensitivity analysis.

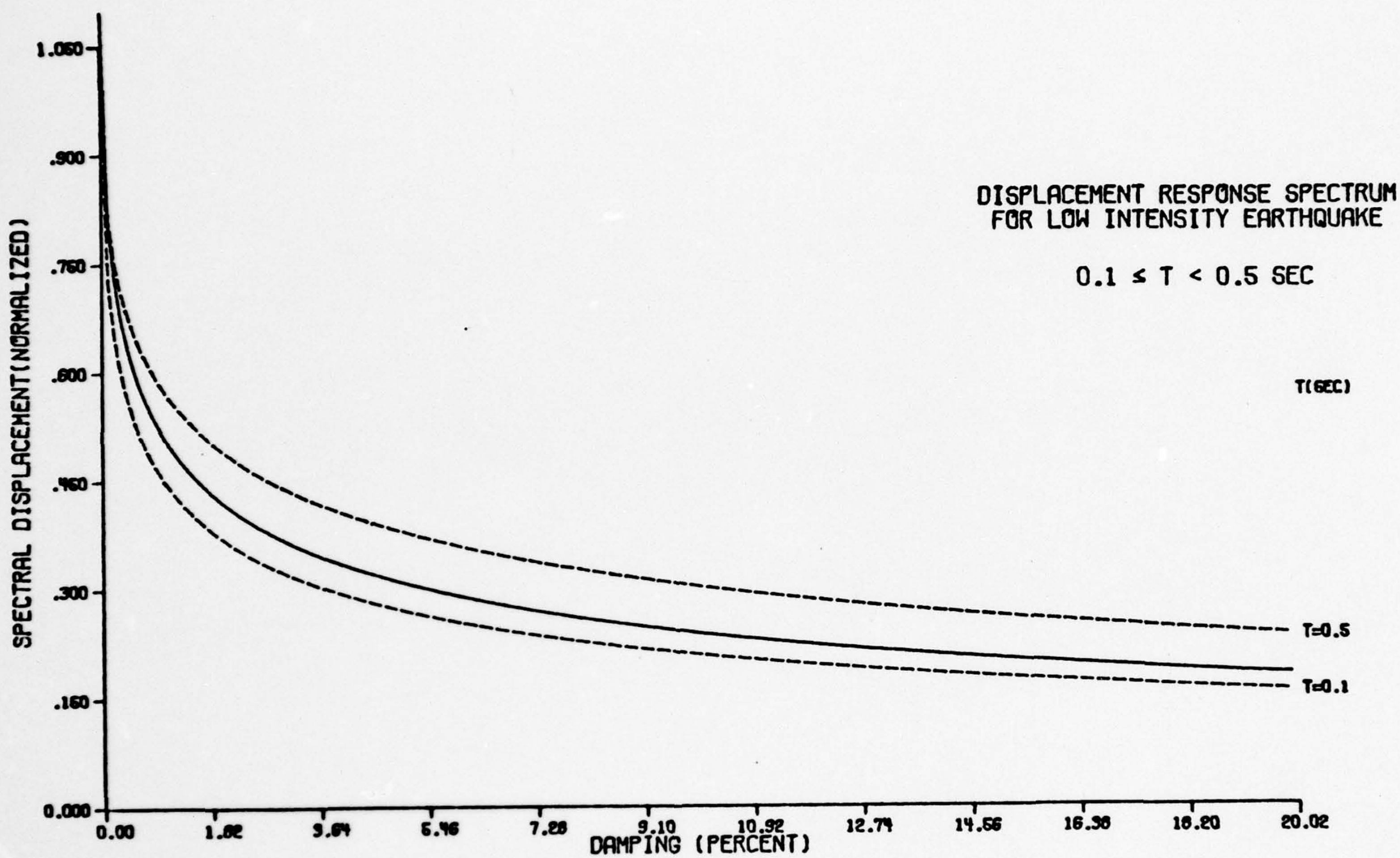

FIGURE C.5
SPECTRAL DISPLACEMENT VS DAMPING

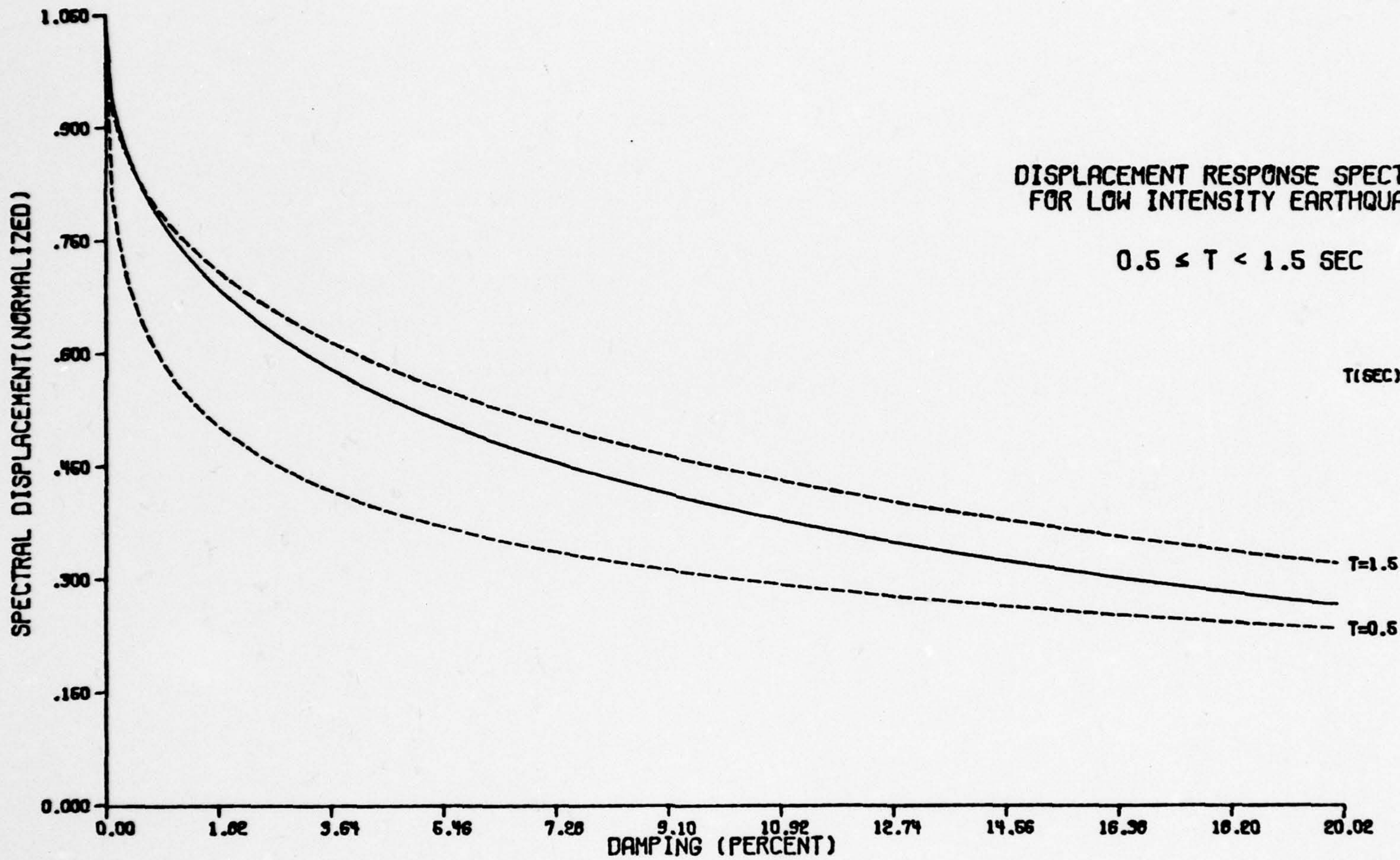

FIGURE C.6
SPECTRAL DISPLACEMENT VS DAMPING

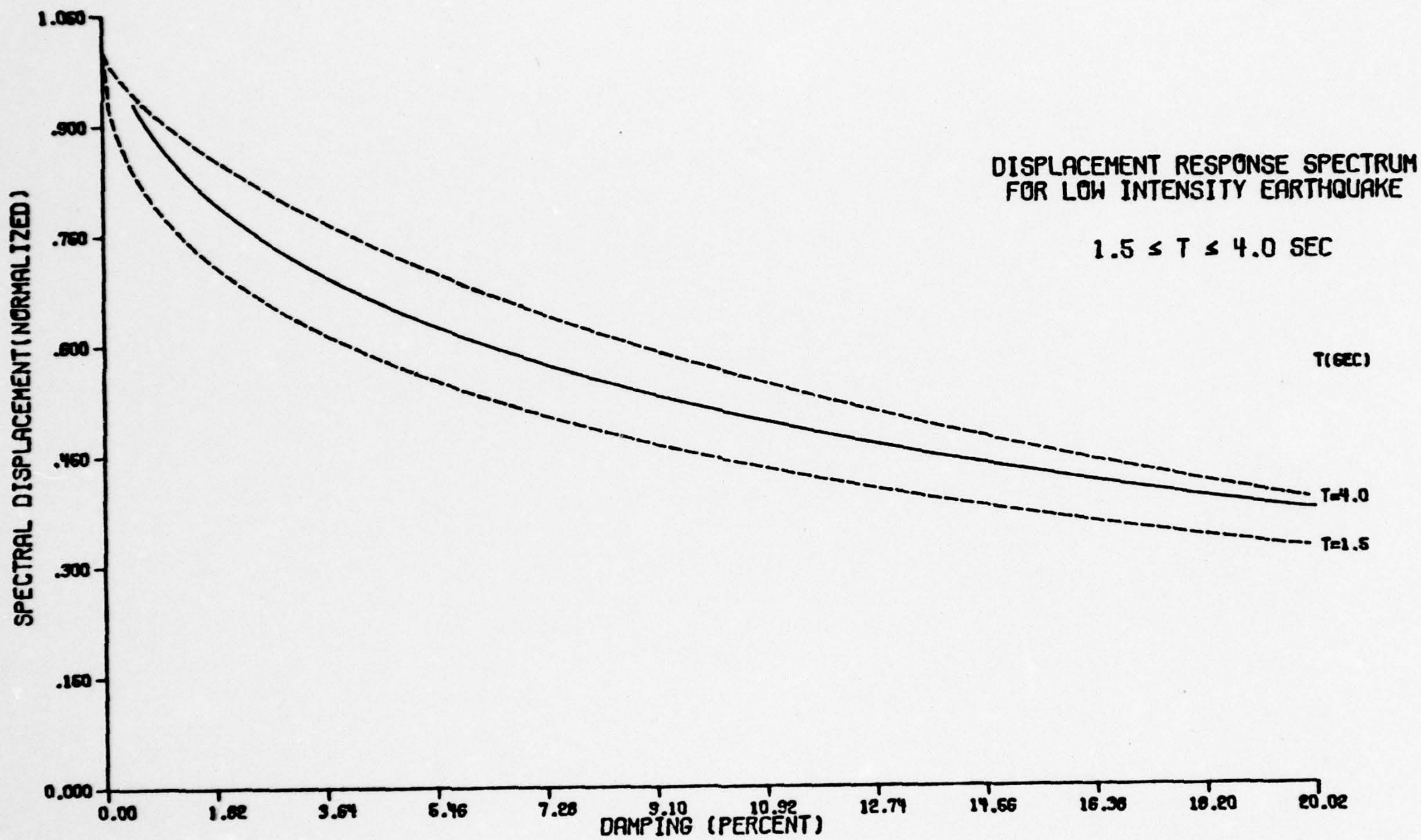

FIGURE C.7
SPECTRAL DISPLACEMENT VS DAMPING

Appendix D

Development of Prediction Equation in the Metric System

The Metric-equivalent form of Eqn. 3-6 is Eqn. 3-7, repeated herein:

$$\zeta = \frac{1}{-.155 + .597e^{(.00328H)^2} + .00041e^{(.0328D)^2} - .078e^{(.00328H)}} \tag{D-1}$$

Since this equation may be somewhat cumbersome to use, a more convenient form was developed. The input data set accumulated for the regression equation development in Chapter III was converted to the Metric system and used for this development. The basic form of Eqn. D-1 was retained in the determination of the new regression coefficients by using the SPSS statistical package. It was felt any equation of this basic form would be more convenient than Eqn. D-1 if the exponential terms could be more easily handled. Thus, the R^2 value was considered as the determining factor in the selection of the best expression.

Several regression equations were run. These are listed in Appendix B. The best equation is:

$$\zeta = \frac{1}{-.037 + .0000074e^{(.01H)^2} + .319e^{(.01D)^2} + .027e^{(.01H)}} \tag{D-2}$$

This equation was developed using mean values of damping as input data. The R^2 value for Eqn. D-2 is equal to 85.1%.

This is just slightly better than the correlation value for Eqn. D-1 (R^2 = 84.2%). As measured by the reference statistic then, these two equations are comparable and the use of either would result in a good prediction for the damping value of a structure. Figs. D.1 and D.2 present Eqn. D-2 graphically for representative values of building width.

The English-equivalent form of Eqn. D-2 is:

$$\zeta = [- .037 + .0000074e^{(.003048H)^2} + .319e^{(.003048D)^2} + .027e^{(.003048H)}]^{-1} \qquad \text{(D-3)}$$

where: H, D in feet.

It should be noted that Eqn. D-3 is a less convenient form than the expression of Eqn. 3-6, which is:

$$\zeta = \frac{1}{- .155 + .597e^{(.001H)^2} + .00041e^{(.01D)^2} - .078e^{(.001H)}} \qquad \text{(D-4)}$$

Two forms of sensitivity analysis were performed using Eqn. D-2. The first used the first order approximation technique to determine the mean and variance (and hence, coefficient of variation) of the displacement response from the mean and variance of the damping value predicted by Eqn. D-2. The displacement response spectrum developed in Appendix C for a low amplitude earthquake is used. The results of this analysis are tabulated in Table D.1.

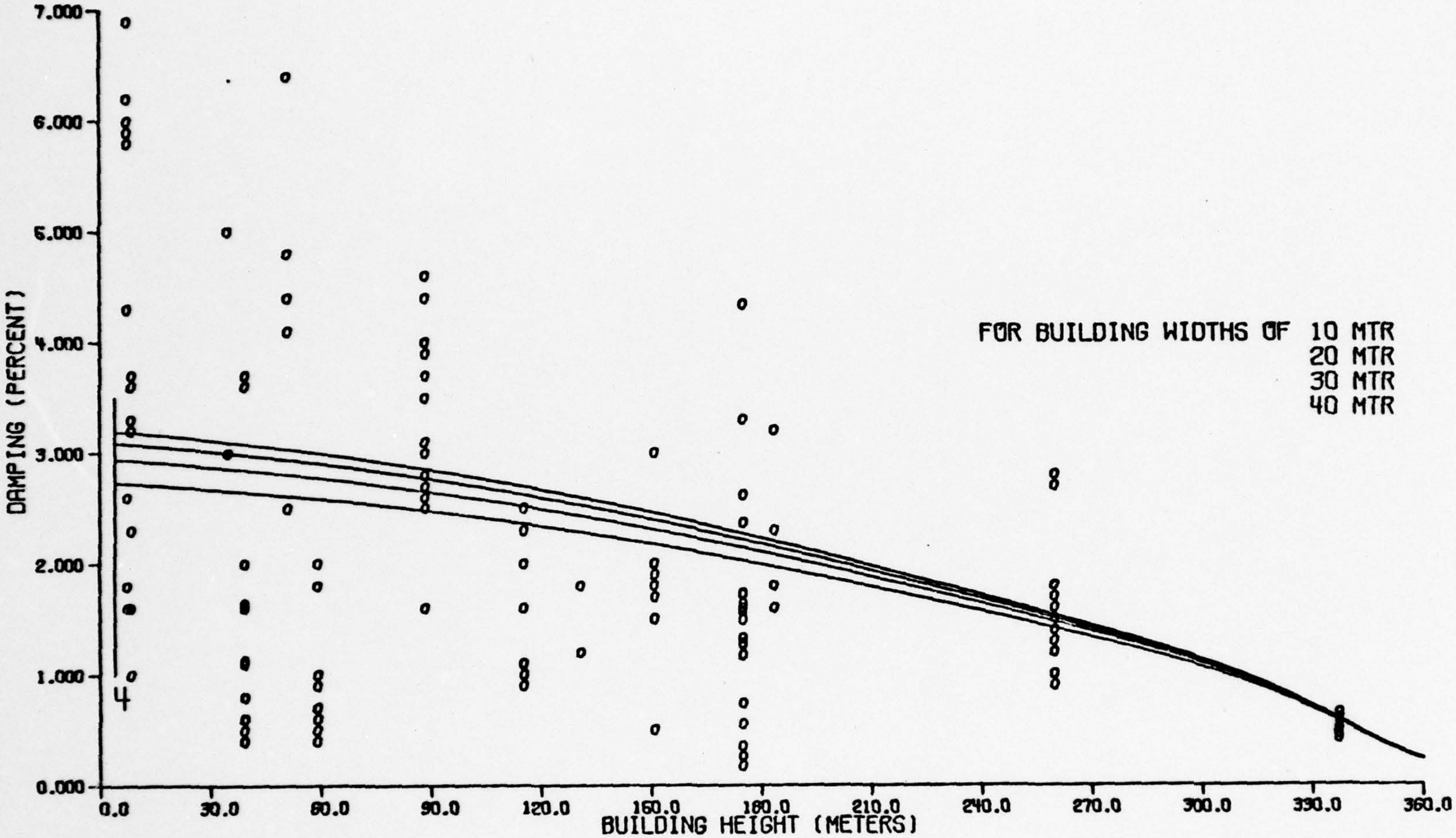

FIGURE D.1
DAMPING FROM EQUATION D-2

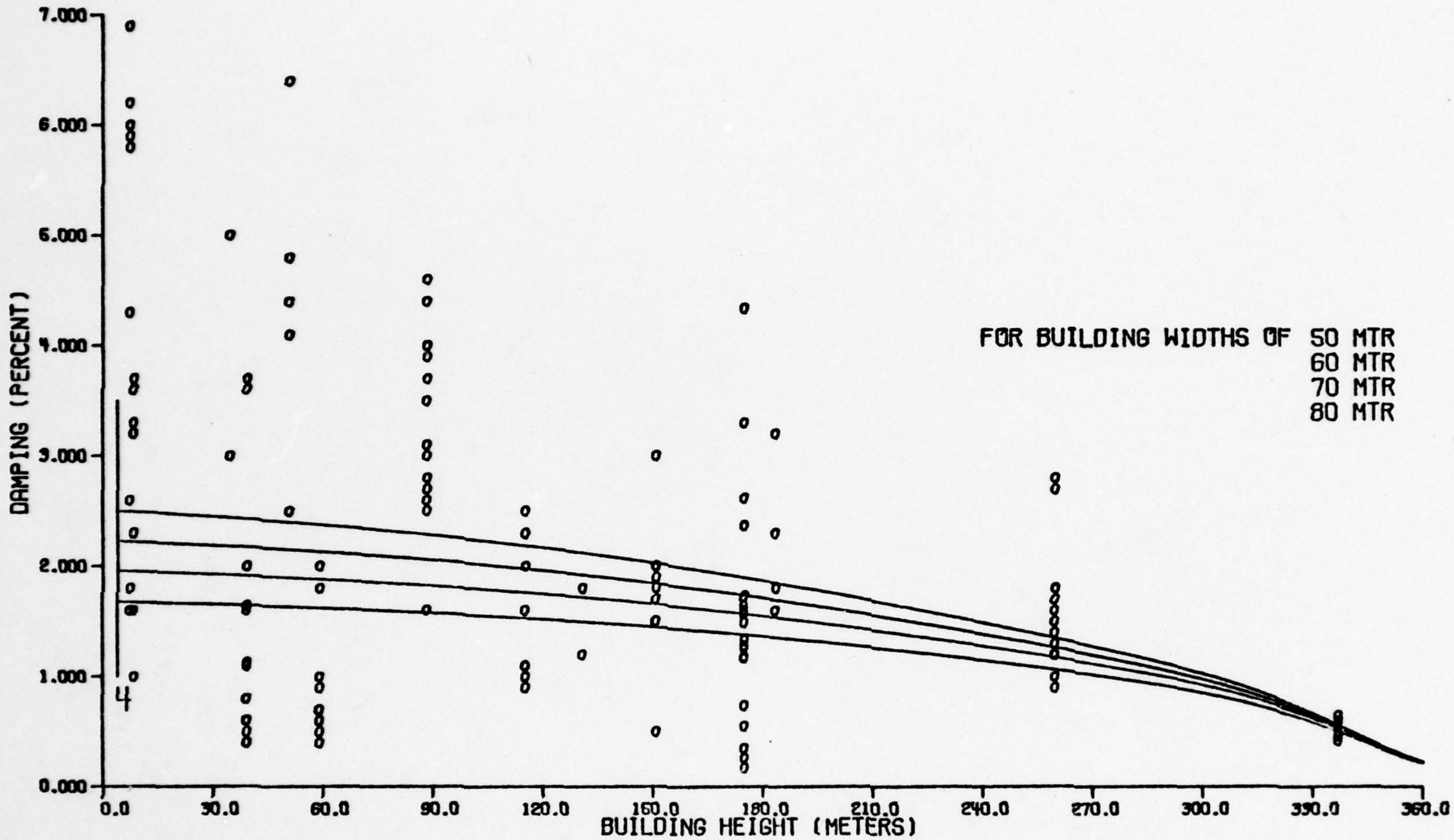

FIGURE D.2
DAMPING FROM EQUATION D-2

TABLE D.1

SENSITIVITY ANALYSIS RESULTS

Bldg Ht, H (Mtr)	7.5	7.5	40	40	51	51	89	89	260
Bldg Wdth, D (Mtr)	6.0	6.5	12	67	51	72.5	21	55	53
No. of stories	2	2	9	9	12	12	22	22	60
$\bar{\zeta}$ fm Eqn (%)	3.20	3.20	3.00	2.00	2.40	1.80	2.80	2.20	1.30
σ_ζ	.484	.484	.484	.484	.484	.484	.484	.484	.484
COV	.151	.151	.139	.242	.204	.265	.175	.223	.367
σ_ζ^2	.234	.234	.234	.234	.234	.234	.234	.234	.234
T (sec)	.449	.872	.500	.413	.930	1.04	2.5	2.6	1.48
$S_{d(0\%)}$ (cm)	.437	.772	.483	.391	.818	.904	2.03	2.11	1.25
$\bar{S}_d$ (cm)	.158	.464	.295	.210	.530	.594	1.5	1.63	.913
$\sigma_{S_d}^2$ $(10)^{-5}$	6.4	36.3	15.7	39.7	64	104	280	421	340
$\bar{x}_{max}$ (cm)	.187	.549	.363	.258	.759	.851	1.94	2.11	1.70
$\sigma_{x_{max}}^2$ $(10)^{-5}$	8.9	50.8	23.8	60.1	131	213	470	707	1179
COV	.050	.041	.042	.095	.048	.054	.035	.040	.064

It is seen from Table D.1 that the COV's are low for the buildings included in the analysis. The worst is for the 60-story building (COV = .367) which is expected. The displacement responses are all small and the resulting COV's are also very low, being less than 10% in all cases.

The second form of sensitivity analysis performed was the comparison of the predicted damping value with the highest and lowest damping values in the experimental data set for a given building height and width. The results are tabulated in Table D.2.

The maximum difference between the displacement response determined from the predicted damping values ($\bar{x}$ in Table D.2) and those determined from the highest and lowest experimental damping values is .383 cm (for the 89 meter high, 55 meter wide building). The average value for all 18 comparisons is .121 cm. The maximum difference in percent is 39.7 (for the 40 meter high, 12 meter wide building), and the average percentage difference between the extreme values and the mean displacement response is 15.6%.

It should be noted the above sensitivity analysis results compare very favorably with those obtained from the sensitivity analyses in Chapter III. It is concluded, therefore, that Eqns. 3-6 and D-2 are comparable.

TABLE D.2

COMPARISON OF PREDICTED AND EXPERIMENTALLY-DETERMINED DAMPING VALUES

Bldg Ht, H (Mtr)	7.5	7.5	40	40	51	51	89	89	260
Bldg Wdth, D (Mtr)	6.0	6.5	12	67	51	72.5	21	55	53
No. of stories	2	2	9	9	12	12	22	22	60
$\bar{\zeta}$, fm Eqn (%)	3.20	3.20	3.00	2.00	2.40	1.80	2.80	2.20	1.30
ζ_{max}(exp'm'l)(%)	6.90	6.00	3.70	2.00	6.40	4.80	4.40	4.60	2.80
ζ_{min}(exp'm'l)(%)	1.80	1.60	0.40	0.50	4.10	2.50	1.60	1.60	0.90
$\bar{x}$ fm mean (cm)	.187	.549	.363	.258	.759	.851	1.94	2.11	1.70
x fm max. (cm)	.142	.449	.343	.203	.563	.690	1.81	1.73	1.45
diff (cm)	.045	.100	.020	.055	.196	.161	.130	.383	.250
%	23.8	18.2	5.5	21.3	25.8	18.9	6.7	18.1	14.7
x fm min. (cm)	.225	.644	.507	.293	.656	.830	2.22	2.14	1.80
diff (cm)	.038	.095	.144	.035	.103	.021	.280	.027	.100
%	20.3	17.3	39.7	13.6	13.6	2.5	14.4	1.3	5.9

VITA

Terrance John Rusnak was born in Hammond, Indiana on September 7, 1942. He attended public schools in Chicago, Illinois from 1948 through 1960. He entered the United States Military Academy at West Point, New York in the summer of 1960 and obtained a Bachelor of Science Degree in June, 1964. He served in various U.S. Army Corps of Engineers assignments from 1964 to 1970 including duty in Korea, Vietnam, Fort Belvoir, Virginia, and Washington, D.C. While serving as an Assistant PMS at Purdue University from 1970 to 1972, he was a part-time student and obtained a Master of Science degree in Industrial Management in August 1972. He began full-time graduate work in 1972 also at Purdue University and received a Master of Science Degree in Civil Engineering in May, 1973. From 1973 until 1976, he was a project manager for the U.S. Air Force Regional Civil Engineer's Office in Atlanta, Georgia. He began work as a doctoral student at Purdue University in the summer of 1976.

He is a registered Professional Engineer in the State of Virginia. He presently is a Major in the United States Army, and is a member of the Corps of Engineers.